

The faint radio sky: radio astronomy becomes mainstream

Paolo Padovani

Received: June 7, 2016 / Accepted: August 9, 2016

Abstract Radio astronomy has changed. For years it studied relatively rare sources, which emit mostly non-thermal radiation across the entire electromagnetic spectrum, i.e. radio quasars and radio galaxies. Now it is reaching such faint flux densities that it detects mainly star-forming galaxies and the more common radio-quiet active galactic nuclei. These sources make up the bulk of the extragalactic sky, which has been studied for decades in the infrared, optical, and X-ray bands. I follow the transformation of radio astronomy by reviewing the main components of the radio sky at the bright and faint ends, the issue of their proper classification, their number counts, luminosity functions, and evolution. The overall “big picture” astrophysical implications of these results, and their relevance for a number of hot topics in extragalactic astronomy, are also discussed. The future prospects of the faint radio sky are very bright, as we will soon be flooded with survey data. This review should be useful to all extragalactic astronomers, irrespective of their favourite electromagnetic band(s), and even stellar astronomers might find it somewhat gratifying.

Keywords Radio continuum · Galaxies: active · Galaxies: starburst · Quasars: general · Galaxies: statistics · surveys

Contents

1	Introduction	2
2	The main components of the radio sky	3
2.1	Radio galaxies	3
2.2	Radio quasars and blazars	4
2.3	Radio-quiet AGN	5

P. Padovani
 European Southern Observatory, Karl-Schwarzschild-Str. 2, D-85748
 Garching bei München, Germany
 Tel.: +49-89-32006478
 E-mail: ppadovan@eso.org

2.4	Star-forming galaxies	6
2.5	FR 0 radio galaxies	7
3	Radio number counts	7
3.1	Number count basics	7
3.2	Observed radio number counts and their complications	8
4	The bright radio sky population	10
5	The faint radio sky population	11
5.1	Source classification	11
5.2	The importance of selection effects	14
5.3	Radio number counts by population	15
5.4	Luminosity functions	16
5.4.1	SFGs	17
5.4.2	RL AGN	17
5.4.3	RQ AGN	18
5.4.4	SFGs and AGN	18
5.5	Evolution	18
5.5.1	SFGs	19
5.5.2	RL AGN	19
5.5.3	RQ AGN	20
6	The big picture: what does it all mean?	20
6.1	Astrophysics of faint radio sources	20
6.1.1	SFGs and cosmic star formation history	20
6.1.2	RL AGN and quiescent galaxies	21
6.2	The origin of radio emission in (sub-mJy) RQ AGN	21
6.3	Radio emitting AGN in the larger context	23
7	The future	23
7.1	New radio facilities	23
7.2	How many sources, and of what type, will the new radio facilities detect?	24
7.2.1	Predictions	24
7.2.2	Source classification in the era of the SKA and its precursors	25
7.3	The astrophysical impact of future radio observations	26
7.3.1	SFGs and cosmic star formation history	26
7.3.2	Galaxy evolution	26
7.3.3	Why do RL AGN exist?	27
7.3.4	And more	28
8	Conclusions	29
8.1	Messages to all astronomers	29
8.2	Messages to radio astronomers	29
	Abbreviations	29
	References	30



Fig. 1 The radio sky at 4.85 GHz above an optical photograph of the NRAO site in Green Bank, West Virginia (USA). The former 300-foot telescope made this image, which is about 45° across. Increasing radio brightness is indicated by lighter shades to indicate how the sky would appear to someone with a “radio eye” 300 feet (~ 91 metres) in diameter. The flux density limit is ~ 25 mJy (Gregory et al., 1996). Copyright NRAO.

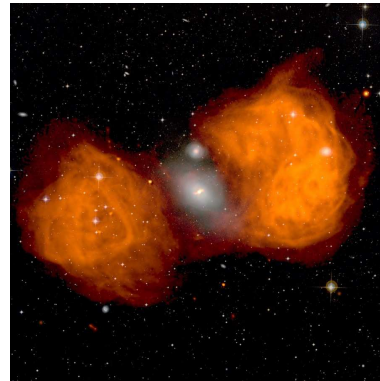
1 Introduction

The radio sky is very different from the optical sky. When we look at the sky with the naked eye, we practically see only stars. These approximate blackbody radiators and therefore their emission covers a relatively narrow range of frequencies, centred at values ranging from the ultraviolet (UV) to the infrared (IR), depending on the star temperature. Therefore, most bright stars are extremely faint at radio frequencies. Figure 1 displays the radio sky as it would appear to someone with a “radio eye” with a diameter equal to that of the former National Radio Astronomy Observatory (NRAO) Green Bank 300-foot radio telescope. Most of the “dots” in the figure, which are unresolved radio sources, are actually distant ($z \approx 0.8$; Condon, 1989) luminous radio galaxies (RGs) and quasars. The very few extended sources are mostly Galactic supernova remnants. Radio emission from RGs and quasars is due to ultra-relativistic ($E \gg m_e c^2$) electrons moving in a magnetic field and thereby emitting synchrotron radiation, which, unlike blackbody emission, can cover a very large range in frequency, reaching ~ 10 decades in some sources.

As one goes fainter by using telescopes, galaxies take over even in the optical sky: for $AB \gtrsim 20 - 22$ mag, depending on the filter, galaxies outnumber stars by a large margin (Windhorst et al., 2011). The Hubble Ultra Deep Field (HUDF), which covers 11 arcmin^2 in four filters (B to z) down to approximately uniform limiting magnitudes



(a) 3C 31



(b) Fornax A

Fig. 2 (a): large scale radio map at 1.4 GHz of 3C 31, showing filamentary plumes extending over 400 kpc from the galaxy. Copyright NRAO 1996. Image from <http://www.cv.nrao.edu/~abridle/images.htm>. (b): Radio emission (orange) associated with the giant elliptical galaxy NGC1316 (centre of the image), consisting of two large radio lobes, each extending over ~ 180 kpc. Image courtesy of NRAO/AUI and J. M. Uson.

$AB \sim 29$ for point sources, contains at least 10,000 objects, almost all of them galaxies (Beckwith et al., 2006). Nevertheless, these galaxies are very different from those seen in the radio “bright”¹ sky. Radio quasars and RGs, in fact, are somewhat rare, atypical, mostly non-thermal sources across the entire electromagnetic spectrum, in which a large fraction of the total emission comes from relativistic jets, that is streams of plasma with speeds getting close to the speed of light, and associated lobes (Fig. 2). Most of the galax-

¹ The standard flux density unit in radio astronomy is the Jansky (Jy), which is equivalent to $10^{-23} \text{ erg cm}^{-2} \text{ s}^{-1} \text{ Hz}^{-1}$. By today’s standards, strong radio sources have $S_r \gtrsim 1$ Jy, intermediate ones have $1 \text{ mJy} \lesssim S_r \lesssim 1$ Jy, while weak radio sources are below the mJy (soon μJy) level.

ies detected in the HUDF, on the other hand, are undergoing episodes of star formation (SF) and therefore are strong thermal emitters.

This review² aims to discuss very recent developments in our understanding of the faint radio sky and how our radio view of the Universe has changed and got much similar to the optical one. By going radio faint one is in fact detecting the bulk of the active galactic nuclei (AGN) population, and not only the small minority of radio quasars and RGs, and also plenty of star-forming galaxies (SFGs). These developments are having (or should have) a strong effect on radio astronomy, but should also change the perception that astronomers working in other bands have of it. One of the main messages of this review, in fact, is that radio astronomy is not a “niche” activity but is extremely relevant also to more classical aspects of extragalactic astronomy, such as star formation and galaxy evolution.

I wrote this review primarily with non radio-astronomers in mind but I believe that some radio astronomers might still be not fully aware of their changing landscape and especially of what is in store for them. Therefore, this review should be useful to all extragalactic astronomers irrespective of their preferred electromagnetic band(s). Stellar astronomers might still find some satisfaction in learning that the faint radio sky is dominated by SF related processes (which is another “take home” message)!

The structure of this review is as follows: Sect. 2 discusses the main astronomical components of the radio sky, while Sect. 3 deals with the radio number counts. In Sect. 4 and 5 I describe the bright and faint radio sky populations respectively, expanding in the latter on source classification, radio number counts by class, luminosity functions (LFs), and evolution. Sect. 6 puts these results into the bigger picture by discussing some astrophysical implications, while Sect. 7 dwells on future prospects by discussing upcoming radio facilities and their astrophysical impact, predictions for deeper radio surveys, and the issue of source classification of very faint ($\lesssim 1 \mu\text{Jy}$) radio sources. Finally, Sect. 8 gives my conclusions and some messages. Throughout this paper, spectral indices are defined by $S_\nu \propto \nu^{-\alpha}$, magnitudes are in the AB system, and the values $H_0 = 70 \text{ km s}^{-1} \text{ Mpc}^{-1}$, $\Omega_m = 0.27$, and $\Omega_\Lambda = 0.73$ have been used. The state of the art of this field until early 2009 is reviewed by de Zotti et al. (2010).

² There was obviously no way I could mention *all* papers dealing with the many topics related to this review, which have appeared in the literature. I have therefore had to make choices and often resorted to the sentence “and references therein”. Moreover, I here deal exclusively with extragalactic sources; see, e.g., Sect. 3.8 of Norris et al. (2013) for a discussion of radio surveys of the Galactic plane.

2 The main components of the radio sky

I describe here the main properties of the sources, which populate the radio sky, namely galaxies (radio and star-forming), radio quasars and blazars, and radio-quiet AGN. These properties are also extremely important for a proper classification of faint radio sources (Sect. 5.1). A recent review of $z < 0.7$ AGN with radio powers³ $P_{1.4\text{GHz}} > 10^{24} \text{ W Hz}^{-1}$ is given by Tadhunter (2016).

2.1 Radio galaxies

Normal galaxies, with GHz radio powers $\lesssim 4 \times 10^{20} \text{ W Hz}^{-1}$, are thought to have their radio emission dominated by synchrotron radiation from interstellar relativistic electrons (Phillips et al., 1996; Sadler et al., 1989). RGs are instead associated with relativistic jets extending well beyond the host galaxy (see Fig. 2), which is typically a giant elliptical. They are characterised by GHz radio powers $\gtrsim 10^{22} \text{ W Hz}^{-1}$ (e.g., Sadler et al., 1989; Ledlow & Owen, 1996), which represents the faint end of the RG LF (e.g., Urry & Padovani, 1995; van Velzen et al., 2012; Capetti & Raiteri, 2015) and, therefore, is a natural threshold for “radio-loudness” in galaxies (some papers have suggested the presence of non-thermal, jet emission in early type galaxies as faint as $10^{20} \text{ W Hz}^{-1}$; e.g., Balmaverde & Capetti, 2006). Fanaroff & Riley (1974) recognized that RGs separate into two distinct luminosity classes, each with its own characteristic radio morphology. High-luminosity Fanaroff-Riley (FR) IIs have radio lobes with prominent hot spots and bright outer edges, while in low-luminosity FR Is the radio emission is more diffuse (Fig. 2). The distinction is fairly sharp at 178 MHz, with FR Is and FR IIs lying below and above, respectively, the fiducial luminosity $P_{178\text{MHz}} \approx 10^{26}/(H_0/70)^2 \text{ W Hz}^{-1}$. This translates to $P_{1.4\text{GHz}} \approx 2 \times 10^{25}/(H_0/70)^2 \text{ W Hz}^{-1}$, with some apparent dependency also on optical luminosity (Ledlow & Owen, 1996), which however appears not to be confirmed by more recent studies (Gendre et al., 2013, and references therein).

RGs are characterised by GHz radio spectra having $\alpha_r \approx 0.7$. This is the signature of extended sources emitting synchrotron radiation at relatively high frequencies where they are optically thin, which implies the existence of fast electrons moving in a magnetic field. Compact sources, instead, have flatter radio spectra, which are attributed to synchrotron self-absorption (Rybicki & Lightman, 2004). More specifically, different parts of the compact region become optically thick at different frequencies, which results in a flattened integrated spectrum over a relatively large range in

³ In this review I use W Hz^{-1} , i.e., power per unit frequency, which is commonly used in radio astronomy. It can be converted to erg s^{-1} at 1.4 GHz (νP_ν), for example, by multiplying by 1.4×10^{16} .

frequency. A spectral index $\alpha_r = 0.5$ divides in a remarkably clean way flat-spectrum/compact sources from steep-spectrum/extended sources (e.g., Massardi et al., 2011). An exception to this rule is provided by compact steep-spectrum (CSS) radio sources. These comprise $\approx 30\%$ of the bright radio source population at a few GHz. Together with GHz peaked-spectrum (GPS), they are generally considered to be young radio sources, which will eventually evolve into large radio objects of the FR I and II type (see O’Dea, 1998; Sadler, 2016, for reviews). Quite a few CSS/GPS sources are quasars.

The optical spectra of RGs are, as a rule, typical of so-called “passive” or “quiescent” galaxies, that is they display the absorption features associated with an old stellar population, with some also revealing powerful high ionization emission lines, and others showing at most weak low-ionization emission lines. There appears to be in fact some other fundamental differences between the two classes of RGs, such as their emission line properties (Hine & Longair, 1979), with FR IIs producing, for the same radio power, 5 – 30 times as much emission line luminosity (Zirbel & Baum, 1995). This has led to the suggestion that this dichotomy might arise from differences in their central engines (e.g., Ghisellini & Celotti, 2001), with jets produced by low accretion rate sources being generally weak and mostly displaying FR I-type structure, and galaxies with higher accretion rates giving rise to stronger, mainly FR II-type jets. The environment appears also to have a role: radio sources in rich clusters have a higher probability of being FR Is, which can be explained by the fact that jets are more easily disrupted in dense environments (e.g., Gendre et al., 2013).

The different accretion rates have also been associated with the excitation mode of the narrow line region gas in the host galaxy (Laing et al., 1994). In low-excitation RGs (LERGs) the accretion on to the black hole is thought to be radiatively inefficient (Chiaberge, Capetti, & Celotti, 1999), while high-excitation RGs (HERGs), are instead linked to radiatively efficient accretion discs of the type discussed by Shakura & Sunyaev (1973). Following Heckman & Best (2014) I will use the terms “jet-mode” and “radiative-mode” for the these two classes, respectively. Note that radiative-mode radio-loud AGN include also (by definition) radio quasars (see below). There is considerable overlap between jet-mode RGs and the radio sources morphologically classified as FR Is and also between radiative-mode RGs and FR IIs, although there is a sizeable population of jet-mode FR IIs and a smaller one of radiative-mode FR I (Gendre et al., 2013, and references therein). The two classes have also widely different Eddington ratios⁴ with radiative-mode and jet-mode sources

typically above and below $L/L_{\text{Edd}} \approx 0.01$ respectively (e.g., Heckman & Best, 2014).

2.2 Radio quasars and blazars

Radio quasars are intrinsically the same sources as some RGs. There is in fact plenty of evidence indicating that they are simply FR II/radiative-mode RGs with their jets at an angle $\lesssim 45^\circ$ w.r.t. the line of sight (Orr & Browne, 1982; Barthel, 1989; Antonucci, 1993; Urry & Padovani, 1995). The fact that radio quasars display strong and Doppler broadened lines in their spectra (with fullwidth half maximum [FWHM] $> 1,000$ km/s), unlike RGs, requires also the presence of dust in a flattened configuration (the so-called “torus”), roughly perpendicular to the jet. Only when we look inside the torus (and roughly down the jet) can we see the broad lines, emitted by clouds moving fast close to the black hole, while for RGs the central nucleus and surrounding material (including the broad line emitting clouds) are obscured by the torus. The latter absorbs radiation along some lines of sight re-emitting it in the IR. This so-called “unification model” explains in a natural way why the (projected) sizes of the jets of RGs are larger than those of quasars (Barthel, 1989). Radio quasars and FR II/radiative-mode RGs can easily reach $P_{1.4\text{GHz}} \approx 10^{27} \text{ W Hz}^{-1}$ locally and $P_{1.4\text{GHz}} \gtrsim 10^{28} \text{ W Hz}^{-1}$ at higher redshifts (e.g., Wall et al., 2005; Padovani et al., 2007).

As regards FR I/jet-mode RGs, obscuration towards their nuclei appears to be much smaller than that of their FR II/radiative-mode relatives (e.g., Chiaberge et al., 2002; Evans et al., 2006), which indicates that a torus might be not present. This applies also to the population of FR II/jet-mode RGs, which cannot be radio quasars seen at large angles (Hardcastle et al., 2006): their weak IR emission, in fact, suggests that, like FR I/jet-mode sources, they also lack a torus (Ogle, Whysong, & Antonucci, 2006). Jet-mode RGs, therefore, irrespective of their radio morphology, are “unified” with BL Lacertae objects (BL Lacs), a class of AGN characterised by very weak, if any, emission lines. BL Lacs, together with flat-spectrum radio quasars (FSRQs), make up the class of blazars. FSRQs are defined by their radio spectral index at a few GHz ($\alpha_r \leq 0.5$), which, as mentioned above, is a sign of their radio compactness. (Steep-spectrum radio quasars [SSRQs], not surprisingly, have $\alpha_r > 0.5$, extended radio emission, and jets that are at angles w.r.t. the line of sight, which are intermediate between FSRQs and FR II/radiative-mode RGs.) Blazars are AGN hosting jets oriented at a very small angle ($\lesssim 15 - 20^\circ$) w.r.t. the line of sight. They have very interesting and somewhat extreme properties, including relativistic beaming, which leads to “Doppler boosting” of their

is balance between radiation pressure (on the electrons) and gravitational force (on the protons).

⁴ The ratio between the observed luminosity and the Eddington luminosity, $L_{\text{Edd}} = 1.3 \times 10^{46} (M/10^8 M_\odot) \text{ erg/s}$, where M_\odot is one solar mass. This is the maximum luminosity a body can achieve when there

flux density (which makes blazars appear more powerful than they really are), superluminal motion, large and rapid variability, and strong, non-thermal emission over the entire electromagnetic spectrum (Urry & Padovani, 1995) and possibly even beyond, into neutrino territory (e.g., Padovani et al., 2015b, 2016). The small angle their jets makes w.r.t. the line of sight implies that blazars are quite rare; nevertheless, given their large flux densities, they are quite common in the bands dominated by non-thermal sources (e.g., radio, sub-mm, and γ -ray). For example, blazars constitute $\sim 51\%$ of the classified sources in the 1 Jy 5 GHz catalogue (Kuehr et al., 1981). Indeed, the first quasar to be discovered, 3C 273 (Schmidt, 1963), is an FSRQ. And of the 2,023 γ -ray sources in the third *Fermi* Large Area Telescope catalogue (3FGL) associated with an astronomical counterpart $\sim 85\%$ of the total, and $\sim 98\%$ of extragalactic sources, are blazars (Acero et al., 2015). I refer the reader interested in the latest developments on blazars and the subtleties of blazar classification to Giommi et al. (2012, 2013); D’Elia et al. (2015) and references therein.

2.3 Radio-quiet AGN

Soon after the discovery of the first quasar, a very strong radio source ($S_{1.4\text{GHz}} \sim 50$ Jy), it was realised that there were many more similar sources, which were undetected by the radio telescopes of the time: they were “radio-quiet” (Sandage, 1965).⁵ These sources were later understood to be only “radio-faint”, as for the same optical power their radio powers were ≈ 3 orders of magnitude smaller than their radio-loud (RL) counterparts, but the name stuck. Radio-quiet (RQ) AGN, which make up the majority ($> 90\%$) of the AGN class, were until recently normally found in optically selected samples and are characterised by relatively low radio-to-optical flux density ratios ($R \lesssim 10$) and radio powers ($P_{1.4\text{GHz}} \lesssim 10^{24}$ W Hz⁻¹ locally; Sect. 5.4).

Innumerable studies have compared the properties of the two AGN classes in various bands to try to shed light on their inherent differences. As a result, the distinction between the two types of AGN has turned out to be not simply a matter of semantics. The two classes represent intrinsically different objects, with RL AGN emitting a *large fraction* of their energy non-thermally and in association with powerful relativistic jets, while the multi-wavelength emission of RQ AGN is *dominated* by thermal emission, directly or indirectly related to the accretion disk⁶.

⁵ Most of the so-called “quasi-stellar galaxies” described by Sandage (1965) actually turned out to be stars (e.g., Kellermann, 2015); but the concept of radio-quiet quasars (i.e., the existence of quasars with much weaker radio emission) proved to be correct.

⁶ The words in italics highlight the presence of a thermal component (the UV bump, due to the accretion disk) in RL quasars and of a hot corona (producing the hard X-ray power law, due to inverse Compton

One of the strongest arguments in support of this statement comes from the hard X-ray – γ -ray bands. It is well established that, while many RL sources emit all the way up to GeV (2.4×10^{23} Hz), and sometimes TeV (2.4×10^{26} Hz), frequencies, RQ AGN have a sharp cut-off at $E_c \gtrsim 50$ KeV reaching $E_c \approx 500$ keV (e.g., Malizia et al., 2014, and references therein, where $F(E) \propto E^{-\Gamma} \exp(-E/E_c)$). While E_c has been measured only in a relatively small number of nearby bright Seyfert galaxies and its determination is non-trivial (given the sensitivity required in the hard X-ray band) such an exponential cut-off *must* be present in the overall RQ AGN population at a few hundred keV in order not to violate the X-ray background above this energy (e.g., Comastri, Gilli, & Hasinger, 2005). Furthermore, as I will discuss in Sect. 6.3, no RQ AGN has so far been detected in γ -rays; this means that, while RQ AGN are actually only radio-weak, they are absolutely γ -ray-quiet⁷. In short, high energy observations do not allow the existence of a single class of AGN!

The host galaxies are also different. Those of RL AGN are bulge-dominated ($L_{\text{bulge}}/L_{\text{host}} > 0.5$), i.e., ellipticals, while for RQ ones the situation is more complicated. Luminous quasars ($M_B \lesssim -24$ or $L_{\text{bol}} \gtrsim 10^{45}$ erg s⁻¹) at low redshifts are mostly hosted by bulge-dominated galaxies (e.g., Dunlop et al., 2003; Hopkins & Hernquist, 2009), while lower luminosity sources cover the full range of morphologies. However, quantitative knowledge of the host properties of bright quasars at $z \gtrsim 0.5$ is still limited. Finally, for many years it has been thought that the optical spectra of the two classes were indistinguishable. This is not true, as long as spectra with high enough signal-to-noise (S/N) ratio and resolution are available (e.g., Zamfir, Sulentic, & Marziani, 2008; Sulentic, Marziani, & Zamfir, 2011, and references therein). I discuss this issue in some detail in Sect. 7.3.3.

As is the case for RL sources, unification applies also to RQ AGN, with Type 2 AGN (e.g., Seyfert 2 galaxies), which show only narrow lines (with FWHM typically $< 1,000$ km s⁻¹), having been unified with Type 1 AGN (e.g., Seyfert 1 galaxies⁸), which display broad lines. The former are then thought to be the same objects as the latter with the central

of the optical/UV photons by high-energy electrons close to the disk in RQ ones.

⁷ At least based on current technology. One cannot exclude a scenario where, for example, the γ -ray flux in RQ AGN scales with S_r and therefore is $\approx 1,000$ times fainter than that of the RL sources detected by *Fermi*. Based on the relative numbers of RQ and RL AGN estimated in Table 1 of Padovani (2011), the RQ AGN contribution to the γ -ray background in this case *might* be non negligible, which would rule out this scenario, as there is no room left for other populations either than blazars, at least above 10 GeV (e.g., Giommi & Padovani, 2015).

⁸ It is generally understood that the distinction at $M_B \sim -23$ used in the past to separate quasars and Seyferts, or stellar and non-stellar (i.e., extended) sources, is not a physical one. In this review I simply consider Seyfert 1’s to be lower luminosity versions of quasars. Nevertheless, this absolute magnitude might still be useful to roughly separate

nucleus obscured by the torus. Netzer (2015) discusses the latest developments for this unified model, while Antonucci (2012) discusses both RL and RQ unifications, with more emphasis on radio sources. RQ radiative-mode sources are the “classical” broad- and narrow-lined AGN (Type 1 and 2), while the jet-mode ones are the so-called LINERs (see Table 4 of Heckman & Best, 2014).

Radio emission in RQ AGN is relatively weak, unlike in RL AGN and RGs, often spread across the host galaxy, and confined to the sub-kpc scale (e.g., Orienti et al., 2015). Most importantly, Seyferts and relatively low redshift RQ quasars follow roughly the far-IR (FIR) – radio correlation (Sect. 2.4) typical of SFGs (e.g., Sopp & Alexander, 1991; Morić et al., 2010; Sargent et al., 2010, see also Sect. 6.2). Furthermore, the FIR flux density in Seyfert galaxies correlates better with the low-resolution kpc-scale radio flux density rather than with the high-resolution pc-scale emission (Thean et al., 2001), which points to a SF origin for the large scale radio emission. This fits with the fact that low-luminosity RQ AGN are usually hosted in late-type galaxies (Sect. 2.4). High resolution studies using very long baseline interferometry (VLBI) imaging, on the other hand, can reveal significant compact radio emission, often variable, sometimes with evidence of weak jets, which can be linked to the central AGN (e.g., Panessa & Giroletti, 2013, and references therein; these studies, until recently, could be carried out mostly for local sources; Sect. 6.2).

Kimball et al. (2011) have carried out sensitive ($S_{6\text{GHz}} \gtrsim 20 \mu\text{Jy}$) Very Large Array (VLA) observations of 179 Sloan Digital Sky Survey (SDSS) quasars ($M_i < -23$) with $0.2 < z < 0.3$ and found a peak in their luminosity distribution at $P_{6\text{GHz}} \approx 3 \times 10^{22} \text{ W Hz}^{-1}$. Their LF suggests that low-redshift, low radio power quasars ($P_{6\text{GHz}} < 10^{23} \text{ W Hz}^{-1}$ or $P_{1.4\text{GHz}} \lesssim 4 \times 10^{23} \text{ W Hz}^{-1}$) are powered primarily by SF and not by the central black hole. These results have been confirmed by Condon et al. (2013) using the NRAO VLA Sky Survey (NVSS) and including also a high redshift ($1.8 < z < 2.5$) sample.

Zakamska et al. (2016) have recently come to the very different conclusion that radio emission for the RQ quasars in their sample, which have $S_r > 1 \text{ mJy}$, $z < 0.8$, $4 \times 10^{21} \lesssim P_{1.4\text{GHz}} \lesssim 7 \times 10^{24} \text{ W Hz}^{-1}$, and $L_{\text{bol}} > 10^{45} \text{ erg s}^{-1}$, is dominated by quasar activity, not by the host galaxy. Their result is based on a comparison between the observed radio power and the value expected if radio emission were due to SF, using L_{FIR} to derive the SF rate (SFR; see Sect. 6.1.1). However, their L_{FIR} is derived from just one photometric point at $70 \mu\text{m}$ or $160 \mu\text{m}$ using average calibrations, which give luminosities correct only within an order of magnitude (Symeonidis et al., 2008). Moreover, their separation in RQ and RL AGN is done by applying a cut at $P_{1.4\text{GHz}} = 7 \times 10^{24}$

W Hz^{-1} , which is on the high side for low-redshift RQ AGN (see, e.g., Padovani, 1993; Padovani et al., 2015a; Tadhunter, 2016, and discussions therein).

It is fair to say that the mechanism responsible for the *bulk* of radio emission in non-local RQ AGN has been a matter of debate for the past fifty years or so, that is since their discovery. In addition, as mentioned above, it is almost certain that more than one process is at play, with contributions from both the central AGN and the host galaxy. I show later on (Sect. 6.2) that deep radio surveys play a big role in sorting out this issue, which in my opinion has been basically solved (at least at low powers).

In summary, the prevailing picture of the physical structure of AGN is inherently axisymmetric and includes a black hole, an accretion disk, which produces optical/UV and soft X-ray radiation, fast moving clouds giving rise to the broad lines observed in AGN spectra, gas, a torus, and slower moving clouds beyond the obscuring material emitting narrower lines. Outflows of energetic particles can occur along the poles of the disk or torus, escaping and forming collimated jets and sometimes giant radio sources when the host galaxy is an elliptical but forming only much weaker radio sources when the host is a gas-rich spiral. This model implies a radically different AGN appearance at different aspect angles. All of the above applies to relatively large accretions rates: for $L/L_{\text{Edd}} \lesssim 0.01$ the disk becomes radiatively much less efficient, the broad lines disappear, as does the evidence/need for a torus (e.g., Heckman & Best, 2014).

2.4 Star-forming galaxies

SFGs can also be relatively strong radio emitters hosted by spiral and irregular galaxies. These star-forming radio sources dominate the local ($z < 0.4$) radio LF below $P_{1.4\text{GHz}} \approx 10^{23} \text{ W Hz}^{-1}$ but reach only $P_{1.4\text{GHz}} \approx 10^{24} \text{ W Hz}^{-1}$ (e.g., Sadler et al., 2002; Mauch & Sadler, 2007), as compared to $P_{1.4\text{GHz}} \approx 10^{27} \text{ W Hz}^{-1}$ for the powerful RGs. As is the case for RGs, SFGs are also characterised by steep GHz radio spectra ($\alpha_r \approx 0.7$) dominated by synchrotron emission, but have also a flat free-free component, which becomes predominant at $\nu \gtrsim 30 \text{ GHz}$ (Condon, 1992). Unlike RGs, however, where the ultimate prime mover is the central black hole, in SFGs synchrotron emission results from relativistic plasma accelerated in supernova remnants associated with massive ($M \gtrsim 8 M_\odot$) SF (Condon, 1992). Radio observations therefore probe very recent ($\lesssim 10^8 \text{ yr}$) SF activity and trace at some level its location as well. This is corroborated by one of the tightest correlations in observational astrophysics, i.e., the FIR – radio correlation. FIR and radio emission are in fact strongly and virtually linearly correlated in a variety of star-forming sources (e.g., Sargent et al., 2010, and references therein) and it is understood that recent SF drives this correlation.

AGN fainter and brighter than the brightest galaxies (e.g., Condon et al., 2013).

As regards their optical spectra, going from RGs to SFGs one moves along the Hubble sequence from ellipticals to spirals and irregulars. This implies several changes in the optical spectra, including a broad rise in the blue continuum and a dramatic increase in the strengths of the nebular emission lines, especially $H\alpha$ (Kennicutt, 1998). All of the above is however redshift dependent: the fraction of SFGs increases rapidly with redshift (e.g., Ilbert et al., 2013) and indeed even RGs at $z \gtrsim 3$ undergo vigorous SF (e.g., Miley & De Breuck, 2008). In other words, at high redshifts most galaxies are forming stars. For example, while SFRs of a few hundred $M_{\odot} \text{ yr}^{-1}$ are very rare in the local Universe and associated with so-called “starburst (SB) galaxies”, at high redshifts sustained SFRs are the norm, which means that the concept of SB is a relative one. We know now, in fact, that the SF activity of a galaxy can occur in two main different modes: a SB mode, probably triggered by major mergers or dense SF regions; and a more normal one, associated with secular processes, which is observed in the majority of the SFGs (Bonzini et al., 2015, and references therein). For this second mode, a tight correlation between a galaxy’s SFR and its stellar mass M_{\star} has been discovered in the past decade (Noeske et al., 2007; Elbaz et al., 2007; Daddi et al., 2007). This is referred to as the “main sequence” (MS) of SFGs and is generally described as a single power law of the form $\text{SFR} \propto M_{\star}^{\beta}$ with $\beta \sim 0.4 - 1$ (depending on the sample). The slope of the correlation is approximately constant but the normalization increases by about a factor of 20 from the local Universe to $z \sim 2$ (Renzini & Peng, 2015, and references therein).

A more modern definition of SFGs is therefore redshift dependent and denotes galaxies, which belong to the MS, with SB and passive galaxies being significantly above and below, respectively. That is, what is relevant is not the absolute value of the SFR but its relative value compared to the MS.

2.5 FR 0 radio galaxies

There is a relatively new entry in the radio sky: FR 0 RGs⁹! It turns out that $\sim 80\%$ of RGs in a SDSS/NVSS sample having $S_{1.4\text{GHz}} > 5 \text{ mJy}$ and $z \lesssim 0.3$ are unresolved or barely resolved at a radio resolution of 5 arcseconds (Baldi & Capetti, 2010): so no extended emission and therefore no FR I/II division possible. The AGN power estimated from optical line or core radio luminosities is at the same level of classical FR Is but the sample shows a deficit of a factor ~ 100 in extended radio power. Furthermore, $\sim 70\%$ of the local population of RGs at 20 GHz studied by Sadler et al. (2014) have also been classified as FR 0 since their $\sim 1 \text{ GHz}$

emission is unresolved in the NVSS and Sydney University Molonglo Sky Survey (SUMSS) images.

Despite being called with the same name, I think there are some important differences between the two samples. The 20 GHz sample, being selected at high frequencies, is biased towards flat spectrum sources (blazars and GPS; Sect. 3.2); and indeed $\sim 61\%$ of the FR 0s are candidate CSS/GPS sources, with 6–40% of those being possible blazars. Moreover, a good fraction of the radiative-mode FR 0s, which in the 20 GHz sample are mostly hosted in late-type galaxies and make up $\sim 25\%$ of the class, are very likely to be RQ AGN. This is because, as discussed above, in these sources radio emission is very often confined to the host galaxy, and therefore not very extended, but at the same time there can be compact cores, which would be detected at high frequencies. Indeed, 4/12 of the FR 0s studied by Baldi, Capetti, & Giovannini (2015) are RQ AGN and Table 8 of Sadler et al. (2014), which lists the 13 spiral galaxies with $z \leq 0.025$ in their sample, includes many RQ AGN. The remaining 20 GHz jet-mode FR 0s, which are not candidate CSS/GPS ($\sim 33\%$), are very likely to be bona-fide RGs without the extended emission typically associated with FR Is and IIs.

Some of the FR 0 “RGs” could also be low-redshift blazars misclassified as RGs by current classification schemes because their non-thermal radiation is not strong enough to dilute the host galaxy component even in the Ca H&K break region of the optical spectrum (see Giommi et al., 2012, 2013, for more details). In other words, they would look like LERGs in the optical band and like sources more core-dominated than classical FR Is in the radio band, fitting the FR 0 definition. A study of the spectral energy distributions (SEDs) of FR 0s from the radio to the high-energy bands would easily pick out these sources, as their SEDs should be more blazar- than RG-like.

To summarize, the study of FR 0 RGs is still in its infancy but it looks like this class could be quite heterogeneous. If it will be confirmed that the large majority of RGs are true FR 0s, i.e., they look like jet-mode FR Is without the extended radio emission, we will need to figure out why this is the case and what this means, for example, for unified schemes of RL sources.

3 Radio number counts

3.1 Number count basics

The simplest thing one can do when studying a flux-limited sample of astronomical sources is to count them. This requires no additional data but nevertheless number counts provide very useful information, as their shape is tightly related to the evolutionary properties of the sources and also to the geometry of the Universe (since the volume is not simply $\propto D^3$ but also depends on the curvature). This is illustrated

⁹ This name was first used by Ghisellini (2010).

by the following equation, which gives the differential number counts (i.e., the number of objects per flux density per steradian):

$$\frac{n(S)}{4\pi} = \frac{c}{H_0} \int_{z_{\min}(S)}^{z_{\max}(S)} \frac{\Phi[P(S, z), z] D_L^4(z) dz}{(1+z)^{(3-\alpha)} \sqrt{(1+z)^2(1+\Omega_m z) - z(z+2)\Omega_\Lambda}}, \quad (1)$$

where c is the speed of light, $\Phi(P, z)$ is the redshift dependent LF (number of sources per unit power per unit comoving volume), $D_L(z)$ is the luminosity distance, and $z_{\min}(S)$ and $z_{\max}(S)$ represent the flux density dependent redshift range over which the integration is carried out. Eq. 1 shows how the cosmological model (through H_0 , Ω_m , Ω_Λ , and $D_L(z)$) and the shape and evolution of the LF play a role in building the number counts. One can parametrize the LF evolution in a simple way by writing (e.g., de Zotti et al., 2010)¹⁰:

$$\Phi(P, z) = \Phi(P/f_L(z), z=0) f_D(z)/f_L(z), \quad (2)$$

which allows for changes in both power and number. The two extreme cases are: 1. $f_D(z) = 1$, which means that the comoving number density is constant and $P(z) = P_0 f_L(z)$, the so-called pure luminosity evolution (PLE) case; 2. $f_L(z) = 1$, which implies a constant power and a density evolution $\Phi(z) = \Phi_0 f_D(z)$, the so-called pure density evolution (PDE) case. In more complex cases both f_D and f_L can also have a dependence on power. One normally talks about “positive” or “negative” evolution if $f(z) > 1$ or < 1 respectively, meaning that, in the first case, for example, the power or the number density was larger at higher redshifts¹¹.

Radio astronomers plot their differential number counts normalized by the counts expected in a static Euclidean Universe¹², $n_E(S) \propto S^{-5/2}$, by displaying the quantity $S^{5/2} n(S)$.

Figure 3 shows an example of Euclidean normalized 1.4 GHz source counts under different evolutionary assumptions. For simplicity (and based on real data: see Sect. 5.5) I have taken the case of a PLE, with $P(z) = P_0(1+z)^k$, up to $z = 2$ (and constant thereafter). I have considered three cases: $P(z) \propto (1+z)^{2.5}$ (positive evolution [$k > 0$]; solid red line), no evolution ($k = 0$; dashed green line), and $\propto (1+z)^{-2.5}$ (negative evolution [$k < 0$]; dotted blue line). The local LF for SFGs of Mauch & Sadler (2007) has been adopted, and $\alpha_r = 0.7$ was assumed.

Figure 3 shows the following: 1. the counts are Euclidean and evolution independent only at large flux densities ($S \gtrsim$

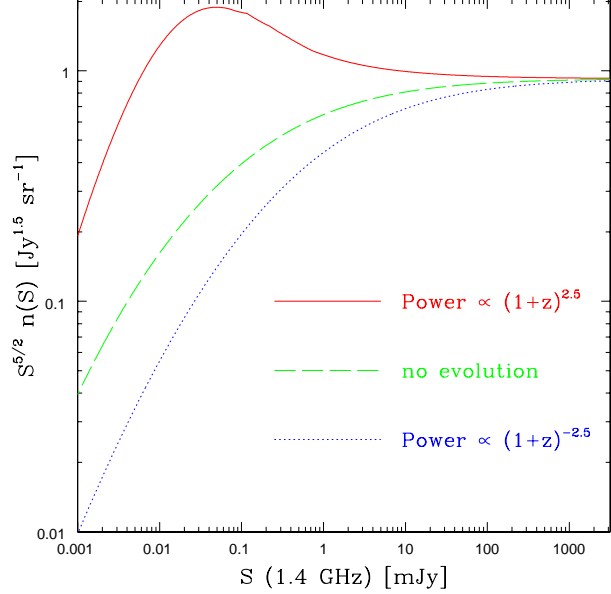


Fig. 3 Euclidean normalized 1.4 GHz source counts derived for different luminosity evolutions up to $z = 2$ (and constant thereafter): $\propto (1+z)^{2.5}$ (solid red line), no evolution (dashed green line), and $\propto (1+z)^{-2.5}$ (dotted blue line). The local LF is that of Mauch & Sadler (2007); $\alpha_r = 0.7$ was assumed.

0.1 Jy in this example); 2. at fainter flux densities the geometry of the Universe starts to have an effect, as clearly visible for the no-evolution case, which soon diverges from the Euclidean one; 3. strong positive evolution manages to counterbalance this, at least down to ~ 0.1 mJy¹³, while negative evolution makes this effect more prominent. In short, once the cosmological model and spectral index are fixed, the number counts are strongly dependent on source evolution, but not only: the same counts, in fact, can be obtained by different combinations of (local) LF and evolution.

3.2 Observed radio number counts and their complications

Figure 4 shows the observed Euclidean normalized 1.4 GHz source counts based on a variety of surveys, which reach $\sim 15 \mu\text{Jy}$. Based on Fig. 3, we can immediately infer the following: 1. strong radio sources have a pronounced positive evolution; 2. their LF is shifted to much higher powers (\approx three orders of magnitude assuming similar evolutions) as compared to the SFG LF used in Fig. 3, since the counts peak at a much larger flux density; 3. below ~ 1 mJy a new population is very likely to make its appearance, as the counts show a marked flattening¹⁴, which one does not

¹⁰ This equation differs from eq. 11 in de Zotti et al. (2010) by a factor $1/f_L(z)$, since they define their LFs as $\Phi(\log P)$; see Sect. 5.4.

¹¹ In terms of cosmic time, rather than redshift, it should be the other way around. Nevertheless, this is how these terms are generally used.

¹² These can be simply derived under the assumption of a uniform distribution of sources and Euclidean space since the number of sources is $\propto D^3 \equiv (L/4\pi S)^{3/2}$. The integral counts, that is the number of objects seen on the sky with flux density $> S$ will then be $n(\geq S) \propto S^{-3/2}$, which translates into differential counts $n(S) \propto S^{-5/2}$.

¹³ This value depends on the LF, the assumed evolution, and on the redshift at which evolution stops.

¹⁴ This is true only for the Euclidean normalized counts: the differential counts actually steepen.

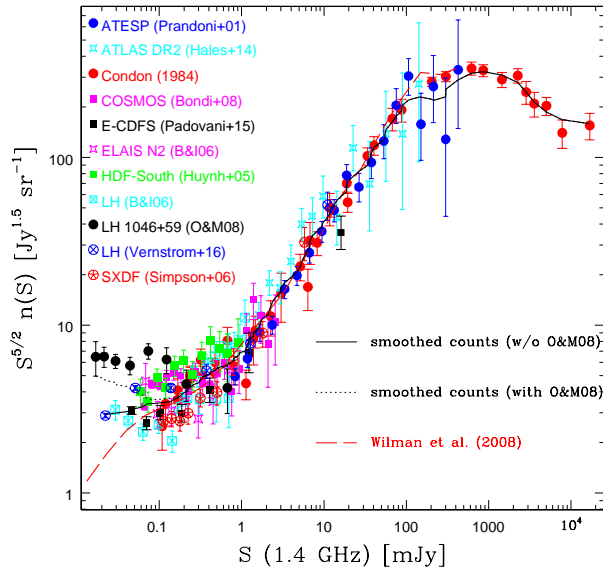


Fig. 4 The Euclidean normalized 1.4 GHz source counts derived from various surveys, as indicated in the legend: Prandoni et al. (2001), Hales et al. (2014b), Condon (1984), Bondi et al. (2008), Padovani et al. (2015a), Biggs & Ivison (2006) (LH stands for Lockman Hole), Huynh et al. (2005), Owen & Morrison (2008), Vernstrom et al. (2016) (converted from 3 GHz assuming $\alpha_r = 0.7$), Simpson et al. (2006). The solid and dotted black lines are a smoothed version of the counts respectively excluding and including the Owen & Morrison (2008) sample. The red dashed line represents the simulated number counts from the SKA Design Study (SKADS; Wilman et al., 2008). See Smolčić et al. (2015) for even more survey data points. Most data and the SKADS counts courtesy of Isabella Prandoni.

expect for normal, well-behaved LFs; 4. below ~ 1 mJy, however, the observed source counts appear also less well constrained with a scatter between different surveys, which can reach a factor of ≈ 3 . I defer discussions of points 1 – 3 to Sect. 5 and elaborate here somewhat on point 4¹⁵.

Undoubtedly, some fraction of the scatter at faint radio flux densities may be due to cosmic variance¹⁶. Nevertheless, this cannot be the full story: for example, in the X-ray band, the scatter between the (integral) number counts in the Great Observatories Origins Deep Survey (GOODS) North and South fields, which cover ~ 0.1 deg², is only $\sim 25\%$ at the faintest fluxes ($\approx 3\sigma$), fully consistent with small field-to-field variations (Luo et al., 2008). Published deep radio source counts, on the other hand, are widely discrepant, even

when made with the same instrument, and even with different researchers using the same instrument in the same field (Condon et al., 2012)! The central problem in understanding radio source counts is the proper balance between source confusion at lower resolution (many faint sources crowding into a single beam) and missing lower surface brightness sources or underestimating flux densities at high resolution (i.e., resolving them out). These issues, while better understood than in the 1950s (see below), still exist today. There is no “correct” resolution that avoids confusion and resolving out sources, but there is an optimum resolution depending on the areal density of sources. As discussed by Norris et al. (2013), some of the largest differences between the various surveys can also be accounted for by different ways of handling many necessary corrections for effects such as, to name a few: clean bias, Eddington bias, and completeness corrections, together with imaging errors such as excessive deconvolution, bandwidth smearing, and insufficient beam sampling in the image plane. Furthermore, some authors measure the number of radio components, while others measure the number of sources, each of which may consist of several components, the numbers of which in turn may vary as a function of flux density. Resolving these discrepancies is quite critical (but difficult), since this scatter introduces uncertainties in the comparison of observed number counts with detailed, model-based predictions.

I have concentrated on number counts around a few GHz because this is where at present we can reach fainter flux densities. Angular resolution scales with λ , therefore low-frequencies are penalized in this respect. The beam solid angle of a radio telescope scales as ν^{-2} and system noise generally increases with frequency, so the time needed to survey a fixed area of sky to a given limit rises very rapidly at higher frequencies. For example, the deepest image at 150 MHz recently obtained with the Low Frequency ARray (LOFAR) goes down to ~ 0.7 mJy (Williams et al., 2016) (see also vanWeeren et al., 2014, for a deep 62 MHz field), equivalent to $S_{1.4\text{GHz}} \sim 0.15$ mJy (assuming $\alpha_r = 0.7$), while the deepest 15.7 GHz survey reaches 0.1 mJy (Whittam et al., 2016), which corresponds to $S_{1.4\text{GHz}} \sim 0.1 - 0.5$ mJy (for $\alpha_r = 0 - 0.7$, where the first value is more appropriate for flat spectrum cores). These values are $\gtrsim 10$ times larger than the faintest 1.4 GHz flux density limit. It would be good to reach depths comparable to the \sim GHz surveys at lower and higher frequencies to further constrain the number counts and get different and complementary views on radio sources. Steep synchrotron spectra objects, i.e., SFGs and RGs, are better detected at low frequencies, since their flux densities increase rapidly $\propto \nu^{-\alpha_r}$. High frequency surveys, on the other hand, will be by default more biased towards flat spectrum sources i.e., blazars and quasars in general (e.g., Giommi et al., 2009; Mahony et al., 2011; Whittam et al., 2015). This also explains why, despite reaching similar equivalent 1.4

¹⁵ The subject of the “proper” estimation of radio number counts is a very complicated one, fraught with many issues, which go beyond the main scope (and length) of this review (see, for example, Condon et al., 2012; Hales et al., 2014a; Padovani et al., 2015a). Here I briefly touch upon it.

¹⁶ This is the uncertainty in observational estimates of extragalactic objects arising from the underlying large-scale density fluctuations, which is often significant, especially in deep surveys, which tend to cover relatively small areas.

GHz flux densities, the 150 MHz normalized counts display a flattening below 10 mJy ($S_{1.4\text{GHz}} \sim 2$ mJy) while the 15.7 GHz ones do not (see Sect. 5).

In closing this section, I would like to stress the relevance radio number counts have had for cosmology and the Steady-State vs. Big Bang debate. It was in fact the steepness of the earliest radio source counts, which gave the first indications of cosmic evolution (Ryle & Scheuer, 1955, see Fig. 3) but these same results led to the Sidney-Cambridge controversy¹⁷ in the 1950s over the nature of radio sources and their role in cosmology (Mills, Slee, & Hill, 1958), which revolved around understanding source confusion. Note that this was well before the discovery of quasars in 1963! Sadly, as stated by McCrea in Sullivan (1984) “In retrospect, in spite of the confusing side issues, from about 1955 cosmologists would have been safe in accepting that radio astronomy had shown the actual Universe to be not in a steady state. Instead, they waited until a decade later when the discovery of the microwave background had confirmed a positive prediction of big-bang cosmology”.

4 The bright radio sky population

The study of the radio sky goes all the way back to the end of the 1940s, when Bolton, Stanley, & Slee (1949) identified three of the strongest radio sources in the sky, namely Taurus A¹⁸, Virgo A, and Centaurus A. Bolton et al. associated Taurus A with the Crab Nebula, already known to be the expanding shell of SN 1054. They also correctly identified the other two sources with M 87 and NGC 5128 (both FR Is) but, realizing that, were they extragalactic their radio power would be enormous (for the time), they concluded that if the identifications were correct it would imply that M 87 and NGC 5128 had to be within our own Galaxy. Bolton later explained that he understood the true nature of the two sources “but that he was concerned that a conservative Nature referee might hold up publication” (Kellermann, 2015)! By the mid 1950s, however, many RGs were identified with optical counterparts and most high Galactic latitude sources were recognized to be extragalactic with radio powers $\approx 10^7 - 10^{10}$ times larger than that of the Crab Nebula (e.g., 8×10^{42} erg s⁻¹, i.e., $\approx 10^{27}$ W Hz⁻¹ at 100 MHz in the case of Cygnus A: Baade & Minkowski, 1954).

The bright radio sky turned out to be made up almost exclusively of RGs and radio quasars. For example, the second revision of the Third Cambridge Catalogue of Radio Sources (3CRR) (Laing, Riley, & Longair, 1983), which includes all objects with $S_{178\text{MHz}} \geq 10$ Jy, $\delta \geq +10^\circ$, and $|b_{\text{II}}| \geq 10^\circ$,

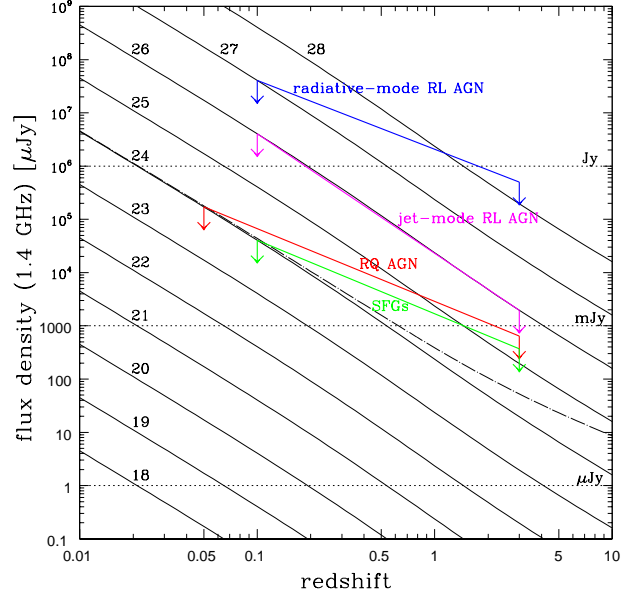


Fig. 5 Flux density at 1.4 GHz vs. redshift for various radio powers (in units of $\log W \text{ Hz}^{-1}$) assuming $\alpha_r = 0.7$ (solid lines). For $P_{1.4\text{GHz}} = 10^{24} \text{ W Hz}^{-1}$ the case $\alpha_r = 0$ is also shown (dot-dashed line). The flux density values corresponding to the maximum radio powers for various classes at $z \sim 0.05 - 0.1$ and $z \sim 3$ are also shown, as detailed in the text. The dotted horizontal lines indicate the 1 μJy , 1 mJy and 1 Jy flux densities.

contains only RGs and RL quasars. And out of the 527 1 Jy 5 GHz sources (Kuehr et al., 1981) only two, NGC 1068 (a Seyfert 2) and M 82 (a starburst), both at very low redshift ($z \leq 0.004$), do not belong to the RG, radio quasar, or blazar classes.

The reason why this is the case is shown graphically in Fig. 5, which plots the 1.4 GHz flux density vs. redshift for a range of radio powers assuming $\alpha_r = 0.7$ (solid lines; for $P_{1.4\text{GHz}} = 10^{24} \text{ W Hz}^{-1}$ the case $\alpha_r = 0$ is also illustrated). It also shows the flux density values corresponding to the maximum radio powers for radiative-mode and jet-mode RL AGN (blue and magenta lines), RQ AGN (red line), and SFGs (green line) at $z \sim 0.05 - 0.1$ and $z \sim 3$ ¹⁹. Figure 5 gives a simple, order of magnitude, picture of the largest flux densities reached by the classes of sources, which populate the radio sky. The average luminosities, being generally close to the break in the LF, and the related more typical flux densities, are much smaller than the maximum ones.

Figure 5 shows the obvious dimming due to the dependence on the inverse square of the luminosity distance, which can be partly offset by luminosity evolution (and some k-corrections). The most important, less trivial, message, is

¹⁷ The interested reader can find a detailed account of this controversy in Sullivan (1984).

¹⁸ In those early days radio sources were named after the constellation in which they appeared followed by a letter. Thus, Taurus A was the first object discovered in the Taurus constellation.

¹⁹ The local maximum powers are from Best et al. (2014) (radiative- and jet-mode RL AGN), Padovani et al. (2015a) (RQ AGN), and Mauch & Sadler (2007) (SFGs). The values at $z \sim 3$ have been estimated by using luminosity evolution models from Urry & Padovani (1995); Padovani et al. (2015a), and Padovani et al., in preparation

that different classes will cover widely different ranges of flux densities, with RL AGN being essentially the only “inhabitants” of the (GHz) $\gtrsim 10 - 100$ mJy sky, apart from SFGs and RQ AGN at very low redshift ($z \lesssim 0.02$), as indeed observed. I now move to the focus of this review, that is the faint radio sky.

5 The faint radio sky population

A turning point in the study of the radio sky was the realisation around 1984 that the Euclidean normalized 1.4 and 5 GHz source counts exhibited a significant flattening below ≈ 1 mJy (Condon & Mitchell, 1984; Fomalont et al., 1984; Windhorst, van Heerde, & Katgert, 1984). Furthermore, Windhorst et al. (1985), based on optical identifications available for less than half of the sample, suggested that “for $1 < S_{1.4} < 10$ mJy a blue radio galaxy population becomes increasingly important; these often have peculiar optical morphology indicative of interacting or merging galaxies”. To really understand which sources were responsible for the flattening and sort out the source population of the $\lesssim 1$ mJy radio sky took more than thirty years. I discuss why next.

5.1 Source classification

A problem common to all astronomical surveys is that of the classification of sources. After having detected them, in fact, one wants to figure out what they are, which is vital to extract astrophysical information. This requires a determination of the redshift, without which the emitted power cannot be calculated, which is still mostly done through optical/near-IR (NIR) spectroscopy²⁰.

In the past, when surveys were much shallower, optical counterparts were relatively bright but telescopes were also smaller than they are today, so one might think that the complexity of the problem has not changed much²¹. To put things into perspective, the median R_{mag} for the Extended *Chandra Deep Field-South* (E-CDFS) VLA sample, which reaches $S_{1.4\text{GHz}} \sim 32.5$ μJy , is ~ 23 ; and this refers only to sources detected in the *R* band, as $\sim 20\%$ of the objects have only an IR counterpart (Bonzini et al., 2012). Getting spectra for such faint sources is very time consuming (prohibitively so for the very faint tail) but can in principle be done. Even if we had optical spectra for all the E-CDFS sources, though,

this would not help us much as often for faint counterparts one can only see a couple of lines. This is enough to get a redshift but not to properly classify the object, as illustrated in Fig. 6, which shows examples of E-CDFS spectra of (from top to bottom) a SFG, a RQ, and a RL AGN having redshifts and magnitudes typical of the sample. And finally, optical based classification is well known to be prone to obscuration biases (see below).

If one adds to all of the above the fact that the faint radio sky is a quite heterogeneous mix (Sect. 2), then the business of source classification turns out to be quite a complex endeavour. I summarize here the main indicators used to classify faint radio sources ranked in *rough* order of practical effectiveness²². These stem from the properties of radio sources as sketched in Sect. 2. I stress that indicators can be ranked low either because they are intrinsically weaker than others or not as sensitive (at least for now).

1. **FIR – radio correlation.** This correlation has been discussed in Sects. 2.3 and 2.4 and is usually parametrized through the so-called q parameter, that is the logarithm of the FIR ($8 - 1,000$ μm) to radio flux density (Helou, Soifer, & Rowan-Robinson, 1985). Even with *Herschel*, which covers the $\sim 55 - 670$ μm range, one needs some extrapolation through templates to estimate the full FIR flux density. However, quite often the total FIR emission cannot be reliably derived because of lack of data at long wavelengths. Therefore q_X is used, where X can be, for example, 24 μm or 70 μm (the longer the wavelength, the better, to decrease the contribution from AGN heated dust [the torus]). Different papers have used the observed or rest-frame q to define a locus, or sometimes a dividing value, to differentiate between sources following the FIR – radio correlation and those which do not. The latter display a “radio excess”, which is characteristic of RL AGN. (Note that a RQ AGN with core radio flux density larger than the extended SF flux density will also have a slight radio excess: Sect. 6.2. It therefore matters where one draws the line.)
2. **X-ray power.** Only AGN can have hard X-ray power ($2 - 10$ keV) $L_X \gtrsim 10^{42}$ erg s⁻¹ (see Szokoly et al., 2004, and references therein). This does not mean that there are *no* AGN below this value, far from it: 1. $\sim 78\%$ of the RL AGN in Padovani et al. (2015a) have $L_X < 10^{42}$ erg s⁻¹; 2. and $\sim 6\%$ of RQ AGN with X-ray detection in the same paper are also below this cut. The first point is simply due to the fact that jet-mode AGN (which make up the majority of the E-CDFS RL sub-sample: see Sect. 5.4.2) are not very strong X-ray emitters, while the second one is related to the (known) existence of

²⁰ The Atacama Large Millimeter/submillimeter Array (ALMA) can also determine redshifts of, for example, SFGs through their molecular emission lines at millimetre wavelengths (e.g., Weiß et al., 2013).

²¹ I thought that for modern radio surveys things have become more complex than they used to be but after chatting with Robert Laing, who played a big role in the optical identification of the 3CRR (Laing, Riley, & Longair, 1983), I am not so sure!

²² What follows below is an evolved and expanded version of Sect. 3 of Bonzini et al. (2013). The ranking order was mainly determined by looking at how many sources had their classification changed by a given indicator after the first three were applied to the E-CDFS sample.

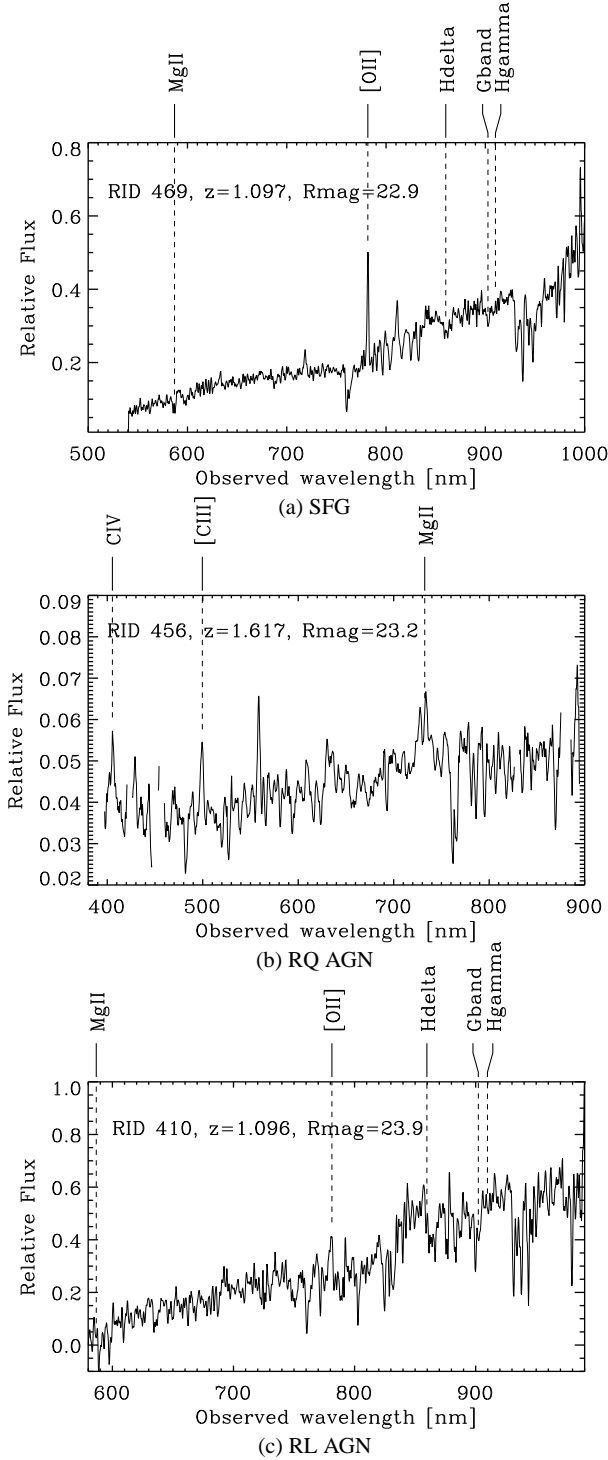


Fig. 6 Examples of E-CDFS spectra of (from top to bottom) a SFG, a RQ, and a RL AGN having redshifts and magnitudes typical of the sample (and $44 \leq S_{1.4\text{GHz}} \leq 75 \mu\text{Jy}$). The SFG is bluer than the RL AGN but redder than the RQ one. The latter displays broad lines but its radio-quietness cannot be established from its spectrum (see Table 5 of Bonzini et al., 2012, and references therein).

low-power radiative mode AGN. Note that this indicator comes from the X-ray band, where (so far) the fraction of jet-mode AGN is small.

3. **IRAC colour - colour diagram.** Different extragalactic sources occupy somewhat different regions of parameter space in *Spitzer* Infrared Array Camera (IRAC) colour - colour diagrams. One version of these plots the ratio $S_{8.0}/S_{4.5}$ versus $S_{5.8}/S_{3.6}$, where the flux densities refer to all four IRAC channels at 3.6, 4.5, 5.8, and 8.0 μm (Donley et al., 2012, and references therein). Quasars (RL and RQ) produce a power-law continuum across these bands, which makes them occupy a specific locus. The completeness of this selection method is therefore high ($\sim 75\%$) at $L_x \geq 10^{44} \text{ erg s}^{-1}$ but relatively low ($\lesssim 20\%$) for $L_x \leq 10^{43} \text{ erg s}^{-1}$. IRAC selection appears also to be incomplete to RGs (Donley et al., 2012). Nevertheless, mid-IR (MIR) selection is very important since it identifies also heavily obscured AGN, many of which are missed even by deep X-ray surveys (Donley et al., 2012).
4. **X-ray spectrum and variability.** Intrinsic X-ray absorption, the presence of a K-shell Fe line at 6.4 keV, and X-ray variability also discriminate between AGN and SFGs (e.g., Vattakunnel et al., 2012, and references therein). These indicators are of a higher order compared to the “simple” flux needed to derive L_x and therefore require a better S/N ratio.
5. **Other radio indicators.**

Radio spectrum. As discussed in Sect. 2.2 and 2.4, SFGs (but also RGs) have steep GHz radio spectra ($\alpha_r \approx 0.7$), while flatter spectra are typical of the compact core emission associated with AGN. An inverted ($\alpha_r < 0$) radio spectrum therefore excludes a SFG but could be equally associated with a RL or RQ AGN.

Radio morphology. The presence of a bright, compact core or clear radio jets/lobes suggests the presence of an AGN. Extended emission on $\sim \text{kpc}$ scales with no obvious peaks or jets/lobes is more likely to originate from SF, which however could also come from the host galaxy of a RQ AGN. This indicator requires resolutions $\lesssim 1 \text{ arcsecond}$ (e.g., Richards et al., 2007).

Radio power. As amply discussed above, RGs and radio quasars are more powerful than RQ AGN and SFGs. Nevertheless, while it might be safe to assume that anything above $P_{1.4\text{GHz}} \approx 10^{24} \text{ W Hz}^{-1}$ has nothing to do with SF, this is only valid at low redshifts given the strong evolution of SFGs (see Fig. 5 and Sect. 5.5). Additionally, such luminous sources are rare and more normal, lower power radio sources can equally be associated with jet-mode RGs, RQ AGN, or SFGs.

6. **Optical indicators.**

Optical spectra. The presence of broad or high-excitation emission lines in optical spectra indicates AGN

activity: after all, this how quasars were discovered. Nevertheless, in modern radio surveys many sources are too faint to get even a spectrum decent enough to determine a redshift. For example, only in $\sim 40\%$ of the sources with redshift information in Padovani et al. (2015a) is the redshift spectroscopic, being photometric in the remaining ones.

BPT diagrams. These use emission line ratios to distinguish galaxies dominated by various photoionization processes, in particular to separate SFGs from AGN (they are named after the three authors of Baldwin, Phillips, & Terlevich, 1981). While until recently these could only be applied at $z \lesssim 0.3$, Kewley et al. (2013) has presented a new diagnostic, which can be used up to $z \sim 3.5$. Good enough optical spectra are however still required.

As a rule, optical-only indicators are then useful solely for relatively bright sources and therefore at relatively low redshifts. However, it is also important to remember that the optical band does not give the full story, being strongly affected by absorption and/or dilution by the host galaxy. For example, there are many cases of sources, which show no sign of nuclear activity in their optical spectra but are strong ($L_x \gtrsim 10^{43} \text{ erg s}^{-1}$) X-ray sources (e.g., Smith, Koss, & Mushotzky, 2014, and references therein). And the identification of low accretion ($L/L_{\text{Edd}} \lesssim 0.01$) AGN will be heavily affected by the properties of their host (Hopkins et al., 2009).

7. **VLBI detection.** VLBI detections of high-luminosity radio cores ($\gg 2 \times 10^{21} \text{ W Hz}^{-1}$) are almost certainly AGN related, whereas lower-luminosity cores may be caused either by AGN or by supernova activity (Middelberg et al., 2011, and references therein). This is a clear cut AGN indicator but its application is hampered by the still limited sensitivity of VLBI observations and for the same reason until recently worked mostly for RL AGN (Bonzini et al., 2013, but see Sect. 6.2).
8. **Radio polarization.** Polarized GHz radio emission is supposed to originate mostly from the jets or lobes of extended AGN²³, where coherent large scale magnetic fields are likely to be present (e.g., Hales et al., 2014b, and references therein). As such, this indicator should single out RGs. Indeed, the number counts of RL AGN in Padovani et al. (2015a) are fully consistent (that is, somewhat above) the surface density of polarized sources derived by Hales et al. (2014b), assuming a typical fractional polarization of 4%. Again, this indicator is of a higher order compared to simply measuring a radio flux density, so polarization observations are less sensitive.
9. **$D_{4000} - P_{1.4\text{GHz}}/M_\star$ plane.** Best et al. (2005a) used the location of sources on the $D_{4000} - P_{1.4\text{GHz}}/M_\star$ plane, where D_{4000} is the strength of the 4,000 Å break (a proxy

for the mean stellar age of a galaxy) to separate SFGs from RL AGN. As for the FIR – radio correlation, this method singles out “radio excess” sources, that is RL AGN. However, at variance with the former, it works only at low redshifts (or requires IR spectra at high redshifts), needs detailed modelling to get the stellar mass, and suffers from the relatively large uncertainties associated with the D_{4000} technique (Ellison et al., 2016).

10. **R value.** The radio-to-optical flux density ratio has been proposed as an indicator of radio-loudness by Schmidt (1970) and a value ~ 10 has been long used since the seminal paper by Kellermann et al. (1989). As discussed by Padovani et al. (2011), this definition is totally insufficient to identify RQ AGN when dealing with a sample, which includes also SFGs and RGs, as both classes are or can be (respectively) characterized by low R values (see Fig. 4 of Bonzini et al., 2013). R was in fact defined for quasar (broad-lined) samples, where it could be assumed that the optical flux was related to the accretion disk, but loses its meaning as an indicator of jet strength if the optical band is dominated by the host galaxy, as is the case for jet-mode RGs. This indicator is mentioned here for historical reasons but does not have much value for the classification of faint radio sources (although a high R does indicate a RL AGN).

In short, to classify faint radio sources one first selects RL AGN using a variant of the IR – radio correlation, then separates the RQ AGN from SFGs using L_x . The IRAC diagram is then used to recover (RQ) AGN missed by the X-ray criterion. Finally, other indicators are applied to catch possible outliers²⁴. Padovani et al. (2011) have also shown that, by applying mainly the first three criteria discussed here to representative, well-known local sources, the correct classification is always recovered.

Table 1 summarizes the role of all indicators, where a “Y” indicates the class(es) for which the relevant indicator is useful and a “~Y” denotes “limited” applicability (e.g., the optical indicator for AGN). SF sources include objects dominated by SF processes in the band under consideration (e.g., those following the FIR – radio correlation).

So far I implicitly assumed that objects can be classified one way or the other. I often see the term “hybrid sources” used in the literature to describe objects having both AGN and SFG features. I find this term somewhat confusing: RQ AGN are often hosted in SF galaxies and therefore black hole and SF related processes are both going to play a role in these sources. Nevertheless, the black hole is the prime driver, which is what we should be interested in. So a RQ

²³ Blazar cores are also polarized, but blazars are relatively rare in the faint radio sky.

²⁴ I have made this sound easy but reality is, as usual, more complex. The reader should consult Sect. 3 of Bonzini et al. (2013) to get a feeling for the many subtleties and possible complications. In particular, not all radio sources are X-ray detected even in the deepest fields.

Table 1 Effectiveness of faint radio source classifiers.

Indicator	AGN		SF sources
	RL	RQ	
FIR - radio correlation	Y		Y
L_x	~Y	Y	
IRAC diagram		~Y	
X-ray spectrum and variability		Y	
other radio		Y	
optical		~Y	~Y
VLBI detection		Y	
radio polarization	Y		
$D_{4000} - P_{1.4\text{GHz}}/M_\star$ plane	~Y		~Y

AGN with its radio emission produced by supernova remnants is still an AGN, not a “hybrid”.

I have spent quite some time on the classification of faint radio sources for two reasons: 1. there appears to be some confusion in the literature on this topic; 2. it is extremely relevant for the classification of the even fainter radio sources, which will be detected in the near future (Sect. 7.2.2).

5.2 The importance of selection effects

Even if the classification problem is complex, it appears nevertheless to be solvable. However, not all indicators discussed above have been available since 1984. And those which were, gave only a biased view.

Optical classification of a sample always starts with the brightest sources, which are obviously easier to observe. This gives rise to a strong selection effect: as shown by Fig. 1 of Padovani et al. (2009), an optical magnitude cut in a radio flux-limited sample produces a bias against sources with large R values, i.e., RL AGN. The fraction of blue, SF sources, therefore, appears artificially increased. Only $\sim 44\%$ of the 93 radio sources forming a complete sample in Windhorst et al. (1985) could be identified through optical imaging and photometry, resulting in two Galactic stars, 10 quasars, and 29 galaxies, most of them of the blue (SF) type. The paper rightly stressed that “it should be remembered that the nature of the *unidentified* sub-mJy radio sources is unknown as yet” but apparently this warning went unheeded. A series of subsequent papers, in fact, perpetuated the SFG mantra. Rowan-Robinson et al. (1993), for example, concluded that faint radio counts ($S_{1.4\text{GHz}} \geq 0.1$ mJy) were dominated by starburst galaxies, on the basis of a sample for which only $\sim 20\%$ of the radio sources had optical identifications. Grupponi, Mignoli, & Zamorani (1999), on the other hand, with a fraction of optical identifications close to 50%, deduced that $\sim 44\%$ of radio sources with $0.2 \leq S_{1.4\text{GHz}} \leq 1$ mJy were instead early-type galaxies.

Another problem was the fact that the sensitivity of deep radio surveys usually decreases with the distance from the

centre of the field of view²⁵. This means that the evaluation of the true fraction of sources of a given class needs to take that into account by weighing appropriately each object by the inverse of the area accessible at the flux density of the source (e.g., Padovani et al., 2007, i.e., a source whose flux density could be reached only in 10% of the area is worth ten sources, which could instead be detected over the full survey). Neglecting this correction can obviously lead to wrong values if the population mix changes with flux density, as indeed observed.

A more important, but subtler, cause of misinterpretation is the (simple) fact that radio-based diagnostics will give radio-only information! An AGN in which most of the radio emission is related to SF in its host galaxy, as discussed in Sect. 2.3, will be classified as a SF, neglecting the rest (and dominant part) of its emitted power, which ultimately comes from black hole related processes. Only by including other, and broader, classification criteria, as detailed above, can one paint the full picture of a radio source. Which leads me to the most important of all selection effects: the lack of multi-wavelength data!

Imagine in fact to be an astronomer in the late 1980s – early 1990s. The Infrared Astronomical Satellite (IRAS), launched in 1983, which provided the first high sensitivity all-sky map at 12, 25, 60 and 100 μm , reached ≈ 200 mJy at 25 μm (Moshir, Kopman, & Conrow, 1992). For $q_{24\mu\text{m}} \sim 1.26$ (Sargent et al., 2010), a SFG with $S_{1.4\text{GHz}} \sim 1$ mJy has a MIR flux $f_{24\mu\text{m}} \approx 18$ mJy, i.e., a factor of 10 smaller. One could not then use the IR – radio correlation indicator. Only when the Infrared Space Observatory (ISO) was launched in 1995 could these flux densities be reached and even surpassed (e.g., Gruppioni et al., 2003). The *Spitzer* satellite, launched in 2003, which reaches $f_{24\mu\text{m}} \approx 40$ μJy (B  thermin et al., 2010) (on very small areas), can actually detect SFGs all the way down to $S_{1.4\text{GHz}} \approx 2$ μJy . And the first IRAC colour–colour cuts for AGN selection started to appear only in 2004 – 2005 (e.g., Lacy et al., 2004; Hatziminaoglou et al., 2005).

²⁵ Nowadays the images corresponding to a few individual pointings are typically combined to form a mosaic image so this is less of an issue (e.g., Miller et al., 2013). Still, it needs to be taken into account.

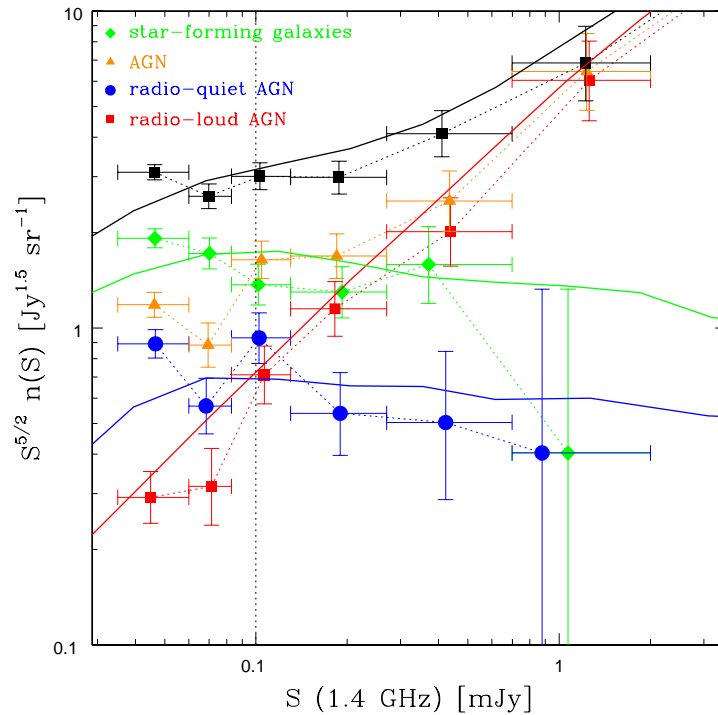


Fig. 7 Euclidean normalized 1.4 GHz source counts for the whole E-CDFS sample (black filled squares) and the various sub-classes of radio sources: SFGs (green diamonds), all AGN (orange triangles), RQ AGN (blue circles), and RL AGN (red squares). The solid lines are the SKADS simulated number counts (Wilman et al., 2008). Error bars correspond to 1σ Poisson errors (Gehrels, 1986). The vertical dotted line marks the 0.1 mJy flux density. Adapted from Padovani et al. (2015a).

The story is roughly the same for the X-ray band. Before the launch of the *Chandra* and *XMM-Newton* satellites in 1999 the best one could do with ROSAT was a soft X-ray limit $f_x \approx 10^{-15}$ erg cm $^{-2}$ s $^{-1}$ in *one* very small area of the sky (~ 0.3 deg 2 ; Lehmann et al., 2001). A RQ AGN with $S_{1.4\text{GHz}} \sim 1$ mJy has $f_x \approx 5 \times 10^{-15}$ erg cm $^{-2}$ s $^{-1}$ (Padovani, 2011), so the application of the L_x criterion was possible only for the nine radio/X-ray sources in that area, seven of which indeed had sub-mJy (5 GHz) flux densities (Cileigi et al., 2003). The first results from the deep *Chandra* and *XMM-Newton* surveys appeared in 2001 (Giacconi et al., 2001; Hasinger et al., 2001). They reached a 0.5–2 keV flux $\sim 2 - 3 \times 10^{-16}$ erg cm $^{-2}$ s $^{-1}$, opening the way to their use for the identification of faint radio sources (and much more; Brandt & Alexander, 2015).

5.3 Radio number counts by population

Armed with the classifiers I have described, we can now “solve” the question of the detailed composition of the sub-mJy radio sky.

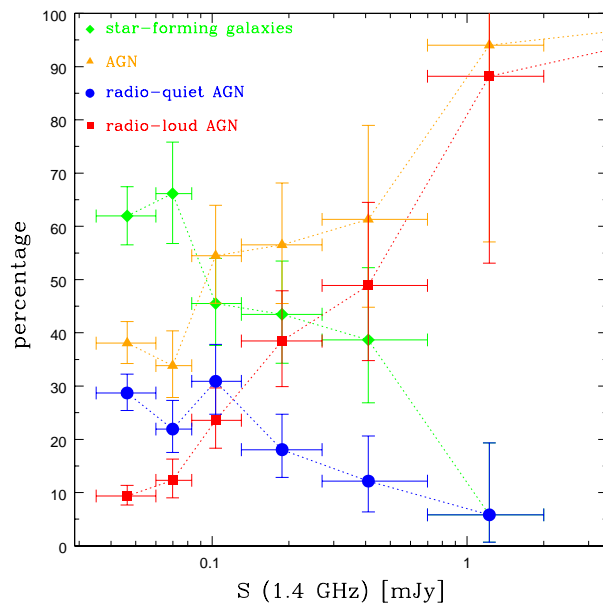


Fig. 8 Relative fractions (in percentage) of the various sub-classes of E-CDFS radio sources as a function of flux density: SFGs (green diamonds), all AGN (orange triangles), RQ AGN (blue circles), and RL AGN (red squares). Error bars correspond to 1σ Poisson errors (Gehrels, 1986).

Figure 7 presents the Euclidean normalized number counts for the various sub-classes of the E-CDFS sample²⁶ (full details in Padovani et al., 2015a). These show the familiar steep slope followed by a flattening below 1 mJy. Having classified the sources, however, one can go beyond this well known behaviour, and see which classes are doing what. The three main features of this figure are: 1. the fast drop of AGN, due to RL sources; 2. the rise of SFGs; 3. the rise of RQ AGN. These features are better appreciated in Fig. 8, which shows the relative fractions of the different E-CDFS sub-classes. AGN go from being totally dominant at large flux densities ($\gtrsim 1$ mJy) to being a minority ($\sim 40\%$), and a very small one ($\sim 10\%$) as regards RL sources. SFGs, on the other hand, are negligible at high flux densities but become the dominant population below $\lesssim 0.1$ mJy, reaching $\sim 60\%$ at the survey limit. AGN make up 43% of sub-mJy sources, which shows that there are still plenty of them in the faint radio sky, while SFGs represent 57%. RQ AGN constitute 26% of sub-mJy sources (or 61% of all AGN) but their fraction appears to increase at lower flux densities, where they make up 75% of all AGN and $\approx 29\%$ of all sources at the survey limit, up from $\approx 6\%$ at ≈ 1 mJy. So the “magical” flux density is not 1 mJy but ≈ 0.1 mJy, which is where SFGs overtake AGN and also, for a strange coincidence, RQ AGN surpass RL ones.

RQ AGN were very slow to appear in the deep radio field arena. King & Rowan-Robinson (2004) and Jarvis & Rawlings (2004) were the first, to the best of my knowledge, to include RQ AGN in the modelling of radio number counts, while Simpson et al. (2006) showed for the first time the existence of RQ AGN in a deep ($S_{1.4\text{GHz}} \geq 0.1$ mJy) radio field, making the suggestion that these sources (were a significant fraction of them very absorbed) may dominate the population responsible for the flattening of the normalized radio counts. The first observed radio number counts to include RQ AGN were those of Padovani et al. (2009). Perhaps the “radio-quiet” name has (unconsciously) fooled researchers for many years into thinking that they were really “radio silent”?

²⁶ I stress that I have not picked the E-CDFS sample to put together Fig. 7 and 8 (and Fig. 9) because this is my own survey. After Sect. 2.3 and Fig. 5, in fact, one should expect the presence of RQ AGN in radio surveys but the only radio counts I know of which include *all* classes of astrophysical sources, which make up the faint radio sky are those published by our group (Padovani et al., 2009, 2011, 2015a). Having a deep, sizeable radio sample, which is almost completely identified and where most of the sources have a redshift (spectroscopic or photometric) is not easy. But the real reason, I think, has to do with X-ray data: as shown by Table 1 the best indicator of RQ AGN is X-ray power (i.e., once RL AGN are singled out using the FIR – radio correlation, RQ ones are easily identified through their L_x). For that one needs very deep X-ray data in a region of the sky where there are very deep radio data as well: and this means the E-CDFS, which at present reaches $f_{0.5-2\text{keV}} \sim 5 \times 10^{-18}$ erg cm⁻² s⁻¹ (Lehmer et al., 2012). Note that we still do not detect *all* radio sources in the X-ray band but $\sim 60\%$ in the central region (Vattakunnel et al., 2012).

5.4 Luminosity functions

The determination of the LF requires a complete, flux density-limited sample of sources, with redshift, at distances large enough that peculiar velocities cancel out ($z \gtrsim 0.003$). For relatively small power ranges one can consider a single power law of the type $\Phi(P) \propto P^{-\epsilon}$, while for broader ranges a two power-law LF $\Phi(P) \propto 1/[(P/P_*)^{\epsilon_1} + (P/P_*)^{\epsilon_2}]$ with a break at P_* might give a better fit. More complex models (e.g., a Schechter LF) are of course also possible and often better.

All LFs in the Universe have $\epsilon > 0$, that is more powerful sources are rarer than less powerful ones. The detection of the former, therefore, requires large sampling volumes, which can be more easily obtained through relatively shallow but wide area surveys. These, however, penalize intrinsically faint objects, which are more easily detected by going deep, which can be done effectively only on small regions of the sky (for example, at a given redshift a lower flux density implies a lower radio power; or alternatively, at a given radio power a lower flux density implies a larger redshift: Fig. 5). Because of these two conflicting requirements, many extragalactic surveys now follow the so-called “wedding cake” strategy, in which multiple surveys are made covering different depths and areas (with the two being inversely proportional). In the radio band the NVSS, for example, covered the whole sky at 1.4 GHz north of -40° declination down to ~ 2.5 mJy (Condon et al., 1998), while a series of deeper surveys have been carried out on much smaller areas (Fig. 4).

Figure 7 and 8 demonstrate clearly the changing mix of radio sources as a function of flux density. As a result, because of deeper surveys, the focus of the LF derivation has shifted greatly in recent years from what it used to be. In a radio sky dominated by RGs, radio quasars, and blazars the emphasis was on flat vs. steep sources, FSRQs vs. FR IIs, BL Lacs vs. FR Is (Urry & Padovani, 1995; de Zotti et al., 2010, and references therein). Figure 1 of Padovani (2011) shows the relatively small surface densities most of these classes are predicted to have once one enters the sub-mJy regime. For example, only ≈ 10 blazars are expected in the E-CDFS area (0.285 deg²), out of 765 sources. Nowadays the focus is on SFGs, RL, and RQ AGN.

Figure 9 shows the local differential 1.4 GHz LFs (derived using the $1/V_a$ method, a variation of the $1/V_{\text{max}}$ one: see Schmidt, 1968; Padovani et al., 2015a, for details) for E-CDFS SFGs ($z < 0.5$; green diamonds), RL AGN ($z < 0.4$; red squares), and RQ AGN (whole sample de-evolved to $z = 0$ using the best fit evolutionary parameter from a maximum likelihood fit; blue circles). The best-fit local LFs from maximum likelihood fits are also shown (Padovani et al., 2015a, and Padovani et al., in preparation). These are somewhat model dependent but by making maximal use of the data provide additional information on the low redshift LF,

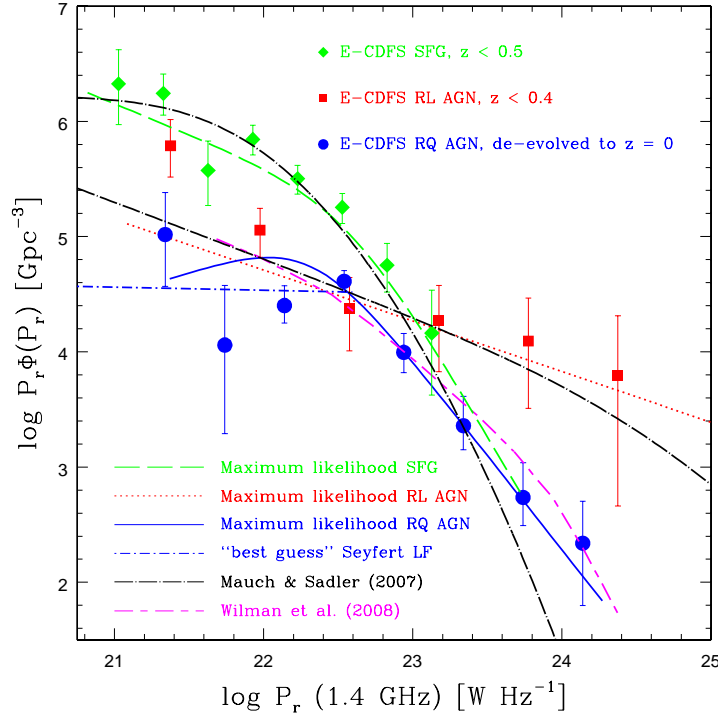


Fig. 9 The local differential 1.4 GHz LFs in a $P \times \phi(P)$ form for E-CDFS SFGs ($z < 0.5$; green diamonds), RL AGN ($z < 0.4$; red squares), and RQ AGN (whole sample de-evolved to $z = 0$ using the $1/V_a$ method and the best fit evolutionary parameter from a maximum likelihood fit; blue circles). The best-fit local LFs from a maximum likelihood fit are also shown, together with my “best guess” of the radio LF of Seyfert galaxies for $P_{1.4\text{GHz}} \lesssim 3 \times 10^{22} \text{ W Hz}^{-1}$, the $z < 0.3$ LFs from Mauch & Sadler (2007) for SFGs and AGN (upper and lower curve respectively), and the local LF for RQ AGN assumed in the SKADS simulation of Wilman et al. (2008). Error bars correspond to 1σ Poisson errors added in quadrature with the cosmic variance uncertainties for SFG and RL AGN and with the variations of the number density associated with a 1σ change in the evolutionary parameter for RQ AGN.

which is based on relatively small samples (plus they are free from arbitrary binning). Finally, the figure displays also the $z < 0.3$ LFs from Mauch & Sadler (2007) for SFGs and AGN and the local LF for RQ AGN assumed in the SKADS simulation of Wilman et al. (2008) (Sect. 7.2.1). The LFs are shown in a $P \times \Phi(P)$ form, which is almost equivalent to the $\phi(M_B)$ form²⁷ normally used in the optical band. I now discuss the (large amount of) information conveyed by Fig. 9 taking every population in turn first.

5.4.1 SFGs

The local LF for SFGs is best fitted by two power laws with $\Phi(P) \propto P^{-1.5^{+0.1}_{-0.2}}$ and $\propto P^{-3.2 \pm 0.2}$, respectively below and

²⁷ $P \times \Phi(P) = 2.5/\ln(10) \times \Phi(M) \sim 1.09 \times \Phi(M)$, where the units of $\Phi(M)$ are $\text{mag}^{-1} \text{ volume}^{-1}$. Note that these units are also sometimes used in the radio band: e.g., Condon (1989); Sadler et al. (2002); Mauch & Sadler (2007). The conversion, instead, to units of $\text{Mpc}^{-3} \text{ dex}^{-1}$ used, for example, by Simpson et al. (2012), is done by dividing my values by $10^9/\ln(10)$. The $P \times \Phi(P)$ form allows an easy separation of luminosity and density evolution as the former simply translates the LF to higher powers with no change in number, while the opposite is true for the latter.

above $P_* \sim 4 \times 10^{22} \text{ W Hz}^{-1}$ (Padovani et al., in preparation). The E-CDFS derivation is consistent with previous ones based on sub-mJy data (e.g., Smolčić et al., 2009a; Padovani et al., 2011; Mao et al., 2012, not shown for clarity) but reaches $\sim 3 - 10$ lower powers because of its fainter flux density limit. It also agrees impressively well with the local ($z < 0.3$) LF from the sample of Mauch & Sadler (2007), which is based on a correlation of the NVSS with galaxies brighter than $K = 12.75$ mag in the second incremental data release of the 6 degree Field Galaxy Survey (6dFGS). This is no mean feat: the NVSS/6dFGS SFG sample includes 4006 sources, all of them classified using high quality optical spectra. In contrast, the E-CDFS SFG sample includes 91 ($z < 0.5$) or 356 (full sample) sources, classified following the scheme described in Sect. 5. This agreement, therefore, validates on a statistical basis the classification scheme applied to the E-CDFS sources.

5.4.2 RL AGN

The local LF for RL AGN is best fitted by a single power law with $\Phi(P) \propto P^{-1.44 \pm 0.4}$. The comparison with previous determinations based on sub-mJy samples has to be done

carefully because many papers make a distinction between SFGs and AGN but not between RQ and RL AGN. The local LF for *all* E-CDFS AGN compares well, for example, with that of Smolčić et al. (2009b) and Mao et al. (2012), while that of RL AGN agrees with that of Simpson et al. (2012) (once a correction is applied to take into account their different definition of RL AGN). The agreement with the NVSS/6dFGS LF (and also with that of Heckman & Best, 2014) is less good and the E-CDFS LF is a factor ~ 2.2 higher. This is likely to be due partly to small number statistics but mostly to the somewhat different selection criteria. Many of the samples put together by cross-correlating very large surveys, for example those discussed by Heckman & Best (2014), by construction do not sample the whole RL AGN population. They are, in fact, limited to galaxies (and therefore do not include non-stellar and broad-line sources), bivariate (i.e., the result of a cross match between a radio and an optical/NIR survey), and often also restricted to steep-spectrum ($\alpha_r > 0.5$) radio sources. The E-CDFS LF, being simply radio flux density limited, has no such biases and therefore is bound to find larger number densities; cf. the Mao et al. (2012) LF, which is also a factor ~ 3 above the NVSS/6dFGS LF.

Finally, all RL AGN LFs from sub-mJy samples are well above (~ 2 orders of magnitude) the radiative-mode radio AGN LF of Best et al. (2014) and their L/L_{Edd} are mostly $\lesssim 0.01$ (see, e.g., Figs. 6 and 12 of Padovani et al., 2015a, respectively). This shows that the bulk of faint RL AGN are of the jet-mode type. I stress that the number densities of “classical” (i.e., high flux density) RL quasars are orders of magnitude smaller than those of the RL AGN in Fig. 9 (and off-scale: $\lesssim 10 \text{ Gpc}^{-3}$ for $P \gtrsim 10^{26} \text{ W Hz}^{-1}$ for FSRQs; see, e.g., Wall et al., 2005; Padovani et al., 2007).

5.4.3 RQ AGN

The E-CDFS RQ AGN $z \leq 0.4$ sample includes only 6 objects and the corresponding LF is therefore very uncertain. I then use the LF for the full sample de-evolved to $z = 0$ using the best fit evolutionary parameter from the maximum likelihood analysis and the local LF derived from the latter. The local LF for RQ AGN is best fitted by two power laws with $\Phi(P) \propto P^{-0.6^{+0.6}_{-0.7}}$ and $\propto P^{-2.6^{+0.2}_{-0.3}}$, respectively below and above $P_* \sim 2 \times 10^{22} \text{ W Hz}^{-1}$. As discussed in Padovani et al. (2015a) (see their Fig. 8), this LF was found not be inconsistent with the radio LFs for three samples of Seyfert galaxies (within the rather large errors). One can actually use these LFs to estimate the RQ AGN LF at low radio powers ($P_{1.4\text{GHz}} \lesssim 3 \times 10^{22} \text{ W Hz}^{-1}$; with the caveat that, being these bivariate, it is almost certain that the samples are not complete in the radio and therefore the LFs are robust lower limits to the true ones), which is what I have done in Fig. 9 (dot-dashed blue line).

No comparison can be made with previous determinations based on radio-selected samples because none exists. I can compare the derived RQ AGN LF with that *assumed* in the SKADS simulation (magenta short-long-dashed line: see Sect. 7.2.1). This is based on a simple conversion of the AGN X-ray LF to a radio LF using a linear relationship between X-ray and radio power (see details in Wilman et al., 2008). Given the assumptions behind the latter, the agreement between the two is surprisingly good and strongly suggests that: 1. both the SKADS approach and the classification scheme applied to the E-CDFS sources are validated; 2. the sources we are selecting in the radio band are the same as the (RQ) AGN selected in the X-ray band; 3. the “best guess” Seyfert LF is indeed likely to be a lower limit.

5.4.4 SFGs and AGN

The main messages of Fig. 9 come out loud only when the three LFs are considered together. Namely: 1. faint RL AGN have a much flatter radio LF than RQ ones and are always predominant, especially so at $P_{1.4\text{GHz}} \gtrsim 3 \times 10^{22} \text{ W Hz}^{-1}$; 2. the RQ AGN LF appears to be somewhat parallel to, and overlapping with, the SFG one at $P_{1.4\text{GHz}} \gtrsim 5 \times 10^{22} \text{ W Hz}^{-1}$; 3. AGN dominate over SFG at $P_{1.4\text{GHz}} \gtrsim 10^{23} \text{ W Hz}^{-1}$, in agreement with previous studies (e.g., Mauch & Sadler, 2007).

5.5 Evolution

AGN and SFGs evolve strongly (e.g., Merloni & Heinz, 2013; Gruppioni et al., 2013, respectively), i.e., their LF changes with redshift, with their powers and/or they numbers being different from what they are at $z \sim 0$. This was quickly realised for quasars thanks to the first radio surveys and for radio sources in general even before the discovery of quasars (Sect. 3.2). A classic (but not the first) paper is Schmidt (1968), who showed that the space density of 3CR quasars at $z = 1$ was ≈ 100 times the local density. Furthermore, to reproduce the relatively narrow hump in the observed Euclidean normalized counts (Fig. 4), Longair (1966) suggested that not all radio sources evolved equally but that only the most powerful sources could evolve strongly with redshift. Many more papers followed: for example, Dunlop & Peacock (1990), by mostly using a sample with $S_{2.7\text{GHz}} \geq 100 \text{ mJy}$, pointed out that this strong evolution could not continue to very high redshifts but a decrease in the number density of FSRQs, SSRQs, and RGs had to take place around $z \sim 2 - 4$.

This topic is very vast. As is the case for LFs (Sect. 5.4), its focus has recently shifted as we reach fainter radio flux densities. I refer to de Zotti et al. (2010) for a comprehensive review of the evolution of strong radio sources. Here I only mention the fact that there appears to be a consensus

on the strong and positive evolution of FSRQs/SSRQs/FR IIs (i.e., radiative-mode RL AGN), and on the weak, if any, evolution of BL Lacs/FR Is (i.e., jet-mode RL AGN) (see also Padovani et al., 2007; Giommi et al., 2012, and references therein). I now concentrate on the most recent results pertinent to the faint radio sky, taking every sub-population in turn. Before I do that let us have another look at Fig. 7 keeping in mind what we have learnt from Fig. 3: SFGs have normalized counts, which rise at lower flux densities, as is the case for RQ AGN, while RL AGN display the opposite behaviour. This already tells us, without any doubt and need for further information, that the first two sub-samples are undergoing positive evolution, at variance with RL AGN.

5.5.1 SFGs

E-CDFS SFGs evolve strongly, with $P(z) \propto (1+z)^{2.1 \pm 0.1}$ for $0 < z \leq 3.25$; there is also evidence that the strength of the evolution decreases with redshift (Padovani et al., in preparation). Furthermore, Padovani et al. (2011) found suggestive evidence of such a slowing down in the CDFS, with $P(z) \propto (1+z)^{3.5^{+0.4}_{-0.7}}$ and $\propto (1+z)^{1.6^{+0.6}_{-0.7}}$ for $z \leq 1.3$ and $1.3 < z \leq 2.3$ respectively.

Until recently, no *direct* determination of the radio evolution of sub-mJy SFGs was possible, likely for lack of redshifts. For example, Hopkins (2004) combined the constraints from the global (radio to X-ray) SFR density evolution with those derived from the 1.4 GHz sub-mJy source counts to infer $P(z) \propto (1+z)^{2.7 \pm 0.6}$ and $\phi(P) \propto (1+z)^{0.15 \pm 0.60}$ imposing a redshift cutoff at $z = 2$ (i.e., basically a PLE). One of the first direct estimates was that of Smolčić et al. (2009a), who derived $P(z) \propto (1+z)^{2.1-2.5 \pm 0.2}$ for $z \leq 1.3$. This is weaker than found by Padovani et al. (2011), although not significantly so but, as discussed in Bonzini et al. (2013), the method employed by Smolčić et al. (2009a) to separate AGN and SFGs, based on rest-frame optical colours, is not optimal. McAlpine, Jarvis, & Bonfield (2013) obtained $P(z) \propto (1+z)^{2.5 \pm 0.1}$ for $z \leq 2.5$ but their source classification is based only on UV to K band photometry, with their AGN being selected as sources redder than the spiral galaxy templates (i.e., having early type hosts) and SFGs being everything else (which groups at least some of the RQ AGN with the SFGs).

5.5.2 RL AGN

RL AGN are the only sources, which are present in significant numbers both in the bright and faint radio skies. High-power radiative mode objects, however, are more common at large flux densities while low-power jet mode ones are predominant at lower ones (as per Fig. 5). Because of the extra complications in selecting RQ AGN (Sect. 5.1), many papers dealing with the evolution of sub-mJy radio

sources have unfortunately lumped RQ and RL AGN together, obtaining an overall relatively weak evolution (e.g., Smolčić et al., 2009b; McAlpine, Jarvis, & Bonfield, 2013), which masked the big difference between the two AGN subclasses. Padovani et al. (2011) were the first to study them separately in the CDFS sample and found that RL AGN evolve (in number) strongly but negatively ($\phi(P) \propto (1+z)^{-3.7^{+1.1}_{-1.6}}$), while RQ AGN evolve (in power) strongly but positively ($P(z) \propto (1+z)^{2.5^{+0.4}_{-0.5}}$).

Padovani et al. (2015a) have exploited the better statistics of the E-CDFS sample and found that the evolution of RL AGN is still a PDE but a complex one: the number density evolves *positively* as $\phi(P) \propto (1+z)^{2.2^{+1.8}_{-1.6}}$ up to $z_{\text{peak}} = 0.5 \pm 0.1$, beyond which it declines steeply $\propto (1+z)^{-3.9^{+0.7}_{-0.8}}$ (the large error bars at low redshift reflect the small number of RL AGN with $z \leq 0.5$). This is consistent with other results derived at larger flux densities. Rigby et al. (2015) studied various samples of *steep-spectrum* ($\alpha_r > 0.5$) AGN selected from a variety of radio surveys with increasingly smaller areas and flux density limits down to 0.1 mJy. They found that the number density peaks at a luminosity-dependent z_{peak} for $P_{1.4\text{GHz}} \gtrsim 10^{26} \text{ W Hz}^{-1}$, with the most powerful sources peaking at earlier times than the weaker ones. Below this value z_{peak} appears to remain constant. At their lowest powers, $P_{1.4\text{GHz}} \sim 2 \times 10^{24} \text{ W Hz}^{-1}$, $z_{\text{peak}} = 1.1 \pm 0.4$ (or possibly $1.1^{+0.2}_{-1.1}$). Since the median $P_{1.4\text{GHz}}$ of E-CDFS RL AGN is $\sim 10^{24} \text{ W Hz}^{-1}$ a $z_{\text{peak}} \sim 0.5$ is in agreement with their results. The work by Rigby et al. (2015) puts on stronger footing previous results on the high-redshift decline of strong radio sources (see de Zotti et al., 2010).

Best et al. (2014) have also studied samples of (steep-spectrum) radio AGN selected from a variety of surveys down to 0.2 mJy and up to $z = 1$. They classify their sources into radiative-mode and jet-mode AGN using emission line diagnostics. The space density of the jet-mode population with $P_{1.4\text{GHz}} \lesssim 10^{24} \text{ W Hz}^{-1}$ stays constant up to $z \approx 0.5$ and then decreases; at moderate powers, $10^{24} \lesssim P_{1.4\text{GHz}} \lesssim 10^{26} \text{ W Hz}^{-1}$, the space density increases to $z \sim 0.5$ before falling. At the highest powers the space density appears to increase up to $z \sim 1$ but the statistics is somewhat limited (see their Fig. 5). Based on Sect. 5.4.2, the large majority of E-CDFS RL AGN are of the latter type, so the E-CDFS results are similar, taking into account the somewhat more limited coverage of the luminosity – redshift plane. Simpson et al. (2012) also found zero or negative evolution for RL AGN with $P_{1.4\text{GHz}} \lesssim 10^{24} \text{ W Hz}^{-1}$ (although their RL AGN selection is somewhat different: Sect. 5.4.2). As for radiative-mode RL AGN, the evolution in their space density appears to be comparable to the evolution of RQ radiative-mode AGN selected in other bands (e.g., Best et al., 2014).

5.5.3 RQ AGN

The evolution of RQ AGN in the radio band has been first determined by Padovani et al. (2011) and more recently updated by Padovani et al. (2015a) (no other determinations exist to the best of my knowledge). The E-CDFS RQ sample is consistent with a PLE of the type $\propto (1+z)^{2.5 \pm 0.2}$ for $0 \lesssim z < 3.7$, not very different from that of SFGs. As was the case for SFGs, however, there is (2σ) evidence of a slowing down at higher redshifts, with $P(z) \propto (1+z)^{4.0 \pm 0.6}$ and $\propto (1+z)^{2.0 \pm 0.5}$ for $z \leq 1.3$ and $1.3 < z \leq 3.7$ respectively. Radio selected RQ AGN share the strong evolution of the powerful, radiative-mode RL AGN but have radio powers more similar to those of the jet-mode ones, which make up most of the sub-mJy RL AGN (Fig. 9), a situation which can be somewhat confusing.

6 The big picture: what does it all mean?

One obvious question, at this point, is: what are we learning by studying the faint radio sky? In particular, what do the LF and evolution of faint radio sources tell us of astrophysical relevance? I address this next by providing very specific examples.

6.1 Astrophysics of faint radio sources

6.1.1 SFGs and cosmic star formation history

“Once, there were no stars. [...] Understanding how [...] gas evolved into the Universe filled with stars that we observe today [...] remains one of the most important goals of modern astrophysics” (Mac Low, 2013). The solution to this puzzle is related to the time dependence of the SFR density (SFRD, generally expressed in units of $M_\odot \text{ yr}^{-1} \text{ Mpc}^{-3}$), the so-called “Lilly-Madau plot”. This appears to have peaked ≈ 3.5 Gyr after the Big Bang and to have declined exponentially since then (Madau & Dickinson, 2014, and references therein). As mentioned in Sect. 2.4, radio emission in SFGs trace the SFR, so radio observations can also be relevant. Traditionally, however, their role has been somewhat limited (but see, e.g., Haarsma et al., 2000; Seymour et al., 2008; Karim et al., 2011) although other, more “standard” methods all have their own limitations. One issue is that even the deepest radio data at present can only reach relatively high SFR at high redshifts: e.g., $\approx 1000 M_\odot \text{ yr}^{-1}$ at $z \sim 3$ (Madau & Dickinson, 2014, Fig. 1a).

One way one can derive the SFRD is through the power density, defined as $\rho_L = \int P \Phi(P) dP$. Parametrizing the LF as in eq. 2, one obtains the redshift dependence of ρ_L as follows:

$$\rho_L(z) = f_D(z) f_L(z) \int P_0 \Phi(P_0) dP_0 = \rho_L(0) f_D(z) f_L(z), \quad (3)$$

where $\Phi(P_0)$ is the local LF. In other words, the power density at redshift z is the power density at $z = 0$ multiplied by both luminosity and density evolutionary functions (assuming, of course, these have no dependence on power). If $f_D(z) = (1+z)^{k_D}$ and $f_L(z) = (1+z)^{k_L}$ then $\rho_L(z) \propto (1+z)^{k_D+k_L}$ (see also Hopkins, 2004). The power density can then be transformed into a SFRD by using the relevant SFR – power conversion, whose robustness depends on the band at hand. For example, FIR emission is straightforward to understand in the optically thick case for an intensely SFG: $\text{SFR}_{\text{FIR}} [M_\odot \text{ yr}^{-1}] = 4.5 \times 10^{-44} L_{\text{FIR}} [\text{erg s}^{-1}]$ (Kennicutt, 1998). UV and optical indicators, on the other hand, are extremely sensitive to dust, while radio emission is more indirect, since it relies on the complex and not fully understood physics of cosmic-ray generation and confinement (e.g., Condon, 1992; Bell, 2003). As a result, the exact conversion factor of the latter is still debated. Bell (2003) gives $\text{SFR}_{\text{radio}} [M_\odot \text{ yr}^{-1}] = 5.5 \times 10^{-22} P_{1.4\text{GHz}} [\text{W Hz}^{-1}]$ (for $P_{1.4\text{GHz}} \geq 6.4 \times 10^{21} \text{ W Hz}^{-1}$: below this value the relationship is slightly non-linear). The existence of the FIR – radio correlation (Sect. 2.4) is in any case a very strong argument for using radio power as a SFR proxy.

For a *linear conversion* between SFR and power, therefore, $\text{SFRD}(z) \propto f_D(z) f_L(z) \propto (1+z)^{k_D+k_L}$, i.e., the observed slope of the SFRD(z) relationship constrains k_D+k_L . Said differently, when one measures the evolution of the LF of SFGs one is also constraining the evolution of the SFRD in the Universe. Madau & Dickinson (2014) found $\text{SFRD}(z) \propto (1+z)^{2.7}$ for $z \ll 1.9$ and $\propto (1+z)^{-2.9}$ for $z \gg 1.9$, with a smooth transition in between (see their eq. 15)²⁸. The low redshift behaviour is not inconsistent with our current understanding of the radio evolution of SFGs (Sect. 5.5.1). Constraining the high redshift evolution is tougher, though, as shown (again) by Fig. 5: even the E-CDFS can detect at $z \gtrsim 2$ only SFGs with $P_{1.4\text{GHz}} \gtrsim 6 \times 10^{23} \text{ W Hz}^{-1}$, which correspond to the relatively high end of the LF (Fig. 2 of Padovani et al., 2015a, shows that the fraction of E-CDFS SFGs at $z > 2$ is indeed quite small.)

Karim et al. (2011) used a large 1.4 GHz survey of the COSMOS field and a *Spitzer* 3.6 μm selected sample to carry out the most extensive study in the radio band to date. Through stacking in bins of M_\star and (photometric) redshift and converting their mean S_r to SFRs, they computed the integrated SFRD, finding a monotonic decline in the SFRD from $z = 3$ to today. In other words, their results suggest a peak in the SFRD at $z > 3$, at variance with Madau & Dickinson (2014). However, as stated in their paper, their data cannot constrain the situation at high redshifts as strongly as at $z < 1.5$ and therefore they cannot rule out a SFRD peak at $1.5 < z < 3$. This topic is picked up again in Sect. 7.3.1.

²⁸ They note that a solid interpretation of the time dependence of the SFRD from first principles is still missing (e.g., Mac Low, 2013).

6.1.2 RL AGN and quiescent galaxies

AGN are well-known to evolve positively, that is they were more luminous and/or more numerous at higher redshifts. Why is it then that faint RL AGN appear to display the opposite behaviour? This can be understood by looking at AGN evolution from a broader, modern perspective. Our current understanding is that the number density of more luminous AGN peaks at redshifts higher than those of lower luminosity objects (the so-called downsizing). That is, sources in a given luminosity range increase in number from lower to higher redshifts up to a maximum redshift, z_{peak} , above which their numbers decrease, with z_{peak} strongly correlated with power. This behaviour has been seen at many wavelengths (e.g., Hopkins, Richards, & Hernquist, 2007; de Zotti et al., 2010; Merloni & Heinz, 2013, and Sect. 5.5.2 (for the radio)).

The E-CDFS can detect sources as weak as $P_{1.4\text{GHz}} \approx 6 \times 10^{23} \text{ W Hz}^{-1}$ and $\approx 2 \times 10^{24} \text{ W Hz}^{-1}$ up to $z \sim 2$ and ~ 3 , respectively (Fig. 5). For $P_{1.4\text{GHz}} \lesssim 10^{26} \text{ W Hz}^{-1}$ $z_{\text{peak}} \approx 1$ (Rigby et al., 2015). This means that at the median power of RL AGN ($P_{1.4\text{GHz}} \sim 10^{24} \text{ W Hz}^{-1}$) one can probe the evolutionary behaviour of the RL population well beyond z_{peak} and already in its declining phase. Hence the strong negative evolution.

So the real question becomes: what is driving this evolution? Padovani et al. (2011) made, as far as I know, the first connection between the negative evolution of RL AGN²⁹ and that of elliptical galaxies, by noticing the similarity between their results and those of Taylor et al. (2009), who found that the number density of $M_{\star} > 10^{11} M_{\odot}$ red galaxies declined as $\Phi(z) \propto (1+z)^{-1.6}$ for $z \leq 1.8$. Best et al. (2014) took this idea further by assuming that jet-mode (since we are dealing here with low-power sources) RL AGN are hosted in quiescent (i.e., non SF) galaxies and combining the known stellar mass function of the host galaxies with the prevalence of jet-mode RL AGN as a function of M_{\star} . They then came up with a $\Phi(z) \propto (1+z)^{-0.1}$ out to $z = 0.8$ and $\Phi(z) \propto (1+z)^{-6.5}$ at higher redshifts (Rigby et al., 2015, have modified the former into $\propto (1+z)$, which gives a better match to their data). The physical reasons behind this evolution are complex, hotly debated, and not entirely sorted out but are related to SF being “quenched” as time goes by, which translates into a decrease in the number density of quiescent galaxies at higher redshifts (e.g., Peng et al., 2012)³⁰.

As for the radiative-mode AGN (both in the radio and other bands), it has been noted many times that the black hole mass growth rates derived from the AGN bolometric LF

(which evolves strongly and positively with redshift) track closely the cosmic SFRD, which has led to the suggestion that SF and black hole growth are linked. This would make sense, as both mechanisms are fed by the gas in the host galaxy, albeit on quite different spatial scales. Nevertheless, “the differences between accretion histories published in the recent literature would caution that it is premature to consider this comparison to be definitive” (Madau & Dickinson, 2014).

6.2 The origin of radio emission in (sub-mJy) RQ AGN

I have mentioned in Sect. 2.3 that the mechanism responsible for the *bulk* of radio emission in (non-local) RQ AGN has been a matter of debate for the past fifty years or so (see also the Introduction of Condon et al., 2013). Alternatives have included a scaled down version of the RL AGN mechanism (e.g., Miller, Rawlings, & Saunders, 1993; Ulvestad, Antonucci, & Barvainis, 2005), perhaps because the central black hole is rotating more slowly than in RL AGN (Wilson & Colbert, 1995), SF (Sopp & Alexander, 1991), coronal emission (Raginski & Laor, 2016, and references therein), and more (e.g., Orienti et al., 2015, and references therein).

This is a highly non-trivial issue for various reasons: 1. most (> 90%) AGN are RQ; 2. some of the proposed explanations have profound implications on our understanding of AGN physics (jets, accretion, black hole spin, etc.); 3. some others are very relevant for the relationship between AGN and star formation in the Universe and the co-evolution of supermassive black holes and their host galaxies (related to “AGN feedback”), which is a very hot topic in extragalactic research (e.g., Kormendy & Ho, 2013; Heckman & Best, 2014, for recent reviews).

The study of the faint radio sky can help here: for the first time one can select RQ AGN, RL AGN, and SFGs in the radio band and within the same sample. Sub-mJy RQ AGN share many properties with SFGs, including the strong evolution, similar LF, and host galaxies, while not many with the sub-mJy RL AGN. This might suggest that radio emission in RQ AGN is more related to SF than to the central AGN. One can directly test this by comparing the SFR derived from the FIR luminosity as traced by *Herschel*, which is a very robust SFR estimator, with that estimated from the radio power under the assumption that it is due to SF (Sect. 6.1.1). This is exactly what has been done by Bonzini et al. (2015) for the E-CDFS sample, as shown in Fig. 10.

The two SFR estimates for SFGs, not surprisingly, are in agreement over four decades in SFR with a dispersion of 0.2 dex. More interestingly, there is very good agreement between the SFRs derived from the two different tracers also for RQ AGN with only a slightly larger scatter of 0.23 dex. This implies that the *main* contribution to radio emission in

²⁹ The blazar community has been aware of the likely negative evolution of a sub-class of BL Lacs for quite some time: see Giommi et al. (2012) and references therein.

³⁰ This is a very active field with many papers published on the subject in the past few years: see, e.g., Madau & Dickinson (2014); Somerville & Davé (2015) and references therein.

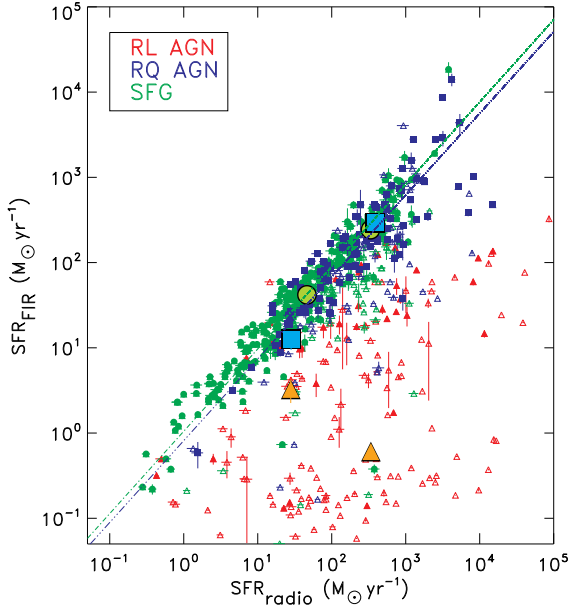


Fig. 10 SFR derived from the FIR luminosity versus the SFR from $P_{1.4\text{GHz}}$ for the E-CDFS sample. SFGs are plotted as green circles, RQ AGN as blue squares, and RL AGN as red triangles. Full symbols represent sources detected in at least one Photoconductor Array Camera and Spectrometer (PACS) filter, while sources shown as empty symbols are *Herschel* non-detections, for which SFR_{FIR} is less robust. Large symbols with lighter colours are the results of a stacking analysis. The two lines are the best fits for the SFGs and RQ AGN with PACS detection. Figure reproduced from Bonzini et al. (2015), Fig. 3, with permission.

sub-mJy radio-selected RQ AGN at $z \sim 1.5$ (the mean redshift of the E-CDFS RQ AGN sample) comes from SF activity in the host rather than from the black hole. This is further supported by the behaviour of RL AGN, which populate the region below the best fit lines, since their $\text{SFR}_{\text{radio}}$ is overestimated because of the strong jet/central AGN contribution. Note that RQ AGN occupy the same locus as SFGs also in the $\text{SFR} - M_{\star}$ plane, suggesting that the majority of the host galaxies of radio-selected RQ AGN are not significantly different from the inactive galaxy population (Bonzini et al., 2015)³¹.

How can these results be reconciled with some of those reviewed in Sect. 2.3? As discussed in Smolčić et al. (2015), at least part of these differences might be attributed to the

³¹ The E-CDFS RQ AGN have been selected mostly based on them falling within the SFG locus in the $q_{24\mu\text{m}} - z$ plane (Bonzini et al., 2013). One could therefore argue that the correlation they follow in Fig. 10 is a consequence of the selection method. However, SFGs and RQ AGN have different MIR characteristics: SFGs, for example, have an average dispersion in $q_{24\mu\text{m}}^{\text{obs}} \sim 0.33$ dex, which is twice as small as that of RQ AGN. This is mainly due to the relatively large AGN contribution at MIR wavelengths in many RQ AGN. In other words, one can effectively use the MIR to discard RL AGN, but this band is not good enough to obtain a reliable estimate of the SFR, for which one needs the FIR (i.e., *Herschel*).

diversity of the samples. Rosario et al. (2013), for example, have shown that in RQ, relatively low-luminosity AGN, much of the observed radio emission is consistent with SF in the AGN hosts, at variance with Zakamska et al. (2016). Since their sources have IR powers $\nu L_{\nu}(12\mu\text{m}) \lesssim 10^{44}$ erg s^{-1} ($L_{\text{bol}} \lesssim 10^{45}$ erg s^{-1}) one might think that there is a dependency on bolometric power, which could be due to the likely different host galaxies, with quasar-like sources being hosted in bulge-dominated galaxies and Seyfert-like ones in disc-dominated galaxies (Sect. 2.3). Indeed, the E-CDFS RQ AGN are also of relatively low power, having $\langle L_{\text{x}} \rangle \sim 10^{43}$ erg s^{-1} (i.e., $L_{\text{bol}} \approx 3 \times 10^{44}$ erg s^{-1}). Nevertheless, this still does not explain the Kimball et al. (2011) and Condon et al. (2013) results, which refer to quasars.

Another complication might have to do with evolution (Padovani et al., 2011): if the AGN related radio component is non-evolving, as is the case for low-power RL AGN (Sect. 5.5.2), while the SF related one follows the evolution of SFGs (Sect. 5.5.1), higher redshift RQ AGN should have their radio emission more SF dominated than lower redshift ones. Both the Kimball et al. (2011) and the Zakamska et al. (2016) samples, however, are at relatively low redshifts ($0.2 < z < 0.3$ and $z < 0.8$ respectively).

Further support for the SF connection in sub-mJy RQ AGN comes from high resolution radio imaging. Richards et al. (2007) have studied 92 radio sources with $S_{1.4\text{GHz}} \geq 40 \mu\text{Jy}$ in the Hubble Deep Field North well resolved by MERLIN and the VLA at $0.2 - 2$ arcsec resolutions. They found that the presence of an AGN is indicated in at least half of the 45 radio starbursts with X-ray counterparts. Furthermore, almost all extended radio starbursts at $z > 1.3$ host X-ray selected obscured AGN (with $L_{\text{x}} < 10^{44}$ erg s^{-1}). These results are fully consistent with a very close relationship between SF and radio emission in relatively high-redshift RQ AGN.

Chi, Barthel, & Garrett (2013) have detected with VLBI 12 out of the 92 sources studied by Richards et al. (2007). Of these, four fulfil the RQ AGN criteria laid out in Sect. 5.1 (based on $q_{24\mu\text{m}}$ and L_{x} , the latter from Richards et al., 2007), and have $0.7 < z < 4.4$ and $S_{\text{VLBI}}/S_{\text{VLA}} \geq 0.5$. This indicates that AGN emission makes up $> 50\%$ of the total in these sources. Nevertheless, these authors estimate that 48/92 sources were bright enough to be detected, which gives a detection rate of only 25%. So the majority of these sources have their arcsecond scale emission completely resolved out by the VLBI beam, which suggests an extended, possibly SF related source for the RQ AGN.

Very recently Maini et al. (2016) have also detected with VLBI compact cores accounting for $\sim 50 - 70\%$ of the total radio emission in two E-CDFS RQ AGN at $z \sim 1.4$ (see also Herrera Ruiz et al., 2016, who observed 18 COSMOS sub-mJy RQ AGN and detected three). Once this core emission

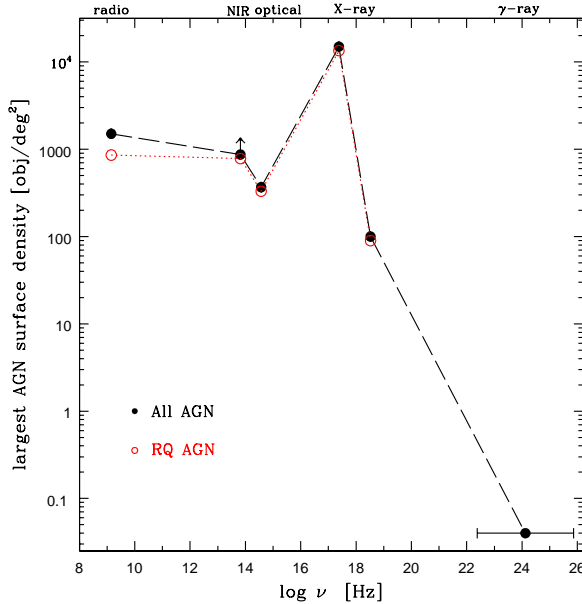


Fig. 11 The largest AGN surface density over the whole electromagnetic spectrum. Black filled points refer to all AGN, while open red points are for RQ AGN. The latter are actually measured only in the radio band, while in the NIR to X-ray bands they have been derived by simply subtracting 10% from the total values. References for the relevant samples and facilities are: E-CDFS/VLA, radio (1.4 GHz: Padovani et al., 2015a); COSMOS/*Spitzer*, NIR (4.5 μ m: Donley et al., 2012); VIMOS VVDS/VLT (Type 1) and zCOSMOS/VLT (Type 2), optical (I band: LeFevre et al., 2013; Bongiorno et al., 2012, respectively); 4 Ms/*Chandra*, soft X-ray (0.5 – 2 keV: Lehmer et al., 2012); *NuSTAR*, hard X-ray (8 – 24 keV: Harrison et al., 2015); 3FGL/*Fermi*, γ -ray (100 MeV – 300 GeV: Acero et al., 2015). Based on the discussion in Sect. 5.1 the surface density in the NIR is only a lower limit to the true value since, by definition, IR selected AGN only account for those objects where the AGN dominates over the host galaxy at the wavelengths of interest, which imposes biases on the sample.

is removed both sources, which had a slight radio excess in Fig. 10, fall nicely on the FIR – radio correlation.

In summary, some sub-mJy RQ AGN show evidence for relatively strong compact radio cores, which suggests that the AGN component might be at the same level as, or even stronger than, the SF one. One needs to keep in mind, though, that VLBI detections might be biased towards AGN-dominated sources, as at present they require relatively large flux densities, and sizeable, complete, and fainter samples should be targeted at VLBI resolutions to get a less biased picture. The *Herschel* results, moreover (Fig. 10), point towards a dominance of SF in the radio emission of sub-mJy RQ AGN at $z \sim 1.5$.

6.3 Radio emitting AGN in the larger context

After the discovery of quasars in 1963 AGN have been observed and detected in all bands, which provide different windows on AGN physics. To put things into perspective,

Fig. 11 shows my best estimates of the largest surface density in various bands covering the whole electromagnetic spectrum for all AGN (black filled points) and RQ AGN only (open red points). There are no RQ AGN detected in the γ -rays³² (Ackermann et al., 2012a).

Figure 11 is a complex mix of physics, selection effects, and technological limitations (perhaps providing enough material for another review!). The main point I want to make is that the surface density of radio-selected RQ AGN is already larger than that reached by the deepest optical surveys and at the same level as the NIR values. The whole idea of looking in an efficient way for RQ AGN in the radio band would have sounded like an oxymoron until only a few years ago! The fact that this is now a reality goes a long way to show how much radio astronomy has changed; and this is just the beginning. The soft X-ray band wins the competition by more than one order of magnitude as the current radio flux density limit is still not as deep as the equivalent one in the X-rays (see Padovani et al., 2015a, and discussion therein). However, it is important to remember that radio observations are unaffected by absorption and therefore are sensitive to all types of AGN, irrespective of their orientation (i.e., Type 1s and Type 2s), unlike soft X-ray ones.

Figure 11 can also be read as describing the “detection potential” of the various bands. The actual number of *detected and identified* AGN is still heavily biased towards the optical/NIR bands, as most of them were discovered through dedicated large-area spectroscopic surveys. For example, of the 510,764 AGN in the Half Million Quasars Catalogue (Flesch, 2015), which includes mostly Type 1 sources, only $\sim 9\%$ and $\sim 11\%$ have been detected in the radio and X-ray bands, respectively. Note that many more sources have been detected (although often not identified) in the radio band. For example, the unified radio catalogue put together by Kimball & Ivezić (2008, 2014)³³ by combining five radio catalogues (FIRST, NVSS, GB6, WENSS, and VLSSr) and the SDSS includes almost three million sources north of -40° . The vast majority of these are going to be AGN, mostly RGs and RL quasars (and there are more radio catalogues covering the sky south of -40°).

7 The future

7.1 New radio facilities

Radio astronomy is at the verge of a revolution, which will usher in an era of large area surveys reaching flux density limits well below current ones. The Square Kilometre Array

³² With the exception of NGC 1068 and NGC 4945, two Seyfert 2 galaxies in which the γ -ray emission is thought to be related to their starburst component (Ackermann et al., 2012b).

³³ http://www.aoc.nrao.edu/~akimball/radiocat_2.0.shtml

(SKA)³⁴, in fact, will offer an observing window between 50 MHz and 20 GHz extending well into the nanoJy (nJy) regime with unprecedented versatility. Phase 1 (SKA1) will constitute about 10% of the full telescope and will take place between 2018 and 2023, with early science observations being conducted as early as 2020 with a partial array. The plan is for SKA1 to be followed by a Phase 2 (SKA2), which will complete the design, and should last until the late 2020s. Around 1 GHz, SKA1 will provide a major advance over existing instruments. Resolution, sensitivity, and survey speed will be an order of magnitude better in most cases, and in combination will occupy a new region of performance.

The SKA will not be the only participant to this revolution. In 2011, a decade long upgrade project has resulted in the VLA expanding greatly its technical capacities and being renamed the “Karl G. Jansky Very Large Array” (JVLA³⁵). LOFAR³⁶ has started operations and is carrying out large area surveys at 15 – 200 MHz (e.g., Morganti et al., 2010; vanWeeren et al., 2014; Heald et al., 2015; Williams et al., 2016), opening up a whole new region of parameter space at low radio frequencies. The Murchison Widefield Array, a low-frequency radio telescope operating between 80 and 300 MHz and one of three telescopes designated as a precursor for the SKA, has also recently become operational and is conducting surveys (Hurley-Walker et al., 2014).

Many other radio telescopes are currently under construction in the lead-up to the SKA, including APERTIF³⁷ (The Netherlands), ASKAP³⁸ (Australia), e-MERLIN³⁹ (UK), and Meerkat⁴⁰ (South Africa), with both ASKAP and Meerkat being the other two of the three telescopes designated as SKA precursors. All these projects will survey the sky vastly faster than is possible with existing radio telescopes producing surveys covering large areas of the sky down to fainter flux densities than presently available, as fully detailed in Norris et al. (2013). Prandoni & Seymour (2015) provide an overview of the radio continuum surveys best suited to enable the top science cases to be tackled by SKA1.

7.2 How many sources, and of what type, will the new radio facilities detect?

7.2.1 Predictions

One would like to have an idea of the number and type of sources likely to be detected by these future deep surveys, for various reasons: 1. predicted surface densities allow one to plan ahead in terms of the sheer number of sources expected; 2. the forecast on the type of sources is important to plan the identification process and particularly to know in advance, which kind of ancillary data will be more relevant.

The “classic” work in this respect is the SKADS (Wilman et al., 2008, 2010), a semi-empirical simulation⁴¹ of the extragalactic radio continuum sky down to 10 nJy at 151, 610 MHz, 1.4, 4.86 and 18 GHz including various source types: RQ AGN, RL AGN (RGs [FR Is and IIs], SSRQs, FSRQs and blazars, and GPS), and SFGs (quiescent and starbursting). Sources are drawn at random from the observed (or suitably extrapolated) radio LFs. As clearly stated in the papers there are numerous uncertainties and limitations in the SKADS simulations, as they had to rely, by necessity, on extrapolations, being based on relatively high flux density samples. This affects particularly the highest redshifts, which can be better probed at fainter flux densities.

Figure 4 shows the SKADS simulated number counts (red dashed line) compared with smoothed versions of the observed counts excluding (solid black line) and including (dotted black line) the Owen & Morrison (2008) sample. (I consider here these two cases separately because the rapid rise observed in the counts for this sample is unique and might be caused by count corrections made for partial resolution of extended sources: Condon et al., 2012; Vernstrom et al., 2016). The agreement between simulations and observations is very good down to 0.1 mJy, which is not surprising as Wilman et al. (2008) did compare their predictions with the data down to this flux density.

Figure 7 shows the SKADS simulated number counts for all sources, SFGs, RL, and RQ AGN. The agreement with the E-CDFS counts is impressively good, for the whole sample but also for all sub-classes, even more so considering the scatter between various surveys shown by Fig. 4. The simulated RL AGN Euclidean normalized counts are dominated (by a factor > 10) by FR I-like sources, in agreement with the observed predominance of jet-mode AGN. Based on the SKADS simulation, a deep survey reaching 1 μ Jy at 1.4 GHz is expected to have a surface density of 6.2×10^4 sources deg^{-2} . Application of eq. 1 using the LFs and evolution derived from the E-CDFS sub-samples gives exactly the same result. The SKADS reaches 10 nJy, while Padovani

³⁴ Everything there is to know about the SKA can be found at <http://www.skatelescope.org>. I give here only a very brief description of the project.

³⁵ <http://science.nrao.edu/facilities/vla>

³⁶ <http://www.astron.nl/radio-observatory/astronomers/lofar-astronomers>

³⁷ <http://www.astron.nl/general/apertif/apertif>

³⁸ <http://www.atnf.csiro.au/projects/askap/>

³⁹ <http://www.e-merlin.ac.uk>

⁴⁰ <http://www.ska.ac.za/meerkat>

⁴¹ The simulation is accessible at http://s-cubed.physics.ox.ac.uk/s3_sex.

(2011) gives *order of magnitude* surface densities down to even smaller flux densities (< 1 nJy).

Another, very different approach to estimate the number of faint sources is the so-called P(D) method (or probability of deflection: Scheuer, 1957), which uses background fluctuations to model the source counts below the limit of a given survey (e.g., Vernstrom et al., 2014, and references therein). Vernstrom et al. (2015) quote a value of 8.9×10^4 sources deg^{-2} for $S_{1.4\text{GHz}} \geq 1 \mu\text{Jy}$, based on Vernstrom et al. (2014). The $\sim 40\%$ difference with the SKADS results (visible also in Fig. 4) is likely due to the (known) limitations of the SKADS simulation.

What type of sources will populate the faint radio sky? Figs. 7 and 8 already hint at the answer: the fraction of SFGs is clearly on the rise, while that of AGN is decreasing overall. This is quantified by the SKADS simulation, which predicts that down to $S_{1.4\text{GHz}} = 1 \mu\text{Jy}$ 80% of the sources will be SFGs, followed by RQ (12%) and RL AGN (8%). Quite similar fractions ($\sim 84\%$, 11% , and 4%) are obtained from the E-CDFS LF and evolution. To the best of our knowledge, therefore, a deep survey reaching $\sim 1 \mu\text{Jy}$ at ~ 1 GHz over 30 deg^2 will detect $\sim 4 \times 10^5$ “potential” AGN (Smolčić et al., 2015), i.e., of the same order of *all* currently known AGN (and candidates) included in the Million Quasars catalogue⁴² and with a surface density roughly equal to that of (current) X-ray selected AGN (Fig. 11). The Evolutionary Map of the Universe (EMU), one of the ASKAP surveys, expects to reach flux densities ~ 2 times larger than those of the E-CDFS over $\sim 3/4$ of the sky, detecting ~ 70 million sources, about half of which will be “potential” AGN (Norris et al., 2011). The “potential” here is important because, as detailed above, the classification of faint radio sources requires a great deal of ancillary, multi-wavelength information, which will not be easy to get at very faint levels or over very large areas, as I am going to discuss now.

7.2.2 Source classification in the era of the SKA and its precursors

It took more than thirty years to figure out the source population of the $\lesssim 1$ mJy radio sky because source classification was complex but above all because the relevant, and necessary, data at other wavelengths were not available (Sect. 5.1 and 5.2). What will the situation be for the $\lesssim 1 \mu\text{Jy}$ (GHz) sky? To answer this question, based on Sect. 5.1, one needs first to have at least order of magnitude estimates of the X-ray, optical/NIR, and MIR – FIR fluxes sub- μJy radio sources are likely to have (where the X-ray, MIR – FIR, and optical/NIR data are needed for source classification and photometric/spectroscopic redshifts respectively). The cur-

rent and, above all, future availability of the relevant multi-wavelength data needs then to be evaluated⁴³.

In the X-ray band, sources with $S_{1.4\text{GHz}} \sim 1 \mu\text{Jy}$ should have $f_{0.5-2\text{keV}} \approx 10^{-17}$, $\approx 10^{-18}$, and well below $10^{-18} \text{ erg cm}^{-2} \text{ s}^{-1}$ for RQ AGN, SFGs, and RL AGN respectively. The deepest X-ray survey currently available is the 4 Ms CDFS, which reaches $f_{0.5-2\text{keV}} \sim 5 \times 10^{-18} \text{ erg cm}^{-2} \text{ s}^{-1}$ over $\sim 0.1 \text{ deg}^2$ (Lehmer et al., 2012); the results of further 3 Ms of data should be available soon (Luo et al., in preparation). The *Athena* mission, selected by the European Space Agency (ESA) as the L2 mission (due for launch in 2028), will reach $f_{0.5-2\text{keV}} \sim 2 \times 10^{-17} \text{ erg cm}^{-2} \text{ s}^{-1}$ in 1 Ms (Barcons et al., 2015) but given its survey speed will be able to cover larger areas much more efficiently than *Chandra*. At these levels, however, *Athena* is not only background but also confusion limited and integrating further will not improve the sensitivity (A. Rau, private communication). This means that even *Athena* surveys will not detect the bulk of the $\gtrsim 1 \mu\text{Jy}$ population (which will likely be made up of SFGs). Below this flux density, very few, if any, radio sources will have an X-ray counterpart in the foreseeable future, as there is no X-ray mission, existent or planned, capable of detecting them.

As regards the MIR – FIR bands *Spitzer*, by reaching $f_{24\mu\text{m}} \approx 40 \mu\text{Jy}$ in the GOODS fields, can detect now SFGs down to $S_{1.4\text{GHz}} \approx 2 \mu\text{Jy}$ (Sect. 5.2). The Space Infrared Telescope for Cosmology and Astrophysics (SPICA), which is under consideration as a medium-class mission under the framework of the ESA Cosmic Vision with a target launch in the mid-2020s, will have a $24 \mu\text{m}$ continuum sensitivity $\sim 10 - 50 \mu\text{Jy}$ (1 hr, 5σ) and in the FIR band will improve upon *Herschel* by almost two orders of magnitude (Nakagawa et al., 2015). The bulk of the $\gtrsim 1 \mu\text{Jy}$ population should then be easily detected in the MIR (and perhaps FIR) band, while deep SPICA exposures should be able to detect many radio sources at $S_{1.4\text{GHz}} \lesssim 0.1 \mu\text{Jy}$.

What does this mean in practice for source classification? Identification of RL AGN should be possible down to $S_{1.4\text{GHz}} \approx 0.1 \mu\text{Jy}$, but these sources are likely to constitute only a minority ($\lesssim 5\%$) of the population. Separation of the (expected small fraction of) RQ AGN from the SFGs will be hard for $S_{1.4\text{GHz}} \gtrsim 1 \mu\text{Jy}$ and impossible at fainter flux densities. At brighter radio flux densities classification will be possible but not on the very large areas covered, e.g., by the EMU survey. Note that the SKA will provide the sub-arcsec resolution essential for disentangling emission from SF and AGN activity (e.g., McAlpine et al., 2015). Nevertheless, this will not solve the classification problem if both coexist in RQ AGN, as discussed in Sect. 6.2.

⁴² <http://quasars.org/milliquas.htm>.

⁴³ I performed both tasks in Padovani (2011), whose main results I summarise and update here. Needless to say, the sensitivities of future facilities are inherently uncertain, especially if the latter have not yet been approved for construction.

As regards the optical/NIR bands, the HUDF reaches $AB \sim 29$ (B to z) over 11 arcmin^2 . The Wide-Field InfraRed Survey Telescope (WFIRST), a NASA space mission under study for launch in 2024, includes a wide-field NIR camera to perform surveys with HST-style imaging and sensitivity, but further in the IR and with hundreds of times the sky coverage (Gehrels et al., 2015). The Large Synoptic Survey Telescope (LSST)⁴⁴, which will be located in Chile, will provide a survey of about half the sky down to $R_{\text{mag}} \sim 27.5$ during 10 years of operation, starting around 2021. This means that the bulk of the $1 \mu\text{Jy}$ population (which should have radio-to-optical flux density ratios $R \lesssim 10$) should be detected by the LSST, i.e., it will have a counterpart in a large area survey, and will be well within the sensitivity of WFIRST. For fainter radio samples optical magnitudes should get fainter, which will make things more difficult, but the precise values depend also on the role that dwarf galaxies and low power ellipticals will play, which is hard to predict (Sect. 7.3.4).

Sources having $R_{\text{mag}} > 27.5$ will be within reach of the James Webb Space Telescope (JWST)⁴⁵, due for launch in 2018, and the Extremely Large Telescopes (ELTs)⁴⁶, with diameters between 25 and 39 m and “first light” expected in the mid-2020s, which however will be covering relatively small fields of view (up to $\approx 0.2 \text{ deg}^2$ for the smallest ELT). It might turn out that WFIRST, JWST, and the ELTs will be the main (only?) facilities to secure optical counterparts of nJy radio sources.

Finally, as regards photometric/spectroscopic redshifts, many of the $S_{1.4\text{GHz}} \gtrsim 1 \mu\text{Jy}$ sources might be too faint for current 8/10 m telescopes to be able to provide a redshift and the situation will get worse at fainter flux densities. This means that JWST and the ELTs might be the main facilities to secure redshifts of μJy radio sources but even they could have problems in the nJy regime. Redshifts could also be obtained through radio HI observations. For example, in 10,000 hours SKA1 should find ≈ 5 million HI galaxies up to $z \sim 0.5$, while SKA2 should detect ≈ 1 billion HI galaxies up to $z \sim 2$ (Abdalla et al., 2015; Santos et al., 2015).

I note that Prandoni & Seymour (2015) have listed facilities and surveys, which will complement the proposed SKA1 surveys. These include imaging and spectroscopic surveys from optical to FIR wavelengths (see their Table 5).

7.3 The astrophysical impact of future radio observations

The new radio facilities described in Sect. 7.1 will undoubtedly revolutionise radio astronomy and will have a huge impact on astrophysics. Readers interested in the research the SKA will foster, for example, can consult the $\sim 2,000$ page volume *Advancing Astrophysics with the Square Kilometre Array*⁴⁷. Here I want to give a small (somewhat biased) flavour of the topics where we can expect major advances in the next few years.

7.3.1 SFGs and cosmic star formation history

In Sect. 6.1.1 I have discussed the importance of studying the cosmic SF history and how, so far, radio surveys have only played a marginal role in this field, for reasons to do mostly with sensitivity. This is going to change quite soon, as detailed in Jarvis et al. (2015). A 100 nJy limit at 1.4 GHz , for example, would detect a galaxy with a $\text{SFR} \sim 20 \text{ M}_{\odot} \text{ yr}^{-1}$ at $z \sim 7$, pushing the radio band at the forefront in terms of sensitivity to SFR in comparison to other bands (see Fig. 1a of Madau & Dickinson, 2014). Said differently, the SKA might provide the most robust measurement of the SF history of the Universe. And a $\sim 1 \mu\text{Jy}$ limit, easily reachable by some of the SKA precursors, would imply a sensitivity to $\sim 50 - 100 \text{ M}_{\odot} \text{ yr}^{-1}$ at $z \sim 6$ (Jarvis et al., 2015), which is already very good.

Madau & Dickinson (2014) quote the difficulty of distinguishing SFGs from AGN in faint radio surveys as a problem in utilizing radio data but this issue is under control, at least for $S_{1.4\text{GHz}} \gtrsim 1 \mu\text{Jy}$ (Sects. 5.1 and 7.2.2). Furthermore, already down to $S_{1.4\text{GHz}} \sim 30 \mu\text{Jy}$ the fraction of RL AGN is only $\sim 10\%$ (Fig. 8) and radio emission in sub-mJy RQ AGN appears to be mainly related to SF processes (Sect. 6.2). Deeper radio surveys, therefore, are expected to include mostly SF-related emitters ($\gtrsim 90\%$ for $S_{1.4\text{GHz}} \gtrsim 1 \mu\text{Jy}$; Sect. 7.2.1), which would also make the identification process much simpler and provide a clean(ish) sample for dealing with this topic.

7.3.2 Galaxy evolution

A huge amount of effort has been devoted in the past few years to study galaxy evolution (e.g., Somerville & Davé, 2015, for a theoretical perspective but also many references to observational work). Radio astronomy should play a stronger role in it (although it has provided jet-mode feedback to the modellers: e.g., Croton et al., 2006). As mentioned in Sect. 6.1.2, Best et al. (2014) has been one of the very few papers to link the observed evolution of jet-mode RL AGN to that of quiescent galaxies. Future radio surveys will provide us with plentiful data and it is imperative that a

⁴⁴ <http://www.lsst.org>

⁴⁵ <http://www.stsci.edu/jwst/>

⁴⁶ These include, in order of decreasing diameter size, the European Extremely Large Telescope (E-ELT; <http://www.eso.org/sci/facilities/eelt/>), the Thirty Meter Telescope (TMT; <http://www.tmt.org/>), and the Giant Magellan Telescope (GMT; <http://www.gmto.org/>).

⁴⁷ Available at <https://www.skatelescope.org/books/>.

stronger connection is built between the evolution of radio sources and that of the general population of galaxies, as has been done, for example, for the RQ AGN population and SFGs (e.g. Hickox et al., 2014; Caplar, Lilly, & Trakhtenbrot, 2015).

We also need to be careful about how to interpret radio data in this respect. In Sect. 5.5.2 I have discussed the finding by Rigby et al. (2015) that the number density of more luminous RL AGN peaks at redshifts higher than those of lower luminosity objects, as found in many other bands. Yuan et al. (2016) have shown that this (apparently) complex behaviour displayed by the steep-spectrum radio sources studied by Rigby et al. (2015) can be easily reproduced by a simple combination of DE and LE. The main idea, very simple in retrospect, is that for a population having a two power-law LF (which is always flat at low powers and steep at high powers), as is the case for RL AGN, the inferred turnover redshift for low-luminosity sources will be lower than that of high-luminosity sources, mimicking a luminosity-dependent density evolution (see their Fig. 3). The very strong implication is that there appears to be no need for different evolution for the low- and high-power RL AGN, which has been the mantra in radio astronomy for many years. This work deserves to be followed up.

7.3.3 Why do RL AGN exist?

The first quasars to be discovered were very strong radio sources. More than fifty years later, we have realised that most AGN are not. But we still do not know why! Said differently, the question “Why do only a minority of galaxies that contain an AGN have jets?” is still unanswered. Without clearing this out first, it is going to be very hard to make progress on galaxy evolution as a whole from a radio perspective (Sect. 7.3.2).

Many papers have been devoted to the issue of the possible bimodality of the radio-to-optical flux density ratio R and/or radio power in quasars (see Baloković et al., 2012, for a recent analysis of, and many references on, this topic). I do not think that this is the real question to ask (see also Condon et al., 2013), and even if a bimodality were to be found it would not answer the fundamental question “Are there really two quasar populations?”⁴⁸. In any case, the answer here is already a definite “yes” (see Sect. 2.3).

The basic issue, therefore, is not if there are or not two AGN populations but why, which takes us back to my original question. There appears to be some interesting differences between RL and RQ AGN, which should help us in answering this question (see also Tadhunter, 2016, for a detailed discussion of the first two topics below for $z < 0.7$ sources). Namely:

- *Environment/Mergers*. RGs appear to be significantly more clustered than normal galaxies. In a sphere of 2 Mpc centred on the RG, the galaxy density is 2.7 times greater than around normal galaxies (e.g., van Velzen et al., 2012). And Chiaberge et al. (2015) find that, at $z > 1$, $\sim 92\%$ of RGs are associated with recent or ongoing merger, while for matched RQ samples this fraction is only $\sim 38\%$.
- *Host galaxy (type and mass)*. Apart from the differences in host galaxies between RL and RQ AGN discussed in Sect. 2.3, the fraction of galaxies that host RL AGN with $P_{1.4\text{GHz}} > 10^{23} \text{ W Hz}^{-1}$ is a strong function of M_* , rising from ~ 0 for $M_* < 10^{10} M_\odot$ to $\gtrsim 30\%$ at $M_* > 5 \times 10^{11} M_\odot$, with a very strong dependence $\propto M_*^{2.5}$ (e.g., Best et al., 2005b). Given the well-known correlation between M_{BH} and M_* (or more likely $M_{*,\text{bulge}}$: e.g., Kormendy & Ho, 2013), this implies also that the black hole masses of RL AGN are larger than those of RQ AGN.
- *Optical properties*. In a series of papers, Sulentic, Marziani and collaborators, building also on previous work, have proposed a four-dimensional parameter space (4D eigenvector 1 [4DE1] based on optical, UV and X-ray spectroscopic properties) in an effort to unify quasar diversity and an alternate population A–B dichotomy (e.g., Sulentic, Marziani, & Zamfir, 2011, and references therein). The optical plane of this 4DE1 parameter space involves the FWHM of broad $H\beta$ and the ratio of the equivalent widths of the Fe II $\lambda 4570$ blend and of the broad $H\beta$ line (R_{FeII}). Pop. A ($\text{FWHM}(H\beta)_{\text{BC}} < 4,000 \text{ km s}^{-1}$) is largely RQ, while Pop. B ($\text{FWHM}(H\beta)_{\text{BC}} > 4,000 \text{ km s}^{-1}$) includes most RL sources and a significant number of spectroscopically indistinguishable RQ objects. This suggests that RL quasars show significant structural and kinematic differences from the majority of RQ sources. The interpretation of the distribution of sources on the optical plane is that the average L/L_{Edd} increases with R_{FeII} , while the dispersion in $\text{FWHM}(H\beta)_{\text{BC}}$ at fixed R_{FeII} is largely an orientation effect (see also Shen & Ho, 2014). In addition, the RL population shifts to larger $\text{FWHM}(H\beta)_{\text{BC}}$ and lower R_{FeII} compared to the RQ population, albeit with a large overlap with RQ sources, as shown in Fig. 12 (from Zamfir, Sulentic, & Marziani, 2008). This is consistent with the notion that RL quasars preferentially reside in more massive and lower L/L_{Edd} systems.

Black hole spin has also been suggested to be different between RL and RQ AGN (e.g., Wilson & Colbert, 1995; Garofalo, Evans, & Sambruna, 2010). Unfortunately, reliable measurements of the black hole spin in AGN are still not available for sizeable and well-selected samples.

RL AGN appear then to be more clustered, undergoing mergers, reside in more massive, bulge-dominated galaxies, display broader $H\beta$, and have lower L/L_{Edd} (and perhaps spin faster or in any case differently) than RQ AGN. As

⁴⁸ By saying “quasar” I refer here only to radiative-mode AGN

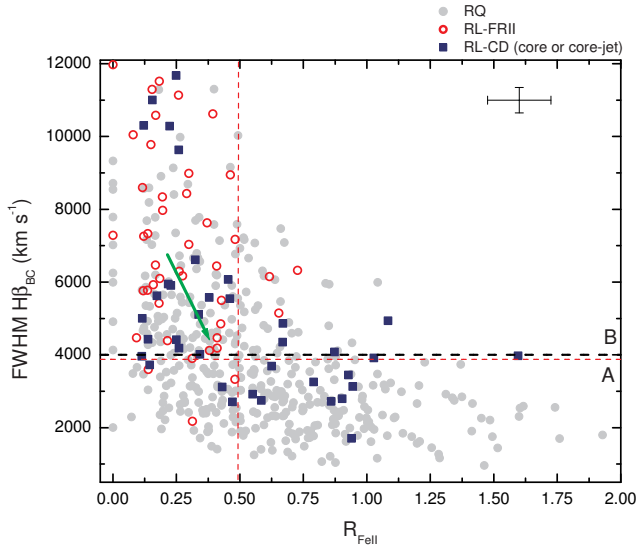


Fig. 12 RL and RQ quasars in the optical plane of the 4DE1 parameter space. RL-FRII are double-lobed quasars, i.e., SSRQs, while RL-CD are core-dominated quasars, i.e., FSRQs. The green arrow indicates the displacement between the median $\text{FWHM}(\text{H}\beta_{\text{BC}})$ and the median R_{FeII} for the two RL classes. The solid light grey symbols are RQ objects. In the upper right corner are indicated the typical 2σ errors. The red dotted lines show the boundaries for the RL/RQ separation based on a 2D Kolmogorov - Smirnov test. Figure reproduced from Zamfir, Sulentic, & Marziani (2008), Fig. 4, with permission.

usual in these cases it would be important to consider the various, sometimes subtle, selection effects that can plague these studies. Nevertheless, if these differences are real, the reason why their combination might explain the presence of jets is still not clear (at least to me!).

We *have* to take advantage of the flood of radio-selected AGN we are going to discover in the near future to tackle, once and for all, this problem.

7.3.4 And more

Based on Sect. 7.2.1 I think that our understanding of what types of sources to expect down to $S_{1.4\text{GHz}} \approx 1 \mu\text{Jy}$ is relatively robust. Below that flux density our vision is more blurred, for obvious reasons. There are however some populations, which are noticeably missing from the simulations but that we know have to be there⁴⁹.

Known unknowns.

The first population is that of low radio power ellipticals. It has been known for quite some time that ellipticals of similar optical luminosity vary widely in radio power. For example, Capetti et al. (2009) have shown that 82% of early-type galaxies in the Virgo cluster with $B_T < 14.4$ are undetected at a flux density limit of $\sim 0.1 \text{ Jy}$, which implies core

radio powers $P_{8.4\text{GHz}} < 4 \times 10^{18} \text{ W Hz}^{-1}$. More recently, Nyland et al. (2016) have studied with the JVLA the nuclear radio emission of a representative subset of the ATLAS^{3D} survey of local early-type galaxies. They detected 51% of their galaxies down to a 5 GHz limit of $\sim 75 \mu\text{Jy}$ with radio powers as low as $10^{18} \text{ W Hz}^{-1}$. These radio faint ellipticals are *not* represented in models of the sub- μJy sky: for example, the lower limit of the RL AGN LF in Wilman et al. (2008) corresponds to $P_{1.4\text{GHz}} \sim 3 \times 10^{20} \text{ W Hz}^{-1}$. Sources with lower powers have $S_{1.4\text{GHz}} > 1 \mu\text{Jy}$ only for $z < 0.3$ (Fig. 5); and a $P_{1.4\text{GHz}} = 10^{18} \text{ W Hz}^{-1}$ object at $z = 1$, for example, will have $S_{1.4\text{GHz}} \sim 0.2 \text{ nJy}$.

The other missing population is that of dwarf galaxies, which are very faint and constitute *the most numerous* extragalactic population. This class includes dwarf spheroidals and ellipticals, dwarf irregulars, and blue compact dwarf galaxies, which all have radio powers reaching $P_{1.4\text{GHz}} < 10^{18} \text{ W Hz}^{-1}$, i.e., below the lower limit of the SFG LF of the simulations of Wilman et al. (2008), which by construction do not include dwarf/irregular galaxies.

The (scanty) available data imply flux density limits $\approx 1 \text{ nJy}$ for both low-power ellipticals and dwarfs, with surface densities comparable to those of RQ AGN and SFGs respectively. Both these classes should therefore be playing a major role in the sub- μJy sky but at present it is hard to be more specific.

Unknown unknowns.

There is also what we do not know, or do not expect to find, or still do not understand, which could be substantial especially at very faint flux densities.

The balloon-borne Absolute Radiometer for Cosmology, Astrophysics and Diffuse Emission (ARCADE2; Fixsen et al., 2011) experiment has measured a sky brightness temperature at 3 GHz ~ 5 times that expected from known populations of radio sources (de Zotti et al., 2010; Seiffert et al., 2011). This means that either there is a population of discrete radio sources with properties somewhat different from those of the faint end of the distribution of known sources or residual emission from our own Galaxy has not been modelled properly (Seiffert et al., 2011). In the former case, this new population has to be exceptionally numerous ($> 10^{13}$ over the all sky), not associated with known galaxies, and with $S_{1.4\text{GHz}} \lesssim 0.03 \mu\text{Jy}$ (Condon et al., 2012). In short, there might be still room for some surprises.

Finally, as stressed by Norris et al. (2013), whenever a new facility has sampled unexplored parts of the observational phase space (be it in frequency, resolution, time domain, area of sky, etc.), many unexpected great discoveries in astronomy have been made, very often not by testing a hypothesis, but just by observing the sky in an innovative way and with an open mind. I am sure the sub- μJy sky will be no exception.

⁴⁹ I have discussed two of them in Padovani (2011) and summarise the main points here.

8 Conclusions

At this point, it should be clear to all astronomers that the faint radio sky plays a vibrant role in a variety of astrophysical topics, including the cosmic star formation history, galaxy evolution, the existence of powerful jets, and radio emission in RQ AGN. This role will grow even further in the near future. Radio observations are also unaffected by absorption, which means, for example, that they are sensitive to all types of AGN, irrespective of obscuration and orientation (i.e., Type 1s and Type 2s).

I conclude this review by sending the following:

8.1 Messages to all astronomers

1. Do not assume that *radio-detected* means *radio-loud*. While this was almost always true when radio surveys only reached the \approx Jy level, this is no longer the case, quite the opposite: a sub-mJy AGN is more likely to be RQ than RL!
2. The “radio-quiet AGN” label is obsolete, misleading, and wrong. The major difference between RL and RQ AGN is, based on the available evidence, the presence or lack of *strong* (relativistic) jets, which in practice translates into them being off or on the FIR – radio correlation. I therefore propose that we start using “jetted AGN” and “non-jetted” AGN. This name has been used already (albeit very sparsely) in the literature⁵⁰. I think it is high time it becomes the norm.
3. Do not look for a bimodality in R or P_r in quasars, as we already know that there are two main classes of AGN: jetted and non-jetted.
4. Most importantly: radio astronomy is not a “niche” activity but is extremely relevant to a whole range of extragalactic studies related, for example, to star formation and galaxy evolution. Take advantage of that and use radio data!

8.2 Messages to radio astronomers

1. The flattening of deep normalized radio counts is not an open issue: we have sorted out the source population of the sub-mJy GHz radio sky and learnt that below \approx 0.1 mJy the radio sky is dominated by SF related processes. This process took more than thirty years because the multi-wavelength data necessary to properly classify sources were not available and radio astronomy was ahead of the other bands. History does not have to repeat itself, although there is some risk that this might

happen. This can be avoided if radio astronomers understand that ...

2. ... radio astronomy is now a fully multi-wavelength enterprise. This is also evinced by the fact that about one third of the papers referenced in this review are *not* radio papers. The full, proper exploitation of data from the SKA and its precursors will *require* (this is not an option!) synergy with other contemporaneous astronomical facilities. These will include, among others, *Athena*, WFIRST, the LSST, the ELTs, JWST, and SPICA.

Acknowledgements I thank Roberto Assef, Angela Bongiorno, Alessandro Capetti, Renato Falomo, Luigina Feretti, Roberto Gilli, Paolo Giommi, Chris Hales, Evanthia Hatziminaoglou, Darshan Kakkad, Robert Laing, Vincenzo Mainieri, Arne Rau, Gordon Richards, an anonymous referee, and particularly Ken Kellermann, for helpful comments and discussions, and the rest of the E-CDFS team, especially Margherita Bonzini, Neal Miller, and Paolo Tozzi, for the work done together over the past few years. Isabella Prandoni kindly provided me with most of the data points in Fig. 4 and the simulated number counts from the SKADS. I also greatly benefited from the NASA’s Astrophysics Data System.

Abbreviations

3CRR	Third Cambridge Catalogue of Radio Sources
6dFGS	6 degree Field Galaxy Survey
AGN	Active Galactic Nuclei
ALMA	Atacama Large Millimeter/submillimeter Array
ARCADE2	Absolute Radiometer for Cosmology, Astrophysics and Diffuse Emission
BL Lacs	BL Lacertae objects
CSS	Compact steep-spectrum
E-CDFS	Extended Chandra Deep Field South
E-ELT	European Extremely Large Telescope
ELT	Extremely Large Telescope
EMU	Evolutionary Map of the Universe
ESA	European Space Agency
FIR	Far-IR
FR	Fanaroff-Riley
FSRQ	Flat-spectrum radio quasar
FWHM	Fullwidth half maximum
GMT	Giant Magellan Telescope
GOODS	Great Observatories Origins Deep Survey
GPS	GHz peaked-spectrum
HERG	High-excitation radio galaxy
HUDF	Hubble Ultra Deep Field
IR	Infrared
IRAC	Infrared Array Camera
IRAS	Infrared Astronomical Satellite
ISO	Infrared Space Observatory
JVLA	Karl G. Jansky Very Large Array
JWST	James Webb Space Telescope
Jy	Jansky

⁵⁰ At the time of writing (mid-2016) I have found 16 refereed papers with the words “jetted AGN” in their abstract.

LERG	Low-excitation radio galaxy
LF	Luminosity function
LOFAR	LOW Frequency ARray
LSST	Large Synoptic Survey Telescope
MIR	Mid-IR
NIR	Near-IR
NRAO	National Radio Astronomy Observatory
NVSS	NRAO VLA Sky Survey
PACS	Photoconductor Array Camera and Spectrometer
PDE	Pure density evolution
PLE	Pure luminosity evolution
R	Radio-to-optical flux density ratio
RG	Radio Galaxy
RL	Radio-loud
RQ	Radio-quiet
S/N	Signal-to-noise
SB	Starburst galaxy
SDSS	Sloan Digital Sky Survey
SED	Spectral energy distribution
SF	Star formation
SFG	Star-forming galaxy
SFR	Star formation rate
SFRD	Star formation rate density
SKA	Square Kilometre Array
SKADS	SKA Design Study
SPICA	Space Infrared Telescope for Cosmology and Astrophysics
SSRQ	Steep-spectrum radio quasar
SUMSS	Sydney University Molonglo Sky Survey
TMT	Thirty Meter Telescope
UV	Ultraviolet
VLA	Very Large Array
VLBI	Very long baseline interferometry
WFIRST	Wide-Field InfraRed Survey Telescope

References

- Abdalla F. B., Bull P., Camera S., Benoit-Lévy A., Joachimi B., Kirk D., Kloeckner H. R., Maartens R., et al. (2015) Cosmology from HI galaxy surveys with the SKA. *Advancing Astrophysics with the Square Kilometre Array (AASKA14)* 17
- Acero F., Ackermann M., Ajello M., Albert A., Atwood W. B., Axelsson M., Baldini L., Ballet J., et al. (2015) Fermi Large Area Telescope Third Source Catalog. *Astrophys J Suppl* 218: 23. doi:10.1088/0067-0049/218/2/23
- Ackermann M., Ajello M., Allafort A., Baldini L., Ballet J., Barbiellini G., Bastieri D., Bechtol K., et al. (2012a) Search for Gamma-ray Emission from X-Ray-selected Seyfert Galaxies with Fermi-LAT. *Astrophys J* 747: 104. doi:10.1088/0004-637X/747/2/104
- Ackermann M., Ajello M., Allafort A., Baldini L., Ballet J., Bastieri D., Bechtol K., Bellazzini R., et al. (2012b) GeV Observations of Star-forming Galaxies with the Fermi Large Area Telescope. *Astrophys J* 755: 164. doi:10.1088/0004-637X/755/2/164
- Antonucci R. (1993) Unified models for active galactic nuclei and quasars. *Annu Rev Astron Astr* 31: 473-521. doi:10.1146/annurev.aa.31.090193.002353
- Antonucci R. (2012) A panchromatic review of thermal and nonthermal active galactic nuclei. *Astronom and Astrophys Trans* 27: 557-602.
- Baade W., Minkowski R. (1954) On the Identification of Radio Sources. *Astrophys J* 119: 215-231. doi:10.1086/145813
- Baldi R. D., Capetti A. (2010) Spectro-photometric properties of the bulk of the radio-loud AGN population. *Astron Astrophys* 519: A48. doi:10.1051/0004-6361/201014446
- Baldi R. D., Capetti A., Giovannini G. (2015) Pilot study of the radio-emitting AGN population: the emerging new class of FR 0 radio-galaxies. *Astron Astrophys* 576: A38. doi:10.1051/0004-6361/201425426
- Baldwin J. A., Phillips M. M., Terlevich R. (1981) Classification parameters for the emission-line spectra of extragalactic objects. *Publications Astron Soc Pacific* 93: 5-19. doi:10.1086/130766
- Balmaverde B., Capetti A. (2006) The host galaxy/AGN connection in nearby early-type galaxies. Is there a miniature radio-galaxy in every "core" galaxy?. *Astron Astrophys* 447: 97-112. doi:10.1051/0004-6361:20054031
- Baloković M., Smolčić V., Ivezić Ž., Zamorani G., Schinnerer E., Kelly B. C. (2012) Disclosing the Radio Loudness Distribution Dichotomy in Quasars: An Unbiased Monte Carlo Approach Applied to the SDSS-FIRST Quasar Sample. *Astrophys J* 759: 30. doi:10.1088/0004-637X/759/1/30
- Barcons X., Nandra K., Barret D., den Herder J.-W., Fabian A. C., Piro L., Watson M. G., the Athena Team, et al. (2015) Athena: the X-ray observatory to study the hot and energetic Universe. *Journal of Physics Conference Series* 610: 012008. doi:10.1088/1742-6596/610/1/012008
- Barthel P. D. (1989) Is every quasar beamed?. *Astrophys J* 336: 606-611. doi:10.1086/167038
- Beckwith S. V. W., Stiavelli M., Koekemoer A. M., Caldwell J. A. R., Ferguson H. C., Hook R., Lucas R. A., Bergeron L. E., et al. (2006) The Hubble Ultra Deep Field. *Astronom J* 132: 1729-1755. doi:10.1086/507302
- Bell E. F. (2003) Estimating Star Formation Rates from Infrared and Radio Luminosities: The Origin of the Radio-Infrared Correlation. *Astrophys J* 586: 794-813. doi:10.1086/367829
- Best P. N., Kauffmann G., Heckman T. M., Ivezić Ž. (2005a) A sample of radio-loud active galactic nuclei in the Sloan Digital Sky Survey. *MNRAS* 362: 9-24. doi:10.1111/j.1365-2966.2005.09283.x
- Best P. N., Kauffmann G., Heckman T. M., Brinchmann J., Charlot S., Ivezić Ž., White S. D. M. (2005b) The host galaxies of radio-loud active galactic nuclei: mass dependences, gas cooling and active galactic nuclei feedback. *MNRAS* 362: 25-40. doi:10.1111/j.1365-2966.2005.09192.x
- Best P. N., Ker L. M., Simpson C., Rigby E. E., Sabater J. (2014) The cosmic evolution of radio-AGN feedback to $z = 1$. *MNRAS* 445: 955-969. doi:10.1093/mnras/stu1776
- Béthermin M., Dole H., Beelen A., Aussel H. (2010) Spitzer deep and wide legacy mid- and far-infrared number counts and lower limits of cosmic infrared background. *Astron Astrophys* 512: A78. doi:10.1051/0004-6361/200913279
- Biggs A. D., Ivison R. J. (2006) A catalogue of μ Jy radio sources in northern legacy fields. *MNRAS* 371: 963-971. doi:10.1111/j.1365-2966.2006.10730.x
- Bolton J. G., Stanley G. J., Slee O. B. (1949) Positions of Three Discrete Sources of Galactic Radio-Frequency Radiation. *Nature* 164: 101-102. doi:10.1038/164101b0
- Bondi M., Ciliegi P., Schinnerer E., Smolčić V., Jahnke K., Carilli C., Zamorani G. (2008) The VLA-COSMOS Survey. III. Further Catalog Analysis and the Radio Source Counts. *Astrophys J* 681: 1129-1135. doi:10.1086/589324
- Bongiorno A., Mignoli M., Zamorani G., Lamareille F., Lanzuisi G., Miyaji T., Bolzonella M., Carollo C. M., et al. (2010) The [O III] emission line luminosity function of optically selected type-2 AGN

- from zCOSMOS. *Astron Astrophys* 510: A56. doi:10.1051/0004-6361/200913229
- Bonzini M., Mainieri V., Padovani P., Kellermann K. I., Miller N., Rosati P., Tozzi P., Vattakunnel S., et al. (2012) The Sub-mJy Radio Population of the E-CDFS: Optical and Infrared Counterpart Identification. *Astrophys J Suppl* 203: 15. doi:10.1088/0067-0049/203/1/15
- Bonzini M., Padovani P., Mainieri V., Kellermann K. I., Miller N., Rosati P., Tozzi P., Vattakunnel S., et al. (2013) The sub-mJy radio sky in the Extended Chandra Deep Field-South: source population. *MNRAS* 436: 3759-3771. doi:10.1093/mnras/stt1879
- Bonzini M., Mainieri V., Padovani P., Andreani P., Berta S., Bethermin M., Lutz D., Rodighiero G., et al. (2015) Star formation properties of sub-mJy radio sources. *MNRAS* 453: 1079-1094. doi:10.1093/mnras/stv1675
- Brandt W. N., Alexander D. M. (2015) Cosmic X-ray surveys of distant active galaxies. The demographics, physics, and ecology of growing supermassive black holes. *Astron Astrophys Rev* 23: 1. doi:10.1007/s00159-014-0081-z
- Capetti A., Kharb P., Axon D. J., Merritt D., Baldi R. D. (2009) A Very Large Array Radio Survey of Early-Type Galaxies in the Virgo Cluster. *Astronom J* 138: 1990-1997. doi:10.1088/0004-6256/138/6/1990
- Capetti A., Raiteri C. M. (2015) Looking below the floor: constraints on the AGN radio luminosity functions at low power. *MNRAS* 449: L128-L131. doi:10.1093/mnras/slv030
- Caplar N., Lilly S. J., Trakhtenbrot B. (2015) AGN Evolution from a Galaxy Evolution Viewpoint. *Astrophys J* 811: 148. doi:10.1088/0004-637X/811/2/148
- Chi S., Barthel P. D., Garrett M. A. (2013) Deep, wide-field, global VLBI observations of the Hubble deep field north (HDF-N) and flanking fields (HFF). *Astron Astrophys* 550: A68. doi:10.1051/0004-6361/201220783
- Chiaberge M., Capetti A., Celotti A. (1999) The HST view of FR I radio galaxies: evidence for non-thermal nuclear sources. *Astron Astrophys* 349: 77-87
- Chiaberge M., Macchetto F. D., Sparks W. B., Capetti A., Allen M. G., Martel A. R. (2002) The Nuclei of Radio Galaxies in the Ultraviolet: The Signature of Different Emission Processes. *Astrophys J* 571: 247-255. doi:10.1086/339846
- Chiaberge M., Gilli R., Lotz J. M., Norman C. (2015) Radio Loud AGNs Are Mergers. *Astrophys J* 806: 147. doi:10.1088/0004-637X/806/2/147
- Cilieggi P., Zamorani G., Hasinger G., Lehmann I., Szokoly G., Wilson G. (2003) A deep VLA survey at 6 cm in the Lockman Hole. *Astron Astrophys* 398: 901-918. doi:10.1051/0004-6361:20021721
- Comastri A., Gilli R., Hasinger G. (2005) Rolling down from the 30 keV peak: Modelling the Hard X-Ray and γ -Ray Backgrounds. *Experimental Astronomy* 20: 41-47. doi:10.1007/s10686-006-9041-6
- Condon J. J. (1984) Cosmological evolution of radio sources found at 1.4 GHz. *Astrophys J* 284: 44-53. doi:10.1086/162382
- Condon J. J., Mitchell K. J. (1984) A deeper VLA survey of the $\alpha = 08^h52^m15^s$, $\delta = +17^\circ 16'$ arcmin field. *Astronom J* 89: 610-617. doi:10.1086/113556
- Condon J. J. (1989) The 1.4 gigahertz luminosity function and its evolution. *Astrophys J* 338: 13-23. doi:10.1086/167176
- Condon J. J. (1992) Radio emission from normal galaxies. *Annu Rev Astron Astr* 30: 575-611. doi:10.1146/annurev.aa.30.090192.003043
- Condon J. J., Cotton W. D., Greisen E. W., Yin Q. F., Perley R. A., Taylor G. B., Broderick J. J. (1998) The NRAO VLA Sky Survey. *Astronom J* 115: 1693-1716. doi:10.1086/300337
- Condon J. J., Cotton W. D., Fomalont E. B., Kellermann K. I., Miller N., Perley R. A., Scott D., Vernstrom T., et al. (2012) Resolving the Radio Source Background: Deeper Understanding through Confusion. *Astrophys J* 758: 23. doi:10.1088/0004-637X/758/1/23
- Condon J. J., Kellermann K. I., Kimball A. E., Ivezić Ž., Perley R. A. (2013) Active Galactic Nucleus and Starburst Radio Emission from Optically Selected Quasi-stellar Objects. *Astrophys J* 768: 37. doi:10.1088/0004-637X/768/1/37
- Croton D. J., Springel V., White S. D. M., De Lucia G., Frenk C. S., Gao L., Jenkins A., Kauffmann G., et al. (2006) The many lives of active galactic nuclei: cooling flows, black holes and the luminosities and colours of galaxies. *MNRAS* 365: 11-28. doi:10.1111/j.1365-2966.2005.09675.x
- Daddi E., Dickinson M., Morrison G., Chary R., Cimatti A., Elbaz D., Frayer D., Renzini A., et al. (2007) Multiwavelength Study of Massive Galaxies at $z \sim 2$. I. Star Formation and Galaxy Growth. *Astrophys J* 670: 156-172. doi:10.1086/521818
- D'Elia V., Padovani P., Giommi P., Turriziani S. (2015) Are many radio-selected BL Lacs radio quasars in disguise?. *MNRAS* 449: 3517-3521. doi:10.1093/mnras/stv573
- de Zotti G., Massardi M., Negrello M., Wall J. (2010) Radio and millimeter continuum surveys and their astrophysical implications. *Astron Astrophys Rev* 18: 1-65. doi:10.1007/s00159-009-0026-0
- Donley J. L., Koekemoer A. M., Brusa M., Capak P., Cardamone C. N., Civano F., Ilbert O., Impey C. D., et al. (2012) Identifying Luminous Active Galactic Nuclei in Deep Surveys: Revised IRAC Selection Criteria. *Astrophys J* 748: 142. doi:10.1088/0004-637X/748/2/142
- Dunlop J. S., Peacock J. A. (1990) The Redshift Cut-Off in the Luminosity Function of Radio Galaxies and Quasars. *MNRAS* 247: 19-42.
- Dunlop J. S., McLure R. J., Kukula M. J., Baum S. A., O'Dea C. P., Hughes D. H. (2003) Quasars, their host galaxies and their central black holes. *MNRAS* 340: 1095-1135. doi:10.1046/j.1365-8711.2003.06333.x
- Elbaz D., Daddi E., Le Borgne D., Dickinson M., Alexander D. M., Chary R.-R., Starck J.-L., Brandt W. N., et al. (2007) The reversal of the star formation-density relation in the distant universe. *Astron Astrophys* 468: 33-48. doi:10.1051/0004-6361:20077525
- Ellison S. L., Teimoorinia H., Rosario D. J., Mendel J. T. (2016) The star formation rates of active galactic nuclei host galaxies. *MNRAS* 458: L34-L38. doi:10.1093/mnras/slw012
- Evans D. A., Worrall D. M., Hardcastle M. J., Kraft R. P., Birkinshaw M. (2006) Chandra and XMM-Newton Observations of a Sample of Low-Redshift FR I and FR II Radio Galaxy Nuclei. *Astrophys J* 642: 96-112. doi:10.1086/500658
- Fanaroff B. L., Riley J. M. (1974) The morphology of extragalactic radio sources of high and low luminosity. *MNRAS* 167: 31P-36P
- Fixsen D. J., Kogut A., Levin S., Limon M., Lubin P., Mirel P., Seiffert M., Singal J., et al. (2011) ARCADE 2 Measurement of the Absolute Sky Brightness at 3-90 GHz. *Astrophys J* 734: 5. doi:10.1088/0004-637X/734/1/5
- Flesch E. W. (2015) The Half Million Quasars (HMQ) Catalogue. *Publications Astron Soc Australia* 32: e010. doi:10.1017/pasa.2015.10
- Fomalont E. B., Kellermann K. I., Wall J. V., Weistrop D. (1984) A deep 6-centimeter radio source survey. *Science* 225: 23-28. doi:10.1126/science.225.4657.23
- Garofalo D., Evans D. A., Sambruna R. M. (2010) The evolution of radio-loud active galactic nuclei as a function of black hole spin. *MNRAS* 406: 975-986. doi:10.1111/j.1365-2966.2010.16797.x
- Gehrels N. (1986) Confidence limits for small numbers of events in astrophysical data. *Astrophys J* 303: 336-346. doi:10.1086/164079
- Gehrels N., Spergel D., on behalf of the WFIRST SDT and Project (2015) Wide-Field InfraRed Survey Telescope (WFIRST) Mission and Synergies with LISA and LIGO-Virgo. *Journal of Physics Conference Series* 610: 012007. doi:10.1088/1742-6596/610/1/012007
- Gendre M. A., Best P. N., Wall J. V., Ker L. M. (2013) The relation between morphology, accretion modes and environmental factors in local radio AGN. *MNRAS* 430: 3086-3101. doi:10.1093/mnras/stt116

- Ghisellini G., Celotti A. (2001) The dividing line between FR I and FR II radio-galaxies. *Astron Astrophys* 379: L1-L4. doi:10.1051/0004-6361:20011338
- Ghisellini G. (2010) The jet/disk connection in blazars. *American Institute of Physics Conference Series* 1242: 43-54. doi:10.1063/1.3460151
- Giacconi R., Rosati P., Tozzi P., Nonino M., Hasinger G., Norman C., Bergeron J., Borgani S., et al. (2001) First Results from the X-Ray and Optical Survey of the Chandra Deep Field South. *Astrophys J* 551: 624-634. doi:10.1086/320222
- Giommi P., Colafrancesco S., Padovani P., Gasparri D., Cavazzuti E., Cutini S. (2009) The number counts, luminosity functions, and evolution of microwave-selected (WMAP) blazars and radio galaxies. *Astron Astrophys* 508: 107-115. doi:10.1051/0004-6361/20078905
- Giommi P., Padovani P., Polenta G., Turriziani S., D'Elia V., Piranomonte S. (2012) A simplified view of blazars: clearing the fog around long-standing selection effects. *MNRAS* 420: 2899-2911. doi:10.1111/j.1365-2966.2011.20044.x
- Giommi P., Padovani P., Polenta G. (2013) A simplified view of blazars: the γ -ray case. *MNRAS* 431: 1914-1922. doi:10.1093/mnras/stt305
- Giommi P., Padovani P. (2015) A simplified view of blazars: contribution to the X-ray and γ -ray extragalactic backgrounds. *MNRAS* 450: 2404-2409. doi:10.1093/mnras/stv793
- Gregory P. C., Scott W. K., Douglas K., Condon J. J. (1996) The GB6 Catalog of Radio Sources. *Astrophys J Suppl* 103: 427-432. doi:10.1086/192282
- Gruppioni C., Mignoli M., Zamorani G. (1999) Optical identifications and spectroscopy of a faint radio source sample: the nature of the sub-mJy population. *MNRAS* 304: 199-217. doi:10.1046/j.1365-8711.1999.02301.x
- Gruppioni C., Pozzi F., Zamorani G., Ciliegi P., Lari C., Calabrese E., La Franca F., Matute I., et al. (2003) The radio-mid-infrared correlation and the contribution of 15- μ m galaxies to the 1.4-GHz source counts. *MNRAS* 341: L1-L6. doi:10.1046/j.1365-8711.2003.06601.x
- Gruppioni C., Pozzi F., Rodighiero G., Delvecchio I., Berta S., Pozzetti L., Zamorani G., Andreani P., et al. (2013) The Herschel PEP/HerMES luminosity function - I. Probing the evolution of PACS selected Galaxies to $z \approx 4$. *MNRAS* 432: 23-52. doi:10.1093/mnras/stt308
- Haarsma D. B., Partridge R. B., Windhorst R. A., Richards E. A. (2000) Faint Radio Sources and Star Formation History. *Astrophys J* 544: 641-658. doi:10.1086/317225
- Hales C. A., Norris R. P., Gaensler B. M., Middelberg E., Chow K. E., Hopkins A. M., Huynh M. T., Lenc E., et al. (2014) ATLAS 1.4 GHz Data Release 2 - I. Observations of the CDF-S and ELAIS-S1 fields and methods for constructing differential number counts. *MNRAS* 441: 2555-2592. doi:10.1093/mnras/stu576
- Hales C. A., Norris R. P., Gaensler B. M., Middelberg E. (2014) ATLAS 1.4 GHz data release 2 - II. Properties of the faint polarized sky. *MNRAS* 440: 3113-3139. doi:10.1093/mnras/stu500
- Hardcastle M. J., Evans D. A., Croston J. H. (2006) The X-ray nuclei of intermediate-redshift radio sources. *MNRAS* 370: 1893-1904. doi:10.1111/j.1365-2966.2006.10615.x
- Harrison F. A., Aird J., Civano F., Lansbury G., Mullaney J. R., Ballantyne D. R., Alexander D. M., Stern D., et al. (2015) The NuSTAR Extragalactic Surveys: The Number Counts of Active Galactic Nuclei and the Resolved Fraction of the Cosmic X-ray Background. *Astrophys J* submitted (arXiv:1511.04183)
- Hasinger G., Altieri B., Arnaud M., Barcons X., Bergeron J., Brunner H., Dadina M., Dennerl K., et al. (2001) XMM-Newton observation of the Lockman Hole. I. The X-ray data. *Astron Astrophys* 365: L45-L50. doi:10.1051/0004-6361:20000046
- Hatziminaoglou E., Pérez-Fournon I., Polletta M., Afonso-Luis A., Hernán-Caballero A., Montenegro-Montes F. M., Lonsdale C., Xu C. K., et al. (2005) Sloan Digital Sky Survey Quasars in the Spitzer Wide-Area Infrared Extragalactic Survey (SWIRE) ELAIS N1 Field: Properties and Spectral Energy Distributions. *Astronom J* 129: 1198-1211. doi:10.1086/428003
- Heald G. H., Pizzo R. F., Orrú E., Breton R. P., Carbone D., Ferrari C., Hardcastle M. J., Jurusik W., et al. (2015) The LOFAR Multifrequency Snapshot Sky Survey (MSSS). I. Survey description and first results. *Astron Astrophys* 582: A123. doi:10.1051/0004-6361/201425210
- Heckman T. M., Best P. N. (2014) The Coevolution of Galaxies and Supermassive Black Holes: Insights from Surveys of the Contemporary Universe. *Annu Rev Astron Astr* 52: 589-660. doi:10.1146/annurev-astro-081913-035722
- Helou G., Soifer B. T., Rowan-Robinson M. (1985) Thermal infrared and nonthermal radio - Remarkable correlation in disks of galaxies. *Astrophys J Lett* 298: L7-L11. doi:10.1086/184556
- Herrera Ruiz N., Middelberg E., Norris R. P., Maini A. (2016) Unveiling the origin of the radio emission in radio-quiet quasars. *Astron Astrophys* 589: L2. doi:10.1051/0004-6361/201628302
- Hickox R. C., Mullaney J. R., Alexander D. M., Chen C.-T. J., Civano F. M., Goulding A. D., Hainline K. N. (2014) Black Hole Variability and the Star Formation-Active Galactic Nucleus Connection: Do All Star-forming Galaxies Host an Active Galactic Nucleus?. *Astrophys J* 782: 9. doi:10.1088/0004-637X/782/1/9
- Hine R. G., Longair M. S. (1979) Optical spectra of 3CR radio galaxies. *MNRAS* 188: 111-130. doi:10.1093/mnras/188.1.111
- Hopkins A. M. (2004) On the Evolution of Star-forming Galaxies. *Astrophys J* 615: 209-221. doi:10.1086/424032
- Hopkins P. F., Richards G. T., Hernquist L. (2007) An Observational Determination of the Bolometric Quasar Luminosity Function. *Astrophys J* 654: 731-753. doi:10.1086/509629
- Hopkins P. F., Hernquist L. (2009) A Characteristic Division Between the Fueling of Quasars and Seyferts: Five Simple Tests. *Astrophys J* 694: 599-609. doi:10.1088/0004-637X/694/1/599
- Hopkins P. F., Hickox R., Quataert E., Hernquist L. (2009) Are most low-luminosity active galactic nuclei really obscured?. *MNRAS* 398: 333-349. doi:10.1111/j.1365-2966.2009.15136.x
- Hurley-Walker N., Morgan J., Wayth R. B., Hancock P. J., Bell M. E., Bernardi G., Bhat R., Briggs F., et al. (2014) The Murchison Wide-field Array Commissioning Survey: A Low-Frequency Catalogue of 14110 Compact Radio Sources over 6 100 Square Degrees. *Publications Astron Soc Australia* 31: e045. doi:10.1017/pasa.2014.40
- Huynh M. T., Jackson C. A., Norris R. P., Prandoni I. (2005) Radio Observations of the Hubble Deep Field-South Region. II. The 1.4 GHz Catalog and Source Counts. *Astronom J* 130: 1373-1388. doi:10.1086/432873
- Ilbert O., McCracken H. J., Le Fèvre O., Capak P., Dunlop J., Karim A., Renzini M. A., Caputi K., et al. (2013) Mass assembly in quiescent and star-forming galaxies since $z \approx 4$ from UltraVISTA. *Astron Astrophys* 556: A55. doi:10.1051/0004-6361/201321100
- Jarvis M. J., Rawlings S. (2004) The accretion history of the universe with the SKA. *New Astronom Rev* 48: 1173-1185. doi:10.1016/j.newar.2004.09.006
- Jarvis M., Seymour N., Afonso J., Best P., Beswick R., Heywood I., Huynh M., Murphy E., et al. (2015) The star-formation history of the Universe with the SKA. *Advancing Astrophysics with the Square Kilometre Array (AASKA14)* 68
- Karim A., Schinnerer E., Martínez-Sansigre A., Sargent M. T., van der Wel A., Rix H.-W., Ilbert O., Smolčić V., et al. (2011) The Star Formation History of Mass-selected Galaxies in the COSMOS Field. *Astrophys J* 730: 61. doi:10.1088/0004-637X/730/2/61
- Kellermann K. I., Sramek R., Schmidt M., Shaffer D. B., Green R. (1989) VLA observations of objects in the Palomar Bright Quasar Survey. *Astronom J* 98: 1195-1207. doi:10.1086/115207
- Kellermann K. I. (2015) The road to quasars. *IAU Symposium* 313: 190-195. doi:10.1017/S1743921315002185

- Kennicutt R. C., Jr. (1998) Star Formation in Galaxies Along the Hubble Sequence. *Annu Rev Astron Astr* 36: 189-232. doi:10.1146/annurev.astro.36.1.189
- Kewley L. J., Maier C., Yabe K., Ohta K., Akiyama M., Dopita M. A., Yuan T. (2013) The Cosmic BPT Diagram: Confronting Theory with Observations. *Astrophys J Lett* 774: L10. doi:10.1088/2041-8205/774/1/L10
- Kimball A. E., Ivezić Ž. (2008) A Unified Catalog of Radio Objects Detected by NVSS, First, WENSS, GB6, and SDSS. *Astronom J* 136: 684-712. doi:10.1088/0004-6256/136/2/684
- Kimball A. E., Ivezić Ž. (2014) An Updated Multi-Wavelength Radio and Optical Catalog of Quasars and Radio Galaxies. *Multiwavelength AGN Surveys and Studies*, IAU Symposium, Volume 304: 238-239. doi:10.1017/S1743921314003901
- Kimball A. E., Kellermann K. I., Condon J. J., Ivezić Ž., Perley R. A. (2011) The Two-component Radio Luminosity Function of Quasistellar Objects: Star Formation and Active Galactic Nucleus. *Astrophys J Lett* 739: L29. doi:10.1088/2041-8205/739/1/L29
- King A. J., Rowan-Robinson M. (2004) Linking radio to infrared: a radio source count model. *MNRAS* 349: 1353-1360. doi:10.1111/j.1365-2966.2004.07605.x
- Kormendy J., Ho L. C. (2013) Coevolution (Or Not) of Supermassive Black Holes and Host Galaxies. *Annu Rev Astron Astr* 51: 511-553. doi:10.1146/annurev-astro-082708-101811
- Kühr H., Witzel A., Pauliny-Toth I. I. K., Nauber U. (1981) A catalogue of extragalactic radio sources having flux densities greater than 1 Jy at 5 GHz. *Astron Astrophys Suppl* 45: 367-430
- Lacy M., Storrie-Lombardi L. J., Sajina A., Appleton P. N., Armus L., Chapman S. C., Choi P. I., Fadda D., et al. (2004) Obscured and Unobscured Active Galactic Nuclei in the Spitzer Space Telescope First Look Survey. *Astrophys J Suppl* 154: 166-169. doi:10.1086/422816
- Laing R. A., Riley J. M., Longair M. S. (1983) Bright radio sources at 178 MHz - Flux densities, optical identifications and the cosmological evolution of powerful radio galaxies. *MNRAS* 204: 151-187. doi:10.1093/mnras/204.1.151
- Laing R. A., Jenkins C. R., Wall J. V., Unger S. W. (1994) Spectrophotometry of a Complete Sample of 3CR Radio Sources: Implications for Unified Models. *The Physics of Active Galaxies* 54: 201
- Ledlow M. J., Owen F. N. (1996) 20 CM VLA Survey of Abell Clusters of Galaxies. VI. Radio/Optical Luminosity Functions. *Astronom J* 112: 9-22. doi:10.1086/117985
- Le Fèvre O., Cassata P., Cucciati O., Garilli B., Ilbert O., Le Brun V., Maccagni D., Moreau C., et al. (2013) The VIMOS VLT Deep Survey final data release: a spectroscopic sample of 35 016 galaxies and AGN out to $z \sim 6.7$ selected with $17.5 \leq i_{AB} \leq 24.75$. *Astron Astrophys* 559: A14. doi:10.1051/0004-6361/201322179
- Lehmann I., Hasinger G., Schmidt M., Giacconi R., Trümper J., Zamorani G., Gunn J. E., Pozzetti L., et al. (2001) The ROSAT Deep Survey. VI. X-ray sources and Optical identifications of the Ultra Deep Survey. *Astron Astrophys* 371: 833-857. doi:10.1051/0004-6361:20010419
- Lehmer B. D., Xue Y. Q., Brandt W. N., Alexander D. M., Bauer F. E., Brusa M., Comastri A., Gilli R., et al. (2012) The 4 Ms Chandra Deep Field-South Number Counts Apportioned by Source Class: Pervasive Active Galactic Nuclei and the Ascent of Normal Galaxies. *Astrophys J* 752: 46. doi:10.1088/0004-637X/752/1/46
- Longair M. S. (1966) On the interpretation of radio source counts. *MNRAS* 133: 421-436. doi:10.1093/mnras/133.4.421
- Luo B., Bauer F. E., Brandt W. N., Alexander D. M., Lehmer B. D., Schneider D. P., Brusa M., Comastri A., et al. (2008) The Chandra Deep Field-South Survey: 2 Ms Source Catalogs. *Astrophys J Suppl* 179: 19-36. doi:10.1086/591248
- McAlpine K., Jarvis M. J., Bonfield D. G. (2013) Evolution of faint radio sources in the VIDEO-XMM3 field. *MNRAS* 436: 1084-1095. doi:10.1093/mnras/stt1638
- McAlpine K., Prandoni I., Jarvis M., Seymour N., Padovani P., Best P., Simpson C., Guidetti D., et al. (2015) The SKA view of the Interplay between SF and AGN Activity and its role in Galaxy Evolution. *Advancing Astrophysics with the Square Kilometre Array (AASKA14)* 83
- Mac Low M.-M. (2013) From Gas to Stars Over Cosmic Time. *Science* 340: 1229229. doi:10.1126/science.1229229
- Madau P., Dickinson M. (2014) Cosmic Star-Formation History. *Annu Rev Astron Astr* 52: 415-486. doi:10.1146/annurev-astro-081811-125615
- Mahony E. K., Sadler E. M., Croom S. M., Ekers R. D., Bannister K. W., Chhetri R., Hancock P. J., Johnston H. M., et al. (2011) Optical properties of high-frequency radio sources from the Australia Telescope 20 GHz (AT20G) Survey. *MNRAS* 417: 2651-2675. doi:10.1111/j.1365-2966.2011.19427.x
- Maini A., Prandoni I., Norris R. P., Giovannini G., Spitler L. R. (2016) Compact radio cores in radio-quiet active galactic nuclei. *Astron Astrophys* 589: L3. doi:10.1051/0004-6361/201628305
- Malizia A., Molina M., Bassani L., Stephen J. B., Bazzano A., Ubertini P., Bird A. J. (2014) The INTEGRAL High-energy Cut-off Distribution of Type 1 Active Galactic Nuclei. *Astrophys J Lett* 782: L25. doi:10.1088/2041-8205/782/2/L25
- Mao M. Y., Sharp R., Norris R. P., Hopkins A. M., Seymour N., Lovell J. E. J., Middelberg E., Randall K. E., et al. (2012) The Australia Telescope Large Area Survey: spectroscopic catalogue and radio luminosity functions. *MNRAS* 426: 3334-3348. doi:10.1111/j.1365-2966.2012.21913.x
- Massardi M., Ekers R. D., Murphy T., Mahony E., Hancock P. J., Chhetri R., de Zotti G., Sadler E. M., et al. (2011) The Australia Telescope 20 GHz (AT20G) Survey: analysis of the extragalactic source sample. *MNRAS* 412: 318-330. doi:10.1111/j.1365-2966.2010.17917.x
- Mauch T., Sadler E. M. (2007) Radio sources in the 6dFGS: local luminosity functions at 1.4GHz for star-forming galaxies and radio-loud AGN. *MNRAS* 375: 931-950. doi:10.1111/j.1365-2966.2006.11353.x
- Merloni A., Heinz S. (2013) Evolution of Active Galactic Nuclei. *Planets, Stars and Stellar Systems. Volume 6: Extragalactic Astronomy and Cosmology* 6: 503-566. doi:10.1007/978-94-007-5609-0_11
- Middelberg E., Deller A., Morgan J., Rottmann H., Alef W., Tingay S., Norris R., Bach U., et al. (2011) Wide-field VLBA observations of the Chandra deep field South. *Astron Astrophys* 526: A74. doi:10.1051/0004-6361/201015406
- Miley G., De Breuck C. (2008) Distant radio galaxies and their environments. *Astron Astrophys Rev* 15: 67-144. doi:10.1007/s00159-007-0008-z
- Miller P., Rawlings S., Saunders R. (1993) The Radio and Optical Properties of the $z < 0.5$ BQS Quasars. *MNRAS* 263: 425-460. doi:10.1093/mnras/263.2.425
- Miller N. A., Bonzini M., Fomalont E. B., Kellermann K. I., Mainieri V., Padovani P., Rosati P., Tozzi P., et al. (2013) The Very Large Array 1.4 GHz Survey of the Extended Chandra Deep Field South: Second Data Release. *Astrophys J Suppl* 205: 13. doi:10.1088/0067-0049/205/2/13
- Mills B. Y., Slee O. B., Hill E. R. (1958) A Catalogue of Radio Sources between Declinations +10 deg and -20 deg. *Australian J of Physics* 11: 360-387. doi:10.1071/PH580360
- Morganti R., Rottgering H., Snellen I., Miley G., Barthel P., Best P., Bruggen M., Brunetti G., et al. (2010) Continuum surveys with LOFAR and synergy with future large surveys in the 1-2 GHz band in *Panoramic Radio Astronomy: Wide-field 1-2 GHz research on galaxy evolution*, Gröningen, The Netherlands, published online at <http://pos.sissa.it/cgi-bin/reader/conf.cgi?confid=89>, 40. arXiv:1001.2384.
- Morić I., Smolčić V., Kimball A., Riechers D. A., Ivezić Ž., Scoville N. (2010) A Closer View of the Radio-FIR Correlation: Dis-

- entangling the Contributions of Star Formation and Active Galactic Nucleus Activity. *Astrophys J* 724: 779-790. doi:10.1088/0004-637X/724/1/779
- Moshir M., Kopman G., Conrow T. A. O. (1992) IRAS Faint Source Survey, Explanatory supplement version 2. Pasadena: Infrared Processing and Analysis Center, California Institute of Technology, 1992, edited by Moshir, M.; Kopman, G.; Conrow, T. A. O.
- Nakagawa T., Shibai H., Onaka T., Matsuhara H., Kaneda H., Kawakatsu Y. (2015) The Next-Generation Infrared Astronomy Mission SPICA Under the New Framework. *Publication of Korean Astron Soc* 30: 621-624. doi:10.5303/PKAS.2015.30.2.621
- Netzer H. (2015) Revisiting the Unified Model of Active Galactic Nuclei. *Annu Rev Astron Astr* 53:365-408. doi:10.1146/annurev-astro-082214-122302
- Noeske K. G., Weiner B. J., Faber S. M., Papovich C., Koo D. C., Somerville R. S., Bundy K., Conselice C. J., et al. (2007) Star Formation in AEGIS Field Galaxies since $z=1.1$: The Dominance of Gradually Declining Star Formation, and the Main Sequence of Star-forming Galaxies. *Astrophys J Lett* 660: L43-L46. doi:10.1086/517926
- Norris R. P., Hopkins A. M., Afonso J., Brown S., Condon J. J., Dunne L., Feain I., Hollow R., et al. (2011) EMU: Evolutionary Map of the Universe. *Publications Astron Soc Australia* 28: 215-248. doi:10.1071/AS11021
- Norris R. P., Afonso J., Bacon D., Beck R., Bell M., Beswick R. J., Best P., Bhatnagar S., et al. (2013) Radio Continuum Surveys with Square Kilometre Array Pathfinders. *Publications Astron Soc Australia* 30: e020. doi:10.1017/pas.2012.020
- Nyland K., Young L. M., Wrobel J. M., Sarzi M., Morganti R., Alatalo K., Blitz L., Bournaud F., et al. (2016) The ATLAS^{3D} Project - XXXI. Nuclear radio emission in nearby early-type galaxies. *MNRAS* 458: 2221-2268. doi:10.1093/mnras/stw391
- O'Dea C. P. (1998) The Compact Steep-Spectrum and Gigahertz Peaked-Spectrum Radio Sources. *Publications Astron Soc Pacific* 110: 493-532. doi:10.1086/316162
- Ogle P., Whysong D., Antonucci R. (2006) Spitzer Reveals Hidden Quasar Nuclei in Some Powerful FR II Radio Galaxies. *Astrophys J* 647: 161-171. doi:10.1086/505337
- Orienti M., D'Ammando F., Giroletti M., Giovannini G., Panessa F. (2015) The physics of the radio emission in the quiet side of the AGN population with the SKA. *Advancing Astrophysics with the Square Kilometre Array (AASKA14)* 87
- Orr M. J. L., Browne I. W. A. (1982) Relativistic beaming and quasar statistics. *MNRAS* 200: 1067-1080. doi:10.1093/mnras/200.4.1067
- Owen F. N., Morrison G. E. (2008) The Deep Swire Field. I. 20 cm Continuum Radio Observations: A Crowded Sky. *Astronom J* 136: 1889-1900. doi:10.1088/0004-6256/136/5/1889
- Padovani P. (1993) The Radio Loud Fraction of QSOS and its Dependence on Magnitude and Redshift. *MNRAS* 263: 461-461. doi:10.1093/mnras/263.2.461
- Padovani P., Giommi P., Landt H., Perlman E. S. (2007) The Deep X-Ray Radio Blazar Survey. III. Radio Number Counts, Evolutionary Properties, and Luminosity Function of Blazars. *Astrophys J* 662: 182-198. doi:10.1086/516815
- Padovani P., Mainieri V., Tozzi P., Kellermann K. I., Fomalont E. B., Miller N., Rosati P., Shaver P., et al. (2009) The Very Large Array Survey of the Chandra Deep Field South. IV. Source Population. *Astrophys J* 694: 235-246. doi:10.1088/0004-637X/694/1/235
- Padovani P. (2011) The microjansky and nanojansky radio sky: source population and multiwavelength properties. *MNRAS* 411: 1547-1561. doi:10.1111/j.1365-2966.2010.17789.x
- Padovani P., Miller N., Kellermann K. I., Mainieri V., Rosati P., Tozzi P. (2011) The VLA Survey of Chandra Deep Field South. V. Evolution and Luminosity Functions of Sub-millijansky Radio Sources and the Issue of Radio Emission in Radio-quiet Active Galactic Nuclei. *Astrophys J* 740: 20. doi:10.1088/0004-637X/740/1/20
- Padovani P., Bonzini M., Kellermann K. I., Miller N., Mainieri V., Tozzi P. (2015a) Radio-faint AGN: a tale of two populations. *MNRAS* 452: 1263-1279. doi:10.1093/mnras/stv1375
- Padovani P., Petropoulou M., Giommi P., Resconi E. (2015b) A simplified view of blazars: the neutrino background. *MNRAS* 452: 1877-1887. doi:10.1093/mnras/stv1467
- Padovani P., Resconi E., Giommi P., Arsioli B., Chang Y. L. (2016) Extreme blazars as counterparts of IceCube astrophysical neutrinos. *MNRAS* 457: 3582-3592. doi:10.1093/mnras/stw228
- Panessa F., Giroletti M. (2013) Sub-parsec radio cores in nearby Seyfert galaxies. *MNRAS* 432: 1138-1143. doi:10.1093/mnras/stt547
- Peng Y.-j., Lilly S. J., Renzini A., Carollo M. (2012) Mass and Environment as Drivers of Galaxy Evolution. II. The Quenching of Satellite Galaxies as the Origin of Environmental Effects. *Astrophys J* 757: 4. doi:10.1088/0004-637X/757/1/4
- Phillips M. M., Jenkins C. R., Dopita M. A., Sadler E. M., Binette L. (1986) Ionized gas in elliptical and S0 galaxies. I - A survey for H-alpha and forbidden N II emission. *Astronom J* 91: 1062-1085. doi:10.1086/114083
- Prandoni I., Gregorini L., Parma P., de Ruiter H. R., Vettolani G., Wieringa M. H., Ekers R. D. (2001) The ATESP radio survey. III. Source counts. *Astron Astrophys* 365: 392-399. doi:10.1051/0004-6361:20000142
- Prandoni I., Seymour N. (2015) Revealing the Physics and Evolution of Galaxies and Galaxy Clusters with SKA Continuum Surveys. *Advancing Astrophysics with the Square Kilometre Array (AASKA14)* 67
- Raginski I., Laor A. (2016) AGN coronal emission models - I. The predicted radio emission. *MNRAS* 459: 2082-2096. doi:10.1093/mnras/stw772
- Renzini A., Peng Y.-j. (2015) An Objective Definition for the Main Sequence of Star-forming Galaxies. *Astrophys J Lett* 801: L29. doi:10.1088/2041-8205/801/2/L29
- Richards A. M. S., Muxlow T. W. B., Beswick R., Allen M. G., Benson K., Dickson R. C., Garrett M. A., Garrington S. T., et al. (2007) Using VO tools to investigate distant radio starbursts hosting obscured AGN in the HDF(N) region. *Astron Astrophys* 472: 805-822. doi:10.1051/0004-6361:20077598
- Rigby E. E., Argyle J., Best P. N., Rosario D., Röttgering H. J. A. (2015) Cosmic downsizing of powerful radio galaxies to low radio luminosities. *Astron Astrophys* 581: A96. doi:10.1051/0004-6361/2526475
- Rosario D. J., Burtscher L., Davies R., Genzel R., Lutz D., Tacconi L. J. (2013) The Mid-infrared Emission of Narrow-line Active Galactic Nuclei: Star Formation, Nuclear Activity, and Two Populations Revealed by Wise. *Astrophys J* 778: 94. doi:10.1088/0004-637X/778/2/94
- Rowan-Robinson M., Benn C. R., Lawrence A., McMahon R. G., Broadhurst T. J. (1993) The evolution of faint radio sources. *MNRAS* 263: 123-130. doi:10.1093/mnras/263.1.123
- Rybicki G. B., Lightman A. P., Radiative Processes in Astrophysics, p. 186 - 190, WILEY-VCH Verlag GmbH & Co. (2004). doi:10.1002/9783527618170
- Ryle M., Scheuer P. A. G. (1955) The Spatial Distribution and the Nature of Radio Stars. *Proceedings of the Royal Society of London Series A* 230: 448-462. doi:10.1098/rspa.1955.0146
- Sadler E. M., Jenkins C. R., Kotanyi C. G. (1989) Low-luminosity radio sources in early-type galaxies. *MNRAS* 240: 591-635.
- Sadler E. M., Jackson C. A., Cannon R. D., McIntyre V. J., Murphy T., Bland-Hawthorn J., Bridges T., Cole S., et al. (2002) Radio sources in the 2dF Galaxy Redshift Survey - II. Local radio luminosity functions for AGN and star-forming galaxies at 1.4 GHz. *MNRAS* 329: 227-245. doi:10.1046/j.1365-8711.2002.04998.x
- Sadler E. M., Ekers R. D., Mahony E. K., Mauch T., Murphy T. (2014) The local radio-galaxy population at 20 GHz. *MNRAS* 438: 796-

824. doi:10.1093/mnras/stt2239
- Sadler E. M. (2016) GPS/CSS radio sources and their relation to other AGN. *Astronomische Nachrichten* 337: 105-113. doi:10.1002/asna.201512274
- Sandage A. (1965) The Existence of a Major New Constituent of the Universe: the Quasistellar Galaxies. *Astrophys J* 141: 1560-1579. doi:10.1086/148245
- Santos M., Bull P., Alonso D., Camera S., Ferreira P., Bernardi G., Maartens R., Viel M., et al. (2015) Cosmology from a SKA HI intensity mapping survey. *Advancing Astrophysics with the Square Kilometre Array (AASKA14)* 19
- Sargent M. T., Schinnerer E., Murphy E., Aussel H., Le Floch E., Frayer D. T., Martínez-Sansigre A., Oesch P., et al. (2010) The VLA-COSMOS Perspective on the Infrared-Radio Relation. I. New Constraints on Selection Biases and the Non-Evolution of the Infrared/Radio Properties of Star-Forming and Active Galactic Nucleus Galaxies at Intermediate and High Redshift. *Astrophys J Suppl* 186: 341-377. doi:10.1088/0067-0049/186/2/341
- Scheuer P. A. G. (1957) A statistical method for analysing observations of faint radio stars. *Proceedings of the Cambridge Philosophical Society* 53: 764-773. doi:10.1017/S0305004100032825
- Schmidt M. (1963) 3C 273: A Star-Like Object with Large Red-Shift. *Nature* 197: 1040. doi:10.1038/1971040a0
- Schmidt M. (1968) Space Distribution and Luminosity Functions of Quasi-Stellar Radio Sources. *Astrophys J* 151: 393-409. doi:10.1086/149446
- Schmidt M. (1970) Space Distribution and Luminosity Functions of Quasars. *Astrophys J* 162: 371-379. doi:10.1086/150668
- Seiffert M., Fixsen D. J., Kogut A., Levin S. M., Limon M., Lubin P. M., Mirel P., Singal J., et al. (2011) Interpretation of the ARCADE 2 Absolute Sky Brightness Measurement. *Astrophys J* 734: 6. doi:10.1088/0004-637X/734/1/6
- Seymour N., Dwelly T., Moss D., McHardy I., Zoghbi A., Rieke G., Page M., Hopkins A., et al. (2008) The star formation history of the Universe as revealed by deep radio observations. *MNRAS* 386: 1695-1708. doi:10.1111/j.1365-2966.2008.13166.x
- Shakura N. I., Sunyaev R. A. (1973) Black holes in binary systems. Observational appearance. *Astron Astrophys* 24: 337-355.
- Shen Y., Ho L. C. (2014) The diversity of quasars unified by accretion and orientation. *Nature* 513: 210-213. doi:10.1038/nature13712
- Simpson C., Martínez-Sansigre A., Rawlings S., Ivison R., Akiyama M., Sekiguchi K., Takata T., Ueda Y., et al. (2006) Radio imaging of the Subaru/XMM-Newton Deep Field - I. The 100- μ Jy catalogue, optical identifications, and the nature of the faint radio source population. *MNRAS* 372: 741-757. doi:10.1111/j.1365-2966.2006.10907.x
- Simpson C., Rawlings S., Ivison R., Akiyama M., Almaini O., Bradshaw E., Chapman S., Chuter R., et al. (2012) Radio imaging of the Subaru/XMM-Newton Deep Field- III. Evolution of the radio luminosity function beyond $z = 1$. *MNRAS* 421: 3060-3083. doi:10.1111/j.1365-2966.2012.20529.x
- Smith K. L., Koss M., Mushotzky R. F. (2014) An Infrared and Optical Analysis of a Sample of XBONGs and Optically Elusive AGNs. *Astrophys J* 794: 112. doi:10.1088/0004-637X/794/2/112
- Smolčić V., Schinnerer E., Zamorani G., Bell E. F., Bondi M., Carilli C. L., Ciliegi P., Mobasher B., et al. (2009a) The Dust-Unbiased Cosmic Star-Formation History from the 20 CM VLA-COSMOS Survey. *Astrophys J* 690: 610-618. doi:10.1088/0004-637X/690/1/610
- Smolčić V., Zamorani G., Schinnerer E., Bardelli S., Bondi M., Birzan L., Carilli C. L., Ciliegi P., et al. (2009b) Cosmic Evolution of Radio Selected Active Galactic Nuclei in the Cosmological Field. *Astrophys J* 696: 24-39. doi:10.1088/0004-637X/696/1/24
- Smolčić V., Padovani P., Delhaize J., Prandoni I., Seymour N., Jarvis M., Afonso J., Magliocchetti M., et al. (2015) Exploring AGN Activity over Cosmic Time with the SKA. *Advancing Astrophysics with the Square Kilometre Array (AASKA14)* 69
- Somerville R. S., Davé R. (2015) Physical Models of Galaxy Formation in a Cosmological Framework. *Annu Rev Astron Astr* 53: 51-113. doi:10.1146/annurev-astro-082812-140951
- Sopp H. M., Alexander P. (1991) A composite plot of far-infrared versus radio luminosity, and the origin of far-infrared luminosity in quasars. *MNRAS* 251: 14P-16P. doi:10.1093/mnras/251.1.14P
- Sulentic J., Marziani P., Zamfir S. (2011) The Case for Two Quasar Populations. *Balt Astronom* 20: 427-434.
- Sullivan W. T., The early years of radio astronomy: reflections fifty years after Jansky's discovery, p. 146 - 165 and p. 365 - 384, Cambridge University Press (1984)
- Symeonidis M., Willner S. P., Rigopoulou D., Huang J.-S., Fazio G. G., Jarvis M. J. (2008) The properties of 70 μ m-selected high-redshift galaxies in the Extended Groth Strip. *MNRAS* 385: 1015-1028. doi:10.1111/j.1365-2966.2008.12899.x
- Szokoly G. P., Bergeron J., Hasinger G., Lehmann I., Kewley L., Mainieri V., Nonino M., Rosati P., et al. (2004) The Chandra Deep Field-South: Optical Spectroscopy. I. *Astrophys J Suppl* 155: 271-349. doi:10.1086/424707
- Tadhunter C. (2016) Radio AGN in the local universe: unification, triggering and evolution. *Astron Astrophys Rev* 24: 10. doi:10.1007/s00159-016-0094-x
- Taylor E. N., Franx M., van Dokkum P. G., Bell E. F., Brammer G. B., Rudnick G., Wuyts S., Gawiser E., et al. (2009) The Rise of Massive Red Galaxies: The Color-Magnitude and Color-Stellar Mass Diagrams for $z_{\text{phot}} \lesssim 2$ from the Multiwavelength Survey by Yale-Chile. *Astrophys J* 694: 1171-1199. doi:10.1088/0004-637X/694/2/1171
- Thean A., Pedlar A., Kukula M. J., Baum S. A., O'Dea C. P. (2001) High-resolution radio observations of Seyfert galaxies in the extended 12- μ m sample - II. The properties of compact radio components. *MNRAS* 325: 737-760. doi:10.1046/j.1365-8711.2001.04485.x
- Ulvestad J. S., Antonucci R. R. J., Barvainis R. (2005) VLBA Imaging of Central Engines in Radio-Quiet Quasars. *Astrophys J* 621: 123-129. doi:10.1086/427426
- Urry C. M., Padovani P. (1995) Unified Schemes for Radio-Loud Active Galactic Nuclei. *Publications Astron Soc Pacific* 107: 803-845. doi:10.1086/133630
- van Velzen S., Falcke H., Schellart P., Nierstenhöfer N., Kampert K.-H. (2012) Radio galaxies of the local universe. All-sky catalog, luminosity functions, and clustering. *Astron Astrophys* 544: A18. doi:10.1051/0004-6361/201219389
- van Weeren R. J., Williams W. L., Tasse C., Röttgering H. J. A., Rafferty D. A., van der Tol S., Heald G., White G. J., et al. (2014) LOFAR Low-band Antenna Observations of the 3C 295 and Boötes Fields: Source Counts and Ultra-steep Spectrum Sources. *Astrophys J* 793: 82. doi:10.1088/0004-637X/793/2/82
- Vattakunnel S., Tozzi P., Matteucci F., Padovani P., Miller N., Bonzini M., Mainieri V., Paolillo M., et al. (2012) The radio-X-ray relation as a star formation indicator: results from the Very Large Array-Extended Chandra Deep Field-South. *MNRAS* 420: 2190-2208. doi:10.1111/j.1365-2966.2011.20185.x
- Vernstrom T., Scott D., Wall J. V., Condon J. J., Cotton W. D., Fomalont E. B., Kellermann K. I., Miller N., et al. (2014) Deep 3 GHz number counts from a P(D) fluctuation analysis. *MNRAS* 440: 2791-2809. doi:10.1093/mnras/stu470
- Vernstrom T., Norris R. P., Scott D., Wall J. V. (2015) The deep diffuse extragalactic radio sky at 1.75 GHz. *MNRAS* 447: 2243-2260. doi:10.1093/mnras/stu2595
- Vernstrom T., Scott D., Wall J., Condon J., Cotton B., Kellermann K., Perley R. (2016) Deep 3-GHz observations of the Lockman Hole North with the Very Large Array - II. Catalogue and μ Jy source properties. *MNRAS* 462: 2934-2949. doi:10.1093/mnras/stw1836
- Wall J. V., Jackson C. A., Shaver P. A., Hook I. M., Kellermann K. I. (2005) The Parkes quarter-Jansky flat-spectrum sample. III. Space

- density and evolution of QSOs. *Astron Astrophys* 434: 133-148. doi:10.1051/0004-6361:20041786
- Weiß A., De Breuck C., Marrone D. P., Vieira J. D., Aguirre J. E., Aird K. A., Aravena M., Ashby M. L. N., et al. (2013) ALMA Redshifts of Millimeter-selected Galaxies from the SPT Survey: The Redshift Distribution of Dusty Star-forming Galaxies. *Astrophys J* 767: 88. doi:10.1088/0004-637X/767/1/88
- Whittam I. H., Riley J. M., Green D. A., Jarvis M. J., Vaccari M. (2015) The faint radio source population at 15.7 GHz - II. Multi-wavelength properties. *MNRAS* 453: 4244-4263. doi:10.1093/mnras/stv1901
- Whittam I. H., Riley J. M., Green D. A., Davies M. L., Franzen T. M. O., Rumsey C., Schammel M. P., Waldram E. M., et al. (2016) 10C continued: a deeper radio survey at 15.7 GHz. *MNRAS* 457: 1496-1506. doi:10.1093/mnras/stv2960
- Williams W. L., van Weeren R. J., Röttgering H. J. A., Best P., Dijkema T. J., de Gasperin F., Hardcastle M. J., Heald G., et al. (2016) LOFAR 150-MHz observations of the Boötes field: Catalogue and Source Counts. *MNRAS* 460: 2385-2412. doi: 10.1093/mnras/stw1056
- Wilman R. J., Miller L., Jarvis M. J., Mauch T., Levrier F., Abdalla F. B., Rawlings S., Klöckner H.-R., et al. (2008) A semi-empirical simulation of the extragalactic radio continuum sky for next generation radio telescopes. *MNRAS* 388: 1335-1348. doi:10.1111/j.1365-2966.2008.13486.x
- Wilman R. J., Jarvis M. J., Mauch T., Rawlings S., Hickey S. (2010) An infrared-radio simulation of the extragalactic sky: from the Square Kilometre Array to Herschel. *MNRAS* 405: 447-461. doi:10.1111/j.1365-2966.2010.16453.x
- Wilson A. S., Colbert E. J. M. (1995) The difference between radio-loud and radio-quiet active galaxies. *Astrophys J* 438: 62-71. doi:10.1086/175054
- Windhorst R. A., van Heerde G. M., Katgert P. (1984) A deep Westerbork survey of areas with multicolor Mayall 4 M plates. I - The 1412 MHz catalogue, source counts and angular size statistics. *Astron Astrophys Suppl* 58: 1-37.
- Windhorst R. A., Miley G. K., Owen F. N., Kron R. G., Koo D. C. (1985) Sub-millijansky 1.4 GHz source counts and multicolor studies of weak radio galaxy populations. *Astrophys J* 289: 494-513. doi:10.1086/162911
- Windhorst R. A., Cohen S. H., Hathi N. P., McCarthy P. J., Ryan R. E., Jr., Yan H., Baldry I. K., Driver S. P., et al. (2011) The Hubble Space Telescope Wide Field Camera 3 Early Release Science Data: Panchromatic Faint Object Counts for 0.2-2 μ m Wavelength. *Astrophys J Suppl* 193: 27. doi:10.1088/0067-0049/193/2/27
- Yuan Z., Wang J., Zhou M., Mao J. (2016) A Mixture Evolution Scenario of the AGN Radio Luminosity Function. *Astrophys J* 820: 65. doi:10.3847/0004-637X/820/1/65
- Zakamska N. L., Lampayan K., Petric A., Dicken D., Greene J. E., Heckman T. M., Hickox R. C., Ho L. C., et al. (2016) Star formation in quasar hosts and the origin of radio emission in radio-quiet quasars. *MNRAS* 455: 4191-4211. doi:10.1093/mnras/stv2571
- Zamfir S., Sulentic J. W., Marziani P. (2008) New insights on the QSO radio-loud/radio-quiet dichotomy: SDSS spectra in the context of the 4D eigenvector1 parameter space. *MNRAS* 387: 856-870. doi:10.1111/j.1365-2966.2008.13290.x
- Zirbel E. L., Baum S. A. (1995) On the FR I/FR II Dichotomy in Powerful Radio Sources: Analysis of Their Emission-Line and Radio Luminosities. *Astrophys J* 448: 521-547. doi:10.1086/175984